NATO STANDARD

AOP-4355

THE LIESKE MODIFIED POINT MASS AND FIVE DEGREES OF FREEDOM TRAJECTORY MODELS

Edition A Version 1
SEPTEMBER 2017

NORTH ATLANTIC TREATY ORGANIZATION

ALLIED ORDNANCE PUBLICATION

Published by the
NATO STANDARDIZATION OFFICE (NSO)

INTENTIONALLY BLANK

NORTH ATLANTIC TREATY ORGANIZATION (NATO)

NATO STANDARDIZATION OFFICE (NSO)

NATO LETTER OF PROMULGATION

14 September 2017

1. The enclosed Allied Ordnance Publication AOP-4355, Edition A, Version 1, THE LIESKE MODIFIED POINT MASS AND FIVE DEGREES OF FREEDOM TRAJECTORY MODELS, has been approved by the nations in the NATO Army Armaments Group, is promulgated herewith. The agreement of nations to use this publication is recorded in STANAG 4355.

2. AOP-4355, Edition A ,Version 1 is effective upon receipt.

3.

4. This publication shall be handled in accordance with C-M(2002)60.

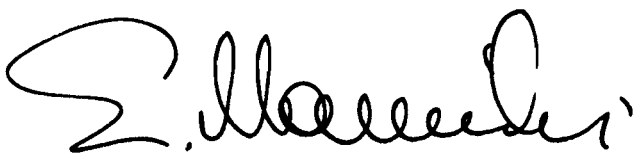

Edvardas MAŽEIKIS
Major General, LTUAF
Director, NATO Standardization Office

INTENTIONALLY BLANK

RESERVED FOR NATIONAL LETTER OF PROMULGATION

INTENTIONALLY BLANK

RECORD OF RESERVATIONS

CHAPTER	RECORD OF RESERVATION BY NATIONS
Note: The reservations listed on this page include only those that were recorded at time of promulgation and may not be complete. Refer to the NATO Standardization Document Database for the complete list of existing reservations.	

INTENTIONALLY BLANK

RECORD OF SPECIFIC RESERVATIONS

[nation]	[detail of reservation]
Note: The reservations listed on this page include only those that were recorded at time of promulgation and may not be complete. Refer to the NATO Standardization Document Database for the complete list of existing reservations.	

INTENTIONALLY BLANK

TABLE OF CONTENTS

CHAPTER 1	AIM	1
CHAPTER 2	AGREEMENT	2
CHAPTER 3	GENERAL	3
CHAPTER 4	DETAILS OF THE AGREEMENT	4
CHAPTER 5	IMPLEMENTATION OF THE AGREEMENT	44
ANNEX A	FORMS OF FIRE CONTROL INPUT DATA	45
ANNEX B	ADDITIONAL TERMS FOR PROJECTILES WITH BOURRELET NUBS	51
ANNEX C	ADDITIONAL TERMS FOR SPIN-STABILIZED ROCKET-ASSISTED PROJECTILES, SPIN-STABILIZED BASE-BURN PROJECTILES, AND FIN-STABILIZED ROCKETS – METHOD 1	53
ANNEX D	ADDITIONAL TERMS FOR SPIN-STABILIZED ROCKET-ASSISTED PROJECTILES, SPIN-STABILIZED BASE-BURN PROJECTILES, AND FIN-STABILIZED ROCKETS – METHOD 2	68
ANNEX E	CALCULATION OF SUBMUNITION TRAJECTORIES	81
ANNEX F	POINT MASS TRAJECTORY MODEL	95
ANNEX G	COORDINATE CONVERSION REQUIRED BY COURSE CORRECTING FUZES	102
ANNEX H	ADDITIONAL TERMS FOR GUIDED MUNITIONS	109
ANNEX I	GLOSSARY OF TERMS	123
ANNEX J	SELECTED BIBLIOGRAPHY	127

INTENTIONALLY BLANK

CHAPTER 1 AIM

1.1. The principal aim of this agreement is to standardize the exterior ballistic trajectory simulation methodology for NATO Army and Naval Forces. The Lieske Modified Point Mass model will be used for spin-stabilized projectiles and the Five Degrees of Freedom model will be used for fin-stabilized rockets. Recommended equations of motion for Aircraft-Dropped Pallets are also presented. This will facilitate the exchange of exterior ballistic data and fire control information.

1.2 Related Documents

STANAG 4106 –	Procedures to Determine the Degree of Ballistic Performance Similarity of NATO Indirect Fire Ammunition and the Applicable Corrections to Aiming Data
STANAG 4119 –	Adoption of a Standard Cannon Artillery Firing Table Format
STANAG 4144 –	Procedures to Determine the Fire Control Inputs for Use in Fire Control Systems
STANAG 4537 –	Sub-Group 2 Shareable (Fire Control) Software Suite (S4)
STANREC 4618 –	The Six/Seven Degrees of Freedom Guided Projectile Trajectory Model
STANAG 6022 –	Adoption of a Standard Gridded Data Meteorological Message
AOP-37 –	NATO Armaments Ballistic Kernel (NABK)
ISO 2533-1975(E) –	The ISO Standard Atmosphere

CHAPTER 2 AGREEMENT

Participating nations agree to use the Lieske Modified Point Mass Trajectory Model for spin-stabilized projectiles and a Five Degrees of Freedom Model for exterior ballistic trajectory simulation of fin-stabilized rockets.

CHAPTER 3 GENERAL

This agreement permits some flexibility by accommodating certain specific national aerodynamic conventions and ballistic data analysis procedures.

CHAPTER 4 DETAILS OF THE AGREEMENT

The details of the agreement are given hereunder and are divided into the following four parts:

4.1 Equations of Motion for Projectiles and Rockets
- A. Equations of Motion for Spin-Stabilized Projectiles
- B. Equations of Motion for Fin-Stabilized Projectiles
- C. Common Equations of Motion

4.2 Equations of Motion for Aircraft-Dropped Pallets
4.3 List of Symbols
4.4 Comparison of Aerodynamic Coefficient Symbols
4.5 List of Data Requirements

4.1 EQUATIONS OF MOTION FOR PROJECTILES AND ROCKETS

The following equations constitute mathematical models representing the flight of:

(1) spin-stabilized projectiles, and
(2) fin-stabilized rockets

that are dynamically stable and possess at least trigonal symmetry. The mathematical modeling is accomplished mainly by: (a) including only the most essential forces and moments, (b) for spin-stabilized projectiles, approximating the actual yaw by the yaw of repose neglecting transient yawing motion, and (c) applying fitting factors to some of the essential forces to compensate for the neglect or approximation of other forces and moments. All vectors have as a frame of reference a right-handed, orthonormal, ground-fixed, Cartesian coordinate system with unit vectors ($\vec{\mathbf{1}}, \vec{\mathbf{2}}$ and $\vec{\mathbf{3}}$) as shown in Figure 4-1.

Assume that the body can be considered a solid of revolution, and assign to the axis of rotational symmetry a unit vector $\vec{x}$ in the chosen coordinate system. Since the rigid body is to represent a projectile or rocket, the direction of $\vec{x}$ from tail to nose is defined as positive. The total angular momentum of the body can now be expressed as the sum of two vectors in the ground-fixed coordinate system:

(1) The angular momentum about $\vec{x}$, and
(2) the angular momentum about an axis perpendicular to $\vec{x}$.

The angular momentum about $\vec{x}$ has the magnitude ($I_X\ p$); where I_X is the moment of inertia of the body about $\vec{x}$, and *p* is the axial spin or angular velocity about $\vec{x}$, in radians per second. Therefore, the total angular momentum about $\vec{x}$ can be represented by the vector ($I_X\ p\ \vec{x}$). In this document, a positive *p* is defined as a rotation which would cause a right-hand screw to advance in the direction of $\vec{x}$.

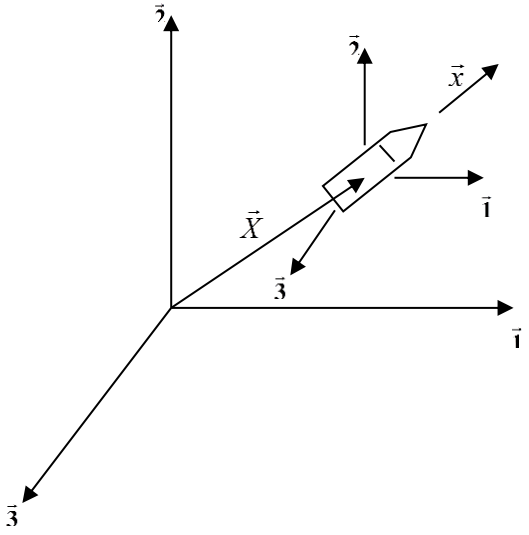

Figure 4-1. Cartesian Coordinate System with Unit Vectors

The total angular velocity of the body about an axis perpendicular to $\vec{x}$ is given by the vector $\left(\vec{x} \times \dot{\vec{x}}\right)$, where the superscript dot refers to differentiation with respect to time. Since the body possesses rotational symmetry about $\vec{x}$, every axis through the center-of-mass and perpendicular to $\vec{x}$ is a principle axis of inertia. If the moment of inertia of the body about any transverse axis is I_Y, the total angular momentum about an axis perpendicular to $\vec{x}$ has the vector representation $I_Y \left(\vec{x} \times \dot{\vec{x}}\right)$.

Let $\vec{H}$ denote the total vector angular momentum of the body. The vector representation of $\vec{H}$ is:

$$\vec{H} = I_X \; p\vec{x} + I_Y \left(\vec{x} \times \dot{\vec{x}}\right) \tag{1}$$

Let $\sum \vec{M}$ be the sum of the vector applied moments, and set $\sum \vec{M}$ equal to the vector rate of change of angular momentum.

$$\dot{\vec{H}} = \sum \vec{M} \tag{2}$$

In addition to these basic equations, two additional expressions are needed for use in the force-moment system.

$$\left(\vec{H} \times \vec{x}\right) = I_Y \; \dot{\vec{x}} \tag{3}$$

$$\left(\vec{H} \cdot \vec{x}\right) = I_X \; p \tag{4}$$

Equation (2) is the basic vector differential equations of angular motion in a fixed coordinate system. The basic equation of motion for the center-of-mass is:

$$\dot{\vec{u}} = \frac{\sum \vec{F}}{m} \tag{5}$$

where $\sum \vec{F}$ denotes the sum of the vector applied forces, m is the mass of the body, and $\dot{\vec{u}}$ is the vector acceleration of the center-of-mass in the fixed coordinate system.

4.1.A. EQUATIONS OF MOTION FOR SPIN-STABILIZED PROJECTILES

Newton's law of motion of the center of mass of the projectile is:

$$\vec{F} = m\dot{\vec{u}} = \overrightarrow{DF} + \overrightarrow{LF} + \overrightarrow{MF} + m\vec{g} + m\vec{\Lambda} \tag{6}$$

where acceleration due to drag force, when *i* is used as a fitting factor, is:

$$\frac{\overrightarrow{DF}}{m} = -\left(\frac{\pi \rho i d^2}{8m}\right)\left(C_{D_0} + C_{D_{\alpha^2}}(Q_D\,\alpha_e)^2 + C_{D_{\alpha^4}}(Q_D\,\alpha_e)^4\right) v\vec{v} \tag{7a}$$

or, when *C* is used as a fitting factor,

$$\frac{\overrightarrow{DF}}{m} = -\left(\frac{\pi \rho m_r}{8Cm}\right)\left(C_{D_0} + C_{D_{\alpha^2}}(Q_D\,\alpha_e)^2 + C_{D_{\alpha^4}}(Q_D\,\alpha_e)^4\right) v\vec{v} \tag{7b}$$

or, when f_D is used as a fitting factor,

$$\frac{\overrightarrow{DF}}{m} = -\left(\frac{\pi \rho d^2}{8m}\right)\left(f_D C_{D_0} + C_{D_{\alpha^2}}(Q_D\,\alpha_e)^2 + C_{D_{\alpha^4}}(Q_D\,\alpha_e)^4\right) v\vec{v} \tag{8}$$

acceleration due to lift force is:

$$\frac{\overrightarrow{LF}}{m} = \left(\frac{\pi \rho d^2 f_L}{8m}\right)\left(C_{L_\alpha} + C_{L_{\alpha^3}}\alpha_e{}^2 + C_{L_{\alpha^5}}\alpha_e{}^4\right) v^2\,\vec{\alpha}_e \tag{9}$$

acceleration due to Magnus force is:

$$\frac{\overrightarrow{MF}}{m} = -\frac{\pi \rho d^3 Q_M\, p C_{mag-f}}{8m}\left(\vec{\alpha}_e \times \vec{v}\right) \tag{10}$$

acceleration due to gravity (*g*) is:
(See Section 4.1.C, Common Equations of Motion)

acceleration due to the Coriolis effect (Λ) is:
(See Section 4.1.C, Common Equations of Motion)

The magnitude of spin acceleration is given by:

$$\dot{p} = \frac{\pi \rho d^4 pv C_{spin}}{8 I_x} \tag{11}$$

where:

$$p = p_0 + \int_0^t \dot{p}\, dt \tag{12}$$

is the magnitude of spin at time = t, and

$$p_0 = \frac{2\pi u_0}{t_c d} \tag{13}$$

is the magnitude of the initial spin of the projectile at the muzzle.

The yaw of repose is given by:

$$\vec{\alpha}_e = -\frac{8 I_X p \left(\vec{v} \times \dot{\vec{u}}\right)}{\pi \rho d^3 (C_{M_\alpha} + C_{M_{\alpha^3}} \alpha_e^2) v^4} \tag{14}$$

where:

$$\vec{\alpha}_{e_0} = \begin{bmatrix} 0 \\ 0 \\ 0 \end{bmatrix} \tag{15}$$

is the initial value of the yaw of repose.

To begin the numerical integration of the modified point mass equations of motion using a predictor-corrector method, one must predict the value of $\dot{\vec{u}}$ using $\vec{\alpha}_{e_0}$ (Eq. (15)) and then use this value of $\dot{\vec{u}}$ to calculate $\vec{\alpha}_e$ using Eq. (14).

See Section 4.1.C for the velocity of the projectile with respect to the ground fixed axis at time = *t*.
See Section 4.1.C for the velocity of the projectile with respect to the air at time = *t*.
See Section 4.1.C for the position of the projectile with respect to the ground axis at time = *t*.

Aerodynamic jump, the initial correction to the trajectory due to the aerodynamic lift force acting on the projectile, is given as a velocity correction:

$$J_A = \Delta\vec{u}_A = -\frac{p_0 I_X f_L C_{L_\alpha} \vec{w}_0}{m d^2 C_{M_\alpha} \vec{v}_0} \tag{16}$$

Windage jump, the correction for wind shear between successive integration steps, is given as a velocity correction:

$$J_w = \Delta\vec{u}_w = \frac{\left(C_{L_\alpha} + C_{L_{\alpha^3}}\ \alpha_e^2 + C_{L_\alpha 5}\ {\alpha_e}^4\right) f_L\ I_X\ p\ (\vec{u} \times \Delta\vec{w})}{(C_{M_\alpha} + C_{M_{\alpha^3}}\ \alpha_e^2)\ m\ d\ v^2} \tag{17}$$

where: $\Delta\vec{w} = \vec{w}_t - \vec{w}_{t-\Delta t}$ (18)

and at $t = 0$, $\vec{w}_t = \vec{w}_0 = 0$.

See Section 4.1.C for the position of the projectile with respect to the spherical earth's surface.

4.1.B. EQUATIONS OF MOTION FOR FIN-STABILIZED ROCKETS

The equations of motion for fin-stabilized rockets are described during four phases of the flight, namely, during launch, from launch to fin opening, from fin opening to the end of motion requiring five degrees of freedom (5 DoF), and from the end of the 5 DoF segment to the end of the 3 DoF phase which normally is the burst point of the warhead. Motor will normally be functioning from t_0 until before (near) the end of Phase 3, Time of End of Five Degrees of Freedom $(t_0 \le t < t_{E5D})$. These phases were chosen to represent those portions of the motion, which require significantly different force and moment descriptions to properly simulate actual flight conditions.

Phase 1: Time Zero to Time of Launch $(t_0 \le t \le t_L)$

Initial Launching Phase

The initial position of the center-of-mass, $\vec{X}_0$, with-respect-to the ground-fixed axis, acceleration, and angular momentum for a rocket are as follows:

The drag force $\left(\overrightarrow{DF}\right)$, thrust force $\left(\overrightarrow{TF}\right)$, acceleration due to gravity and the deceleration due to rocket-launcher friction are considered during the rocket-launching phase. The equation of motion of the center-of-mass during the rocket launch phase is given by:

$$\vec{F} = m\,\dot{\vec{u}} = \left(\overrightarrow{DF} + \overrightarrow{TF}\right) + m|\vec{g}|\left(-\sin QE - \mu_f \cos QE\right)\vec{x}_0 \qquad (19)$$

NOTE: In this phase the rocket does not move before $t = t_{FM}$ and is restricted to forward motion, i.e., for Eq. (19):

$\vec{F} \equiv \vec{0}$ for $t \le t_{FM}$ or whenever $\vec{F} < \vec{0}$

where acceleration due to drag force is:

$$\frac{\overrightarrow{DF}}{m} = -\left(\frac{\pi\, i\, \rho\, d^2}{8\, m}\right) C_{D_0}\, v^2\, \vec{x}_0 \qquad (20)$$

acceleration due to thrust force is:

$$\frac{\overrightarrow{TF}}{m} = \frac{\left(f_T\, \dot{m}_f\, I_{SP} + \left(P_r - P\right) A_e\right)\vec{x}_0}{m} \qquad (21)$$

and acceleration due to gravity $(\vec{g})$ and $\vec{X}_0$ are given in Section 4.1.C.

Initial Angular Momentum at Time of Launch (t_L)

At t_L, the initial angular momentum of the rocket is assigned. $p_{(t_L)}$ is the initial angular velocity (spin) of the rocket about $\vec{x}$, and $\omega_{y_{(t_L)}}$ and $\omega_{z_{(t_L)}}$ are the transverse angular velocities of the rocket at t_L. $\omega_{y_{(t_L)}}$ and $\omega_{z_{(t_L)}}$ are used to match the observed angular performance of the rocket. The initial value of $\vec{H}_{(t_L)}$ is given by:

$$\vec{H}_{(t_L)} = I_{X(t_L)}\ p_{(t_L)}\ \vec{x}_{(t_L)} + I_{Y(t_L)} \begin{bmatrix} -\omega_{y_{(t_L)}} \sin QE \cos \Delta AZ - \omega_{z_{(t_L)}} \sin \Delta AZ \\ +\omega_{y_{(t_L)}} \cos QE \\ -\omega_{y_{(t_L)}} \sin QE \sin \Delta AZ + \omega_{z_{(t_L)}} \cos \Delta AZ \end{bmatrix} \quad (22)$$

where:

$$\vec{x}_{(t_L)} = \vec{x}_0 \quad (23)$$

Phase 2: Time of Launch to Time of Rocket Fins Opening ($t_L \le t \le t_{FO}$)

Use aerodynamics for rockets with fins closed.

Equation of Motion of the Center-of-Mass of the Body

The motion of the center-of-mass of the body is a summation of the accelerations acting on the body and is given by:

$$\vec{F} = m\,\dot{\vec{u}} = \overrightarrow{DF} + \overrightarrow{LF} + \overrightarrow{MF} + \overrightarrow{PDF} + \overrightarrow{TF} + m\,\vec{g} + m\,\vec{\Lambda} \quad (24)$$

where:

acceleration due to drag forces is:

$$\frac{\overrightarrow{DF}}{m} = -\left(\frac{\pi \rho i\, d^2}{8m}\right)\left(C_{D_0} + C_{D_{\alpha^2}}\,(\alpha)^2\right) v\,\vec{v} \quad (25)$$

acceleration due to lift forces is:

$$\frac{\overrightarrow{LF}}{m} = \left(\frac{\pi\, \rho\, d^2\ f_L}{8m}\right)\left(C_{L_\alpha} + C_{L_{\alpha^3}}(\alpha)^2\right)\left(v^2\vec{x} - (\vec{v}\cdot\vec{x})\vec{v}\right) \quad (26)$$

acceleration due to Magnus forces is:

$$\frac{\overrightarrow{MF}}{m} = -\frac{\pi\, \rho\, d^3\, C_{mag-f}}{I_X\ 8m}\left(\vec{H}\cdot\vec{x}\right)\left(\vec{x}\times\vec{v}\right) \quad (27)$$

acceleration due to pitch damping force is:

$$\frac{\overrightarrow{PDF}}{m} = \left(\frac{\pi \ \rho \ d^3 \left(C_{N_q} + C_{N_{\dot{\alpha}}} \right)}{I_Y \ 8 \ m} \right) v \left(\vec{H} \times \vec{x} \right) \tag{28}$$

acceleration due to thrust force is:

$$\frac{\overrightarrow{TF}}{m} = \frac{\left(f_T \ \dot{m}_f \ I_{SP} + \left(P_r - P \right) A_e \right) \vec{x}}{m} \tag{29}$$

acceleration due to gravity (g) is:
(See Section 4.1.C, Common Equations of Motion)

acceleration due to the Coriolis effect (Λ) is:
(See Section 4.1.C, Common Equations of Motion)

NOTE**:** (See Annex C or D for $\dot{m}_f$)

Equation of Angular Momentum of the Body

The angular momentum of the body is the summation of the moments acting on the body and is given by:

$$\dot{\vec{H}} = \overrightarrow{OM} + \overrightarrow{PDM} + \overrightarrow{MM} + \overrightarrow{SDM} + \overrightarrow{FCM} + \overrightarrow{AJDM} + \overrightarrow{TJDM} \tag{30}$$

where:

Angular momentum due to Overturning Moment:

$$\overrightarrow{OM} = \left(\frac{\rho \ d^3 \ \pi}{8} \right) \left(C_{M_\alpha} + C_{M_{\alpha^3}} \ \alpha^2 \right) v \left(\vec{v} \times \vec{x} \right) \tag{31}$$

Angular momentum due to Pitch Damping Moment:

$$\overrightarrow{PDM} = \left(\frac{\rho \ d^4 \ \pi}{8 \ I_Y} \right) \left(C_{M_q} + C_{M_{\dot{\alpha}}} \right) v \left[\vec{H} - \left(\vec{H} \cdot \vec{x} \right) \vec{x} \right] \tag{32}$$

Angular momentum due to Magnus Moment:

$$\overrightarrow{MM} = - \left(\frac{\rho \ d^4 \ \pi}{8 \ I_X} \right) \ C_{mag-m} \left(\vec{H} \cdot \vec{x} \right) \left[\left(\vec{v} \cdot \vec{x} \right) \vec{x} - \vec{v} \right] \tag{33}$$

Angular momentum due to Spin Damping Moment:

$$\overrightarrow{SDM} = \left(\frac{\rho\, d^4\, \pi}{I_X\, 8} \right) C_{spin}\ \ v \left(\vec{H} \cdot \vec{x} \right) \vec{x} \tag{34}$$

Angular momentum due to Fin Cant Moment:

$$\overrightarrow{FCM} = \left(\frac{\rho\, d^3\, \pi}{8} \right) C_{l_\delta}\ \varepsilon\, v^2\ \vec{x} \tag{35}$$

Angular momentum due to Axial Jet Damping Moment:

$$\overrightarrow{AJDM} = \left(\frac{\dot{m}\, r_{ne}^2}{2\, I_X} \right) \left(\vec{H} \cdot \vec{x} \right) \vec{x} \tag{36}$$

Angular momentum due to Transverse Jet Damping Moment:

$$\overrightarrow{TJDM} = \left(\frac{\dot{m}\, r_e\ r_t}{I_Y} \right) \left[\vec{H} - \left(\vec{H} \cdot \vec{x} \right) \vec{x} \right] \tag{37}$$

NOTE: (See Annex C or D for effects of changes in mass during burning.)

The angular momentum and unit vector along the longitudinal axis at time = *t* is:

$$\vec{H} = \vec{H}_{(t_L)} + \int_{t_L}^{t} \dot{\vec{H}}\, dt \tag{38}$$

$$\vec{x} = \vec{x}_{(t_L)} + \int_{t_L}^{t} \dot{\vec{x}}\, dt \tag{39}$$

where $\vec{H}_{(t_L)}$ is defined at Eq. (22), and

$$\vec{x}_{(t_L)} = \vec{x}_0 \tag{40}$$

and

$$\dot{\vec{x}} = \frac{(\vec{H} \times \vec{x})}{I_Y} \tag{41}$$

NOTE: While integrating the equations of motion during the 5 DoF phase, the magnitude of the unit vector $\vec{x}$ should be normalized to the value 1.

The yaw of the symmetric rigid-body (α) is the included angle between $\vec{x}$ and $\vec{v}$. The yaw is defined as a positive quantity and the magnitude is given by:

$$\alpha = \arccos\left[\frac{(\vec{v}\cdot\vec{x})}{|\vec{v}|}\right] \tag{42}$$

The orientation of the yaw (ψ) is the angle of the plane containing $\vec{v}$ and $\vec{x}$ relative to the vertical plane containing $\vec{v}$ measured in a clockwise direction. The orientation of the yaw is given by:

$$\psi = \arctan\left[\frac{(v_1\ x_3 - v_3\ x_1)v}{v_1\ (v_1\ x_2 - v_2\ x_1) - v_3\ (v_2\ x_3 - v_3\ x_2)}\right] \tag{43}$$

<u>Phase 3:</u> Time from Rocket Fins Opening to Time of End of Five Degrees of Freedom ($t_{FO} \le t \le t_{E5D}$)

Same as equations in ($t_L \le t \le t_{FO}$) with aerodynamics for rocket with fins open. Define t_{E5D} to begin after a small time interval after motor burnout (t_{BO}), to allow for aerodynamic settling.

<u>Phase 4:</u> Time from End of Five Degrees of Freedom ($t > t_{E5D}$)

Use point mass equations.

The center of mass of the projectile is:

$$\vec{F} = m\dot{\vec{u}} = \overrightarrow{DF} + m\vec{g} + m\vec{\Lambda} \tag{44}$$

where acceleration due to drag forces is:

$$\frac{\overrightarrow{DF}}{m} = -\left(\frac{\pi\rho i d^2}{8m}\right) C_D v\vec{v} \tag{45}$$

NOTE: ($\vec{g}$, $\vec{u}$, and $\vec{\Lambda}$ are defined in Section 4.1.C)

4.1.C. COMMON EQUATIONS OF MOTION

Acceleration due to gravity is:

$$\vec{g} = -g_0 \left(R^2/r^3\right)\vec{r} = -g_0 \begin{bmatrix} \frac{X_1}{R} \\ 1 - \frac{2X_2}{R} \\ \frac{X_3}{R} \end{bmatrix} \tag{46}$$

where: $g_0 = 9.80665\left[1 - .0026\cos\left(2\,lat\right)\right]$ (47)

$$\vec{r} = \vec{X} - \vec{R}, \tag{48}$$

$$\vec{R} = \begin{bmatrix} 0 \\ -R \\ 0 \end{bmatrix} \tag{49}$$

and $R = 6.356766 \times 10^6$ meters

Acceleration due to the effect of the Coriolis force is:

$$\vec{\Lambda} = -2\left(\vec{\omega} \times \vec{u}\right) \tag{50}$$

where:

$$\vec{\omega} = \begin{bmatrix} \Omega\cos\left(lat\right)\cos\left(AZ\right) \\ \Omega\sin\left(lat\right) \\ -\Omega\cos\left(lat\right)\sin\left(AZ\right) \end{bmatrix} \tag{51}$$

and $\Omega = 7.292115 \times 10^{-5}$ *rad/s*

NOTE**:** For Southern Hemisphere, *lat* is negative.

The position of the projectile or rocket with-respect-to the ground axes is given by:

$$\vec{X} = \vec{X}_0 + \int_0^t \vec{u}\, dt \tag{52}$$

where:

$$\vec{X}_0 = \begin{bmatrix} l_W \cos\left(QE\right)\cos\left(\Delta AZ\right) \\ X_{2_W} + l_W \sin\left(QE\right) \\ l_W \cos\left(QE\right)\sin\left(\Delta AZ\right) \end{bmatrix} \tag{53}$$

is the location of the muzzle, i.e., initial position of the center of mass of the projectile or rocket. For a rocket, $l_W = 0$.

The position of the projectile or rocket with-respect-to the spherical earth's surface is given by the approximation:

$$\vec{E} = \begin{bmatrix} \mathrm{E}_1 \\ \mathrm{E}_2 \\ \mathrm{E}_3 \end{bmatrix} \tag{54}$$

where:

$$\mathrm{E}_1 = \mathrm{R} \times \sin^{-1}\left(\frac{\mathrm{X}_1}{\sqrt{\mathrm{X}_1{}^2 + (\mathrm{R} + \mathrm{X}_2)^2}} \right) \tag{55}$$

$$\mathrm{E}_2 = \sqrt{\mathrm{X}_1{}^2 + \mathrm{X}_3{}^2 + (\mathrm{R} + \mathrm{X}_2)^2} - \mathrm{R} \tag{56}$$

$$\mathrm{E}_3 = \mathrm{R} \times \sin^{-1}\left(\frac{\mathrm{X}_3}{\sqrt{\mathrm{X}_3{}^2 + (\mathrm{R} + \mathrm{X}_2)^2}} \right) \tag{57}$$

The velocity of the projectile or rocket with-respect-to the ground fixed axes at time = *t* is:

$$\vec{u} = \vec{u}_0 + \int_0^t \dot{\vec{u}}\, dt \tag{58}$$

where:

$$\vec{u}_0 = \begin{bmatrix} u_0 \cos(QE)\cos(\Delta AZ) \\ u_0 \sin(QE) \\ u_0 \cos(QE)\sin(\Delta AZ) \end{bmatrix} \tag{59}$$

The velocity of the projectile or rocket with-respect-to the spherical earth's surface is given by the approximation:

$$\dot{\vec{E}} = \begin{bmatrix} \dot{\mathrm{E}}_1 \\ \dot{\mathrm{E}}_2 \\ \dot{\mathrm{E}}_3 \end{bmatrix} \tag{60}$$

where:

$$\dot{\mathrm{E}}_1 = \frac{\partial(\mathrm{E}_1)}{\partial \mathrm{t}} = \mathrm{R} \times \frac{\dfrac{u_1}{\sqrt{\mathrm{X}_1{}^2 + (\mathrm{X}_2 + \mathrm{R})^2}} - \dfrac{\mathrm{X}_1\left[\mathrm{X}_1 u_1 + (\mathrm{X}_2 + \mathrm{R})u_2\right]}{\left[\mathrm{X}_1{}^2 + (\mathrm{X}_2 + \mathrm{R})^2\right]^{3/2}}}{\sqrt{1 - \dfrac{\mathrm{X}_1{}^2}{\mathrm{X}_1{}^2 + (\mathrm{X}_2 + \mathrm{R})^2}}} \tag{61}$$

$$\dot{\mathrm{E}}_2 = \frac{\partial(\mathrm{E}_2)}{\partial \mathrm{t}} = \frac{\left[\mathrm{X}_1 u_1 + \mathrm{X}_3 u_3 + (\mathrm{X}_2 + \mathrm{R}) u_2\right]}{\sqrt{\mathrm{X}_1{}^2 + \mathrm{X}_3{}^2 + (\mathrm{X}_2 + \mathrm{R})^2}} \tag{62}$$

$$\dot{\mathrm{E}}_3 = \frac{\partial(\mathrm{E}_3)}{\partial \mathrm{t}} = \mathrm{R} \times \frac{\dfrac{u_3}{\sqrt{\mathrm{X}_3{}^2 + (\mathrm{X}_2 + \mathrm{R})^2}} - \dfrac{\mathrm{X}_3\left[\mathrm{X}_3 u_3 + (\mathrm{X}_2 + \mathrm{R}) u_2\right]}{\left[\mathrm{X}_3{}^2 + (\mathrm{X}_2 + \mathrm{R})^2\right]^{3/2}}}{\sqrt{1 - \dfrac{\mathrm{X}_3{}^2}{\mathrm{X}_3{}^2 + (\mathrm{X}_2 + \mathrm{R})^2}}} \tag{63}$$

The velocity of the projectile or rocket with-respect-to the air is given by:

$$\vec{v} = \vec{u} - \vec{w} \tag{64}$$

and Mach number:

$$M = v/a \tag{65}$$

where the speed of sound, *a*, is:

$$a = \left[\frac{\gamma P}{\rho}\right]^{1/2} = 20.046796 (T_V + 273.15)^{1/2} \tag{66}$$

γ = ratio of specific heats for air

P = air pressure

ρ = air density = $\dfrac{0.003483678761 P}{T_V + 273.15}$ (67)

T_V = virtual temperature

NOTE: Values used in (66) and (67) referenced from STANAG 6022.

4.2. EQUATIONS OF MOTION FOR AIRCRAFT-DROPPED PALLETS

The equations of motion for aircraft-dropped pallets are described during five phases of the flight, namely, from rest to aircraft ramp, from aircraft ramp to aircraft exit, from aircraft exit to the end of free fall stabilization (main parachute deploy), main parachute inflation, and from the end of main parachute inflation to ground impact. These phases were chosen to represent those portions of the motion, which require significantly different force and moment descriptions to properly simulate actual flight conditions.

Coordinate Frames

All vectors have as a frame of reference a right-handed, orthonormal, Cartesian coordinate system. The origin of this coordinate system is the projected point on the ground of the nose of the carrier aircraft. The aircraft initial orientation is free in rotation about the X_2 (yaw) and X_3 (pitch) axis. No rotation is allowed about the X_1 axis (roll), and the aircraft is always assumed to have zero roll (wing parallel to the ground). Positive values are as defined in Part I – Equations of Motion for Projectiles and Rockets.

Positive Directions for Pallet Drop Coordinate Frame

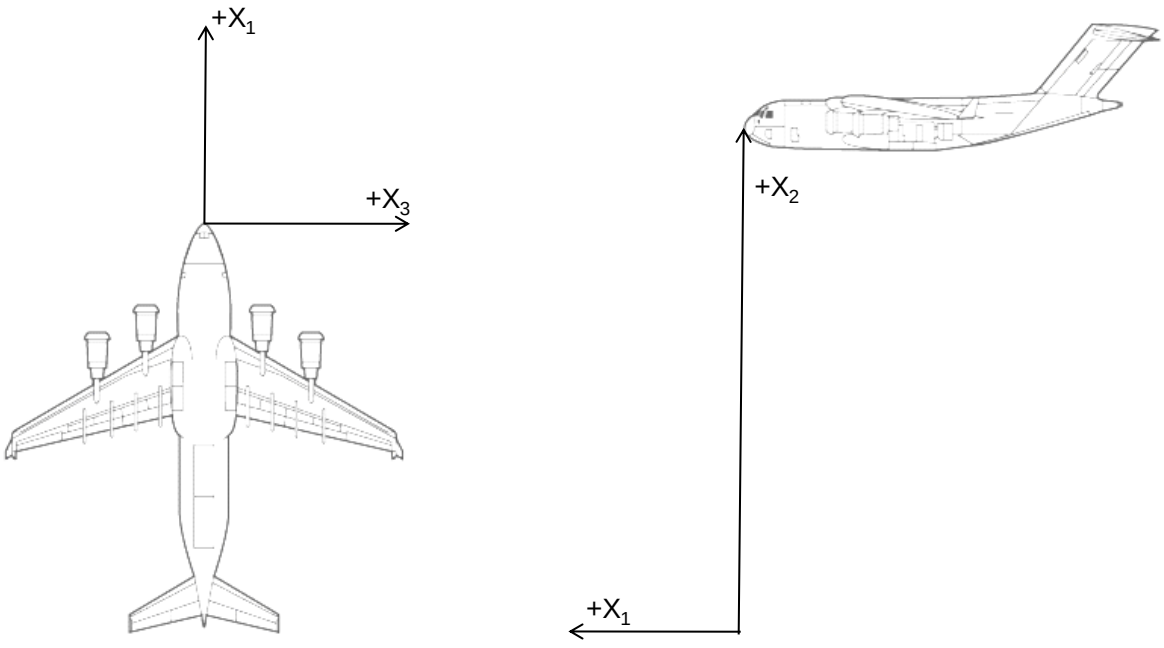

Phase 1: Time Zero to Time at Aircraft Ramp $(t_0 \le t \le t_{AR})$

From Rest to Aircraft Ramp

Phase begins at time zero, when the pallet first moves from rest at its starting station within the aircraft and ends when the pallet center of mass reaches the end of the cargo area. During this phase, the pallet motion is constrained to motion along the aircraft cargo deck.

Phase 1: Time Zero to Time of Aircraft Ramp

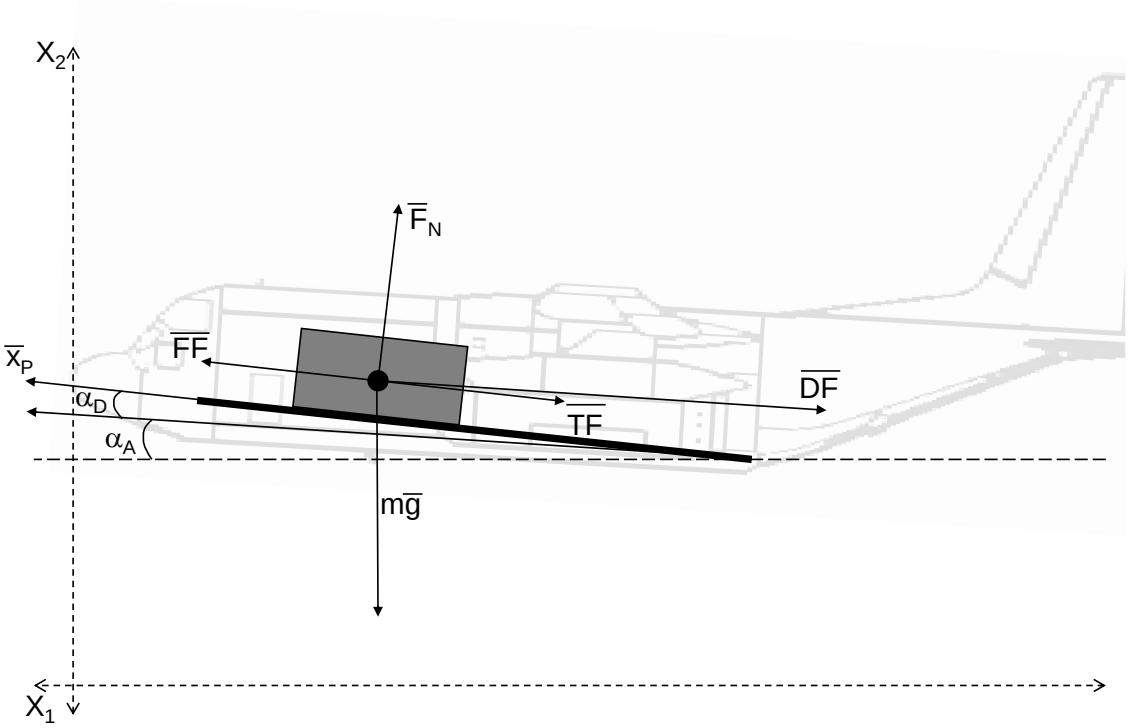

The initial position and acceleration of the center-of-mass, with-respect-to the ground-fixed axis, for a parachute-pallet system are as follows:

The initial position of the pallet with-respect-to the ground fixed coordinate frame is given by:

$$\vec{X}_0 = \begin{bmatrix} X_1 + L_i\left[\cos(\alpha_A + \alpha_D)\cos\Delta AZ\right] \\ X_2 + L_i \sin(\alpha_A + \alpha_D) \\ X_3 + L_i\left[\cos(\alpha_A + \alpha_D)\sin\Delta AZ\right] \end{bmatrix} \quad (68)$$

where:

$L_i =$ initial position, X_1 direction, of pallet within aircraft (69)

The drag force $\left(\overrightarrow{DF}\right)$ of the drogue parachute or the thrust force $\left(\overrightarrow{TF}\right)$ of personnel pushing the pallet, friction force between the pallet skid and the aircraft cargo deck $\left(\overrightarrow{FF}\right)$, normal force of aircraft acting upon the pallet, acceleration due to gravity, and acceleration due to Coriolis are considered during this phase. The pallet is initially at rest with-respect-to the aircraft and is resting on the aircraft cargo deck. The equation of motion of the center-of-mass of the pallet during this phase is given by:

$$\vec{F} = m\,\dot{\vec{u}} = \overrightarrow{DF} + \overrightarrow{TF} + \overrightarrow{FF} + \overrightarrow{F_N} + m\vec{g} + m\vec{\Lambda} \tag{70}$$

where:

mass of the pallet/parachute system is:

$$m = m_p + m_d + m_m \tag{71}$$

acceleration due to drogue parachute drag force is:

$$\frac{\overrightarrow{DF}}{m} = \left(\frac{\rho C_{D_0 D} S_{0D} i_D}{2m}\right) v\left(-\vec{v}\right) \tag{72}$$

where:

$C_{D_0 D} =$ coefficient of drag of drogue parachute
$S_{0D} =$ cross sectional area of drogue parachute
$i_D =$ drag form factor for drogue parachute

acceleration due to thrust force due to personnel pushing is:

$$\frac{\overrightarrow{TF}}{m} = \left(\frac{F_{MP}}{m}\right)\left(-\vec{x}_P\right) \tag{73}$$

where:

$F_{MP} =$ function of force applied by pushing. To be determined.
$\vec{x}_P =$ pallet movement unit vector defined as:

$$\vec{x}_P = \begin{bmatrix} \cos\left(\alpha_A + \alpha_D\right)\cos\Delta AZ \\ \sin\left(\alpha_A + \alpha_D\right) \\ \cos\left(\alpha_A + \alpha_D\right)\sin\Delta AZ \end{bmatrix} \tag{74}$$

where:

$\alpha_A =$ angle of aircraft body axis with-respect-to horizon
$\alpha_D =$ angle of aircraft cargo deck with-respect-to aircraft body axis

acceleration due to friction force between the pallet and aircraft cargo deck is:

$$\frac{\overrightarrow{FF}}{m} = \left(\frac{\mu_f F_N}{m} \right) \vec{x}_P \qquad (75)$$

where:

μ_f = coefficient of sliding friction (See Section 4.1.B)

$\vec{F}_N$ = normal force between the cargo deck and pallet, defined as:

$$\vec{F}_N = \left[\left(\overrightarrow{DF} + m\vec{g} \right) \cdot \left(-\vec{x}_N \right) \right] \vec{x}_N + \left[\left(\overrightarrow{DF} + m\vec{g} \right) \cdot \left(-\vec{x}_S \right) \right] \vec{x}_S \qquad (76)$$

Where the forces in the $\vec{x}_N$ (normal) direction prevent the pallet from falling through the aircraft floor, and the forces in the $\vec{x}_S$ (sideways) direction prevent the pallet from leaving the guide rails on the deck. $\vec{x}_S$ is perpendicular to both $\vec{x}_P$ and $\vec{x}_N$, defined as: $\vec{x}_S = \vec{x}_P \times \vec{x}_N$

and

$F_N \geq 0$

if normal force is negative, then the pallet leaves the deck, and the equations for this phase are not valid.

where:

$\vec{x}_N$ = normal unit vector, perpendicular to the plane of pallet movement with the positive direction pointing towards the aircraft ceiling.

$$\vec{x}_N = \begin{bmatrix} -\sin(\alpha_A + \alpha_D)\cos\Delta AZ \\ \cos(\alpha_A + \alpha_D) \\ -\sin(\alpha_A + \alpha_D)\sin\Delta AZ \end{bmatrix} \qquad (77)$$

acceleration due to gravity (g) is:
(See Section 4.1.C, Common Equations of Motion)

acceleration due to the Coriolis effect (Λ) is:
(See Section 4.1.C, Common Equations of Motion)

Phase 1 ends at time: $t = t_{AR}$ which is defined as the time when the center of mass of the pallet moves to the end of the aircraft cargo deck. The relative movement of the

cargo pallet with-respect-to the aircraft cargo deck must be tracked and the following assumptions must be made.

aircraft speed is constant and is equal to initial values defined as:

$$\dot{\vec{X}}_0 = \begin{bmatrix} \dot{X}_1 \\ \dot{X}_2 \\ \dot{X}_3 \end{bmatrix} \tag{78}$$

relative displacement pallet must move (with-respect-to starting position) to end the phase is given by:

$$L_{EP1} = L_D - L_i \tag{79}$$

<u>Phase 2:</u> Time from Aircraft Ramp to Time of Aircraft Exit $(t_{AR} \le t \le t_{AE})$

Phase begins when the pallet center of mass reaches the end of the cargo area and ends when the pallet center of mass reaches the end of the ramp. This allows for simulation of motion when the aircraft has a ramp oriented at a different angle than the floor of the aircraft cargo section. During this phase, the pallet motion is constrained to motion along the aircraft cargo ramp.

<u>Phase 2:</u> Time from Aircraft Ramp to Time of Aircraft Exit

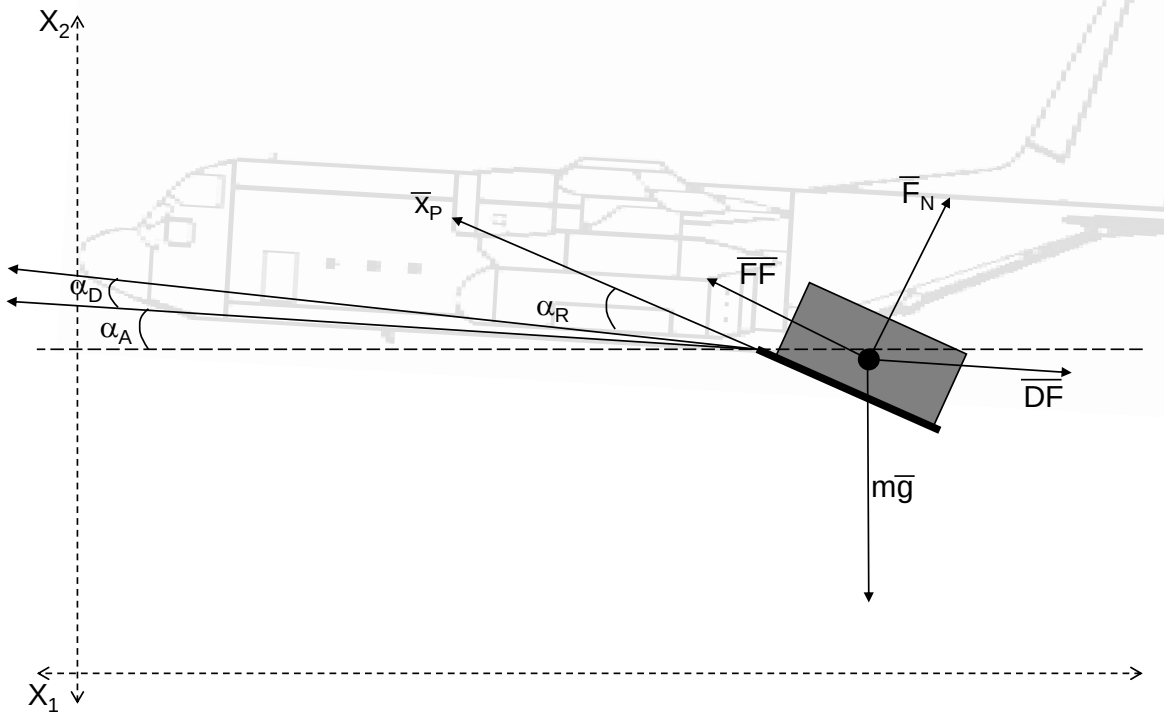

From Aircraft Ramp to Aircraft Exit

The position and acceleration of the center-of-mass, with-respect-to the ground-fixed axis, acceleration for a parachute-pallet system are as follows:

The drag force $\left(\overrightarrow{DF}\right)$ of the drogue parachute, friction force $\left(\overrightarrow{FF}\right)$ between the pallet skid and the aircraft cargo deck, and acceleration due to gravity are considered during this phase. The pallet has is moving on the aircraft cargo deck ramp. The equation of motion of the center-of-mass during this phase is given by Equation (70).

where:

mass of the pallet/parachute system is:
(See Equation 71)

acceleration due to drogue parachute drag force is:
(See Equation 72)

acceleration due to thrust force due to personnel pushing is:

$$\frac{\overrightarrow{TF}}{m} = 0 \tag{80}$$

acceleration due to friction force between the pallet and aircraft cargo deck is:
(See Equation 75)

where:

$\vec{x}_P$ = pallet movement unit vector defined as:

$$\vec{x}_P = \begin{bmatrix} \cos\left(\alpha_A + \alpha_D + \alpha_R\right)\cos\Delta AZ \\ \sin\left(\alpha_A + \alpha_D + \alpha_R\right) \\ \cos\left(\alpha_A + \alpha_D + \alpha_R\right)\sin\Delta AZ \end{bmatrix} \tag{81}$$

α_A = angle of aircraft body axis with-respect-to horizon
α_D = angle of aircraft cargo deck with-respect-to aircraft body axis
α_R = angle of aircraft cargo ramp axis with-respect-to aircraft cargo deck

and:

$\vec{x}_N$ = pallet movement normal unit vector defined as:

$$\vec{x}_N = \begin{bmatrix} -\sin(\alpha_A + \alpha_D + \alpha_R)\cos\Delta AZ \\ \cos(\alpha_A + \alpha_D + \alpha_R) \\ -\sin(\alpha_A + \alpha_D + \alpha_R)\sin\Delta AZ \end{bmatrix} \quad (82)$$

acceleration due to gravity (g) is:
(See Section 4.1.C, Common Equations of Motion)

acceleration due to the Coriolis effect (Λ) is:
(See Section 4.1.C, Common Equations of Motion)

Phase 2 ends at time: $t = t_{AE}$ which is defined as the time when the center of mass of the pallet moves to the end of the aircraft cargo ramp and exits the aircraft. The relative movement of the cargo pallet with-respect-to the aircraft cargo deck must be tracked and the following assumptions must be made.

aircraft speed is constant and is equal to initial values defined as:
(See Equation 78)

relative displacement pallet must move (with-respect-to starting position) to end the phase is given by:

$$L_{EP2} = L_{EP1} + L_R \quad (83)$$

<u>Phase 3:</u> Time of Aircraft Exit to Time of Main Parachute Deploy ($t_{AE} \le t \le t_P$)

When pallet reaches the end of the aircraft ramp, it is no longer constrained by the aircraft and is in a free fall stabilizing motion with either no parachute or the drogue parachute deployed.

Phase 3: Time of Aircraft Exit to Time of Main Parachute Deploy

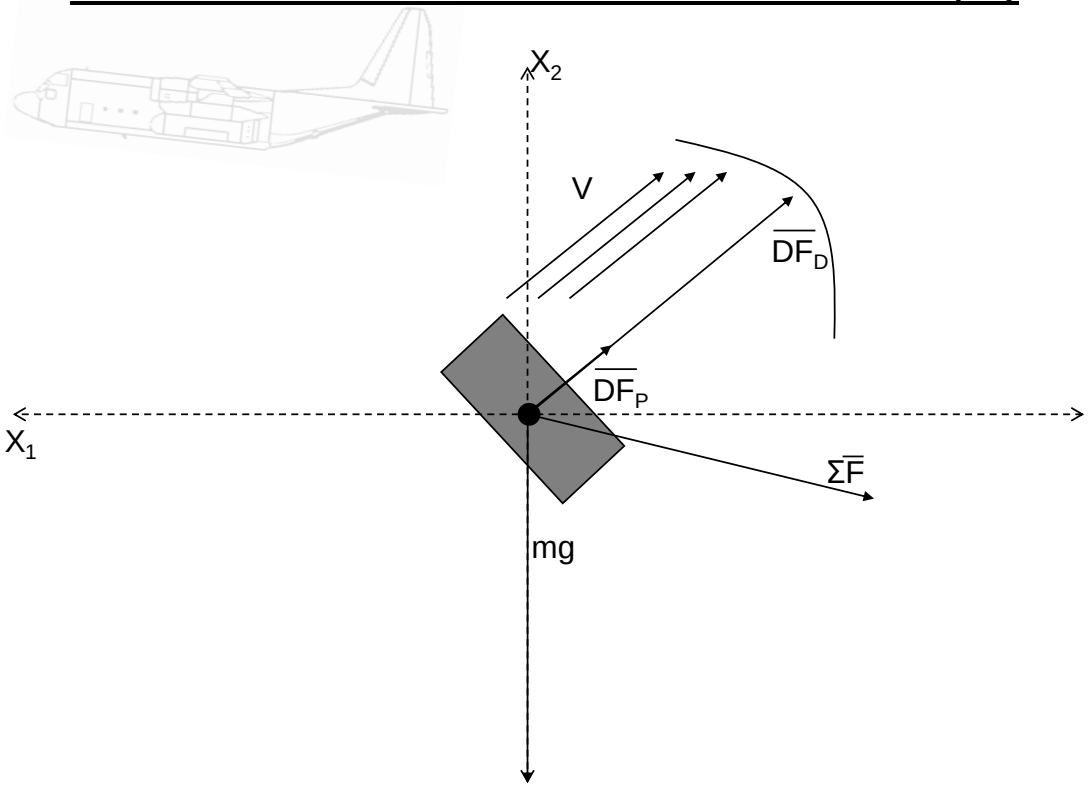

where:

$t_P = 8\text{sec}$

(best estimate, equation as a function of mass and altitude TBD)

Equation of Motion of the Center-of-Mass of the Body

The motion of the center-of-mass of the body is a summation of the accelerations acting on the body and is given by:

$$\vec{F} = m\,\dot{\vec{u}} = \overrightarrow{DF_P} + \overrightarrow{DF} + m\,\vec{g} + m\,\vec{\Lambda} \qquad (84)$$

where:
mass of the pallet/parachute system is:
(See Equation 71)

acceleration due to drag force of the pallet is:

$$\frac{\overrightarrow{DF_P}}{m} = \left(\frac{\rho C_{D_{0P}} S_{0P} i_P}{2m}\right) v\left(-\vec{v}\right) \qquad (85)$$

where:

$C_{D_0P} =$ drag coefficient of pallet

$S_{0P} =$ cross sectional area of pallet

$i_P =$ drag form factor of pallet

acceleration due to drag force of the drogue parachute is:
(See Equation 72)

acceleration due to gravity (g) is:
(See Section 4.1.C, Common Equations of Motion)

acceleration due to the Coriolis effect (Λ) is:
(See Section 4.1.C, Common Equations of Motion)

Phase 4: Time of Main Parachute Deploy to Time of Main Parachute Inflation ($t_P \le t \le t_M$)

Parachute-pallet system deploys main parachute after free-fall stabilization. Use aerodynamics for pallet without drogue parachute deployed and gradually include drag of main parachute as it unfolds and inflates. Phase ends when the main parachute is fully inflated.

Equation of Motion of the Center-of-Mass of the Body

The motion of the center-of-mass of the body is a summation of the accelerations acting on the body and is given by Equation 17:

where:

mass of the pallet/parachute system is:

$$m = m_p + m_m \tag{86}$$

acceleration due to drag force of the pallet is:
(See Equation 85)

acceleration due to drag force of the main parachute is:

$$\frac{\overrightarrow{DF}}{m} = \left(\frac{\rho C_{D_0MI} S_{0M} i_M}{2m} \right) v\left(-\vec{v}\right) \tag{87}$$

where:

$S_{0M} =$ cross sectional area of main parachute

$i_M =$ drag form factor of main parachute

$C_{D_0MI} =$ drag coefficient of main parachute during inflation

given by the equation:

$$C_{D_0MI} = 0 \qquad \text{for } (t_P \le t < t_P + t_{de}) \qquad (88a)$$

$$C_{D_0MI} = \frac{C_{D_0M}}{t_i}\{t - (t_P + t_{de})\} \qquad \text{for } (t_P + t_{de} \le t \le t_P + t_{de} + t_i) \qquad (88b)$$

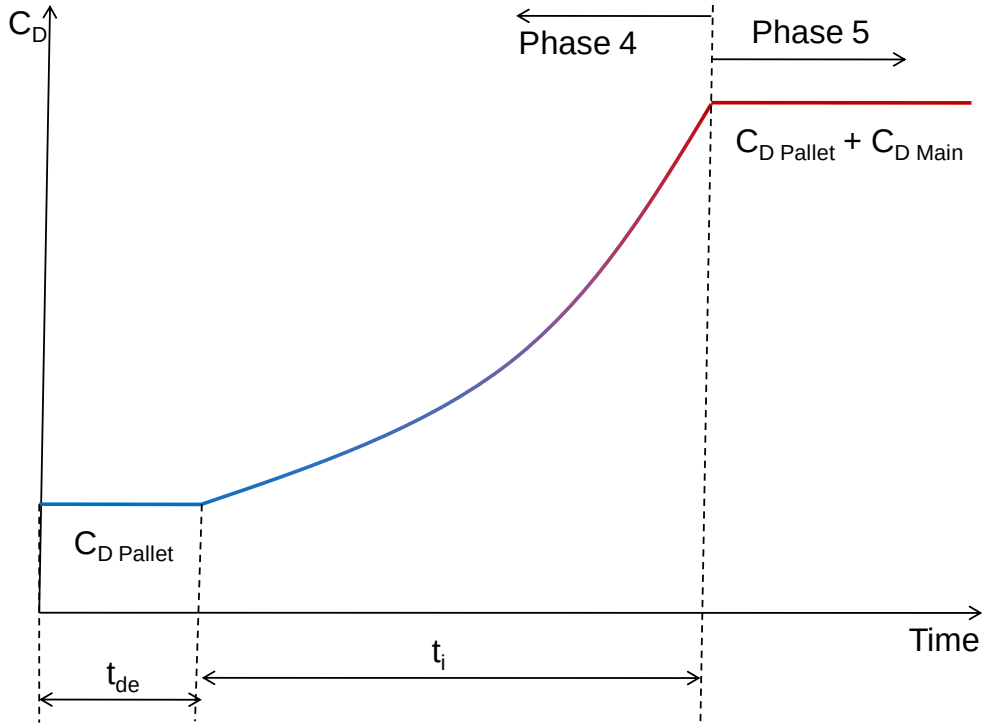

Time vs. Total Coefficient of Drag during Parachute Inflation

where:

t_{de} = time of delayed inflation (input)

t_i = time for main parachute inflation and is given by the equation:

$$t_i = \frac{2D_0}{3\pi V_s\left(\frac{9}{70} - \frac{C_e}{3}\right)} \qquad (89)$$

where:

$D_0 =$ circumferential diameter of the fully inflated parachute

$C_e =$ effective porosity of parachute fabric

$V_s =$ velocity at beginning of inflation ($t = t_P + t_{de}$)

acceleration due to gravity (g) is:

(See Section 4.1.C, Common Equations of Motion)

acceleration due to the Coriolis effect (Λ) is:
(See Section 4.1.C, Common Equations of Motion)

<u>Phase 5:</u> Time of Main Parachute Inflation to Time of Ground Impact ($t_M \leq t \leq t_G$)

Parachute-pallet system has main parachute fully inflated. Use aerodynamics for pallet with main parachute deployed. System is in a state of equilibrium at terminal velocity, perturbed only by changes in air density and wind speed and direction.

<u>Phase 5: Time of Parachute Deploy to Time of Ground Impact</u>

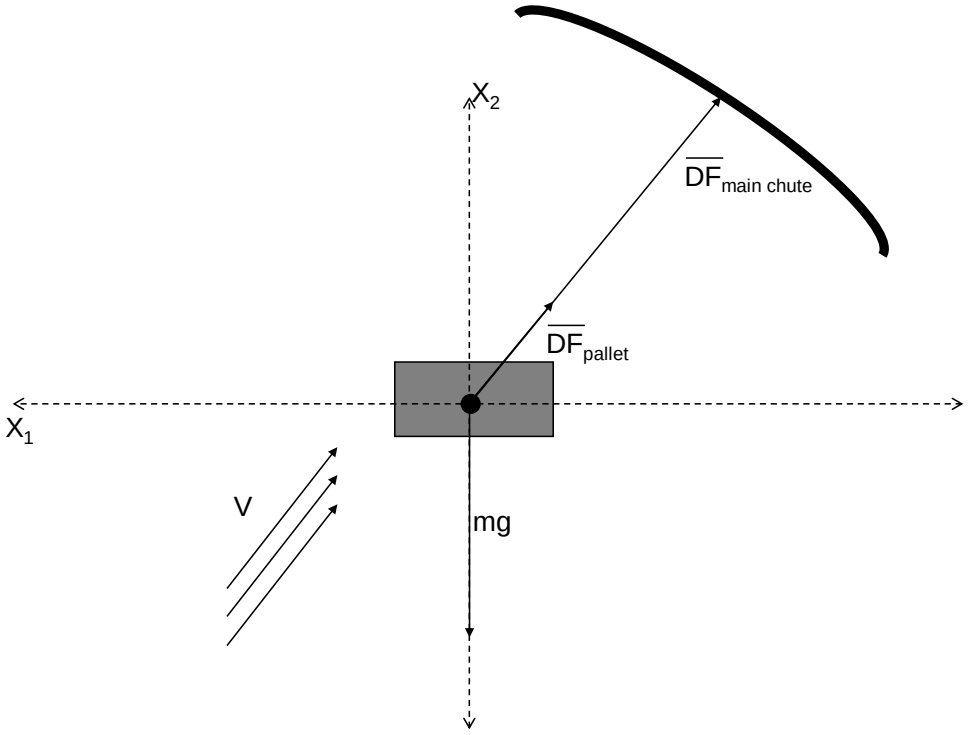

<u>Equation of Motion of the Center-of-Mass of the Body</u>

The motion of the center-of-mass of the body is a summation of the accelerations acting on the body and is given by Equation 84:

where:

mass of the pallet/parachute system is:
(See Equation 85)

acceleration due to drag force of the pallet is:
(See Equation 86)

acceleration due to drag force of the main parachute is:

$$\frac{\overrightarrow{DF}}{m} = \left(\frac{\rho C_{D_0 M} S_{0M} i_M}{2m} \right) v(-\vec{v}) \qquad (90)$$

where:

$C_{D_0 M}$ = drag coefficient of main parachute (fully inflated)

S_{0M} = cross sectional area of main parachute (fully inflated)

i_M = drag form factor of main parachute (fully inflated)

acceleration due to gravity (g) is:
(See Section 4.1.C, Common Equations of Motion)

acceleration due to the Coriolis effect (Λ) is:
(See Section 4.1.C, Common Equations of Motion)

Additional Data Requirements for Aircraft Dropped Cargo Pallets

(1) Physical Data	***Symbol***
Pallet mass	m_p
Drogue parachute or delay element mass	m_d
Main parachute mass	m_m
Total length of aircraft cargo deck	L_D
Total length of aircraft cargo ramp	L_R
Length (from initial position) to end phase 1	L_{EP1}
Length (from initial position) to end phase 2	L_{EP2}
Angle of aircraft body with-respect-to horizon	α_A
Initial aircraft position with-respect-to ground fixed coordinates	X_1, X_2, X_3
Initial pallet position with-respect-to ground fixed coordinates	$\vec{X}_0$
Initial pallet velocity with-respect-to ground fixed coordinates	$\dot{\vec{X}}_0$
Initial position, in X_1 direction, of pallet within aircraft	L_i
Angle of aircraft cargo deck with respect aircraft body	α_D
Cross sectional area of drogue parachute	S_{0D}
Drag form factor for drogue parachute	i_D
Angle of aircraft cargo ramp with respect aircraft cargo deck	α_R
Cross sectional area of pallet	S_{0P}
Drag form factor of pallet	i_P
Cross sectional area of main parachute	S_{0M}
Drag form factor of main parachute	i_M
Function of force applied by pushing. To be determined.	F_{MP}
Circumferential diameter of the fully inflated main parachute	D_0
Effective porosity of parachute fabric	C_e
Cross sectional area of main parachute (fully inflated)	S_{0M}

Drag form factor of main parachute (fully inflated)	i_M
Time of delayed inflation	t_{de}
Time of parachute opening	t_P

(2) Aerodynamic Data	***Symbol***
Drag coefficient of drogue parachute	C_{D_0D}
Drag coefficient of pallet	C_{D_0P}
Drag coefficient of main parachute during inflation	C_{D_0MI}
Drag coefficient of main parachute (fully inflated)	C_{D_0M}

4.3. LIST OF SYMBOLS

Symbol	Definition	Units
a	Local speed of sound in air	m/s
A_e	Exit area of the motor jet	m^2
$\overrightarrow{AJDM}$	Angular momentum due to axial jet damping moment	$kg\ m^2\ rad/s^2$
AZ	Azimuth (Bearing) of $\vec{1}$ axis measured clockwise from true North	mil *
C	Ballistic coefficient	kg/m^2
C_D	Drag force coefficient	*none*
C_{D_0}	Zero-yaw drag force coefficient	*none*
$C_{D_{\alpha^2}}$	Quadratic drag force coefficient	$1/rad^2$ **
$C_{D_{\alpha^4}}$	Quartic drag force coefficient	$1/rad^4$
C_{L_α}	Lift force coefficient	$1/rad$
$C_{L_{\alpha^3}}$	Cubic lift force coefficient	$1/rad^3$
$C_{L_{\alpha^5}}$	Quintic lift force coefficient	$1/rad^5$
C_{l_δ}	Fin cant moment coefficient	$1/rad$
C_{M_α}	Overturning moment coefficient	*none*
$C_{M_{\alpha^3}}$	Cubic overturning moment coefficient	$1/rad^2$
C_{mag-f}	Magnus force coefficient	$1/rad^2$

---

* 1 mil = 1/6400 of a circle = 2π/6400 radians.
** To aid in understanding, we use the symbol “rad” in place of the

	number 1 (one) for this dimensionless derived unit.	
C_{mag-m}	Magnus moment coefficient	*1/rad*
$C_{M_q} + C_{M_{\dot{\alpha}}}$	Pitch damping moment coefficient	*1/rad*
$C_{N_q} + C_{N_{\dot{\alpha}}}$	Pitch damping force coefficient	*1/rad*
C_{spin}	Spin damping moment coefficient	*none*
d	Reference diameter of projectile	*m*
$\overrightarrow{DF}$	Drag force	*kg m/s²*
$\vec{E}$	Position of the center of mass of the body with-respect-to spherical earth's surface	*m*
$\vec{F}$	Total force acting on the center of mass of the projectile or rocket	*kg m/s²*
f_D	Drag factor	*none*
f_L	Lift Factor	*none*
f_T	Thrust factor for rocket motor	*none*
$\overrightarrow{FCM}$	Angular momentum due to fin cant moment	$kg\ m^2\ rad/s^2$
$\vec{g}$	Acceleration due to gravity	*m/s²*
g_0	Magnitude of acceleration due to gravity at mean sea level	*m/s²*
$\vec{H}$	Total angular momentum of the body	$kg\ m^2\ rad/s$
$\dot{\vec{H}}$	Rate of change of the total angular momentum of the body	$kg\ m^2\ rad/s^2$
$\vec{H}_{(t_L)}$	Total angular momentum of the body at t_L	$kg\ m^2\ rad/s$
I_{SP}	Specific impulse of rocket motor fuel	$N\ s/kg$

I_x	Axial moment of inertia	$kg\ m^2$
$I_{X_{(t_L)}}$	Axial moment of inertia of the rocket at (t_L)	$kg\ m^2$
I_Y	Transversal moment of inertia of the body	$kg\ m^2$
$I_{Y_{(t_L)}}$	Transversal moment of inertia of the rocket at (t_L)	$kg\ m^2$
i	Form factor	*none*
l_W	Distance from weapon trunnion to muzzle	m
lat	Latitude of launch point; for southern hemisphere lat is negative	*deg*
$\overrightarrow{LF}$	Lift force	$kg\ m/s^2$
m	Fuzed projectile or rocket mass at time t	kg
$\dot{m}$	Fuzed projectile or rocket mass rate of change at time t	kg/s
$\dot{m}_f$	Mass flow rate of the motor fuel	kg/s
m_r	Reference fuzed projectile or rocket mass	kg
M	Local Mach number	*none*
$\overrightarrow{MF}$	Magnus Force	$kg\ m/s^2$
$\overrightarrow{MM}$	Angular momentum due to Magnus moment	$kg\ m^2\ rad/s^2$
$\overrightarrow{OM}$	Angular momentum due to overturning moment	$kg\ m^2\ rad/s^2$
p	Axial spin rate of projectile	*rad/s*
p_0	Initial spin rate of projectile	*rad/s*
$p_{(t_L)}$	Axial spin rate of rocket at t_L	*rad/s*
P	Local atmospheric air pressure	*Pa*
P_r	Standard atmospheric air pressure at sea level	*Pa*

	$(1.01325 \times 10^5$ Pa)	
$\overrightarrow{PDF}$	Pitch damping force	N
$\overrightarrow{PDM}$	Angular momentum due to pitch damping moment	$kg\ m^2\ rad/s^2$
Q_D	Yaw drag fitting factor	*none*
QE	Quadrant elevation	*mil*
Q_M	Magnus force fitting factor	*none*
$\vec{R}$	Position of the center of the sphere, locally approximating the geoid	m
R	Radius of the sphere, locally approximating the geoid	m
$\vec{r}$	Position of the center of mass of the projectile or rocket with respect to the center of the sphere, locally approximating the geoid	m
r	Distance of the center of mass of the projectile or rocket from the center of the sphere, locally approximating the geoid	m
r_e	Distance from the body center-of-mass to the motor nozzle exit	m
r_{ne}	Radius of the motor's mass flow exit	m
r_t	Distance from the body center-of-mass to the motor nozzle throat	m
$\overrightarrow{SDM}$	Angular momentum due to spin damping moment	$kg\ m^2\ rad/s^2$
t	Time variable (computed time of flight)	s
t_c	Twist of rifling at muzzle	*calibers/rev*
t_{FM}	Time of first rocket motion	s
t_L	Time at end of rocket launch phase	s

t_{FO}	Time at rocket fin opening	s
t_{E5D}	Time at end of 5DOF phase for rockets	s
$\overrightarrow{TF}$	Thrust force due to rocket motor thrust	N
$\overrightarrow{TJDM}$	Angular momentum due to transverse jet damping moment	$kg\ m^2\ rad/s^2$
T_V	Virtual temperature	$°C$
t_0	Time zero (beginning of calculations)	s
$\vec{u}$	Velocity of the projectile or rocket with-respect-to ground-fixed axes	m/s
$\dot{\vec{u}}$	Acceleration of center-of-mass in the fixed coordinate system	m/s^2
u_0	Initial speed of projectile or rocket with-respect-to ground-fixed axes	m/s
v	Speed of projectile or rocket with-respect-to air	m/s
$\vec{v}$	Velocity of the projectile or rocket with-respect-to air	m/s
$\vec{w}$	Velocity of the air with-respect-to the ground (wind velocity)	m/s
$\vec{x}$	Unit vector along longitudinal axis of the rigid body	$none$
$\vec{x}_0$	Unit vector along longitudinal axis of the rigid body, Initially	$none$
$\vec{x}_{(t_L)}$	Unit vector along longitudinal axis of the rigid body, at t_L	$none$
$\dot{\vec{x}}$	Rate of change of unit vector along longitudinal axis of the body	rad/s
$\vec{X}$	Position vector of the center of mass of the projectile or	m

	rocket in the ground-fixed coordinate system	
$\vec{X}_0$	Initial position vector of the center of mass of the projectile or rocket	*m*
X_{2_w}	Height of weapon trunnion above mean sea level	*m*
α	Total angle of attack	*rad*
$\vec{\alpha}_e$	Yaw of repose approximation	*rad*
ΔAZ	Difference between the weapon azimuth (bearing) and the $\vec{1}$ axis measured clockwise	*mil*
Δt	Integration time step	*s*
$\Delta\vec{w}$	Difference in wind speed between the integration steps	*m/s*
$\Delta\vec{u}$	Velocity correction for windage jump	*m/s*
ε	Fin cant angle	*rad*
γ	Ratio of specific heats of air, 1.4	*none*
$\vec{\Lambda}$	Acceleration due to Coriolis effect	m/s^2
μ_f	Coefficient of sliding friction	*none*
ρ	Density (specific mass) of air	kg/m^3
ψ	Orientation of the yaw	*rad*
$\vec{\omega}$	Angular velocity of the coordinate system due to the angular speed of the earth	*rad/s*
$\omega_{y_{(t_L)}}$	Transverse angular velocity of the body at (t_L) about an axis perpendicular to the quadrant elevation of the weapon in the vertical plane.	*rad/s*
$\omega_{z_{(t_L)}}$	Transverse angular velocity of the body at (t_L) in the vertical plane containing the weapon.	*rad/s*

Ω	Angular speed of the earth	*rad/s*
$\bullet$	Denotes differentiation with-respect-to time when appears over variable or function	s^{-1}
$\rightarrow$	Denotes vector when appears over variable	*none*

4.4. COMPARISON OF AERODYNAMIC COEFFICIENT SYMBOLS

Three different conventions have been widely used to describe the aerodynamic coefficients associated with the force and moment system used to describe the motion of the center of mass of a projectile. Table 4-1 provides a concise comparison of the symbols. The first column lists the aerodynamic coefficient symbols used throughout this document. These symbols are associated with a drag force and lift force whose directions are defined with-respect-to the velocity vector of the center of mass of the shell and perpendicular to that vector (in the plane of yaw) respectively. The NACA symbols are associated with axial drag and normal forces whose directions are defined with-respect-to the axis of the shell and perpendicular to that axis (also in the plane of yaw) respectively. Consequently a rotational transformation is necessary to completely relate these two sets of symbols:

$$C_{D_0} = C_{x_0} \tag{91}$$

$$C_{D_{\alpha^2}} = C_{x_{\alpha^2}} + C_{z_\alpha} - \frac{1}{2} C_{x_0} \tag{92}$$

$$C_{L_\alpha} = C_{z_\alpha} - C_{x_0} \tag{93}$$

$$C_{L_{\alpha^3}} = C_{z_{\alpha^3}} - \frac{1}{2} C_{z_\alpha} - C_{x_{\alpha^2}} \tag{94}$$

The ballistic symbols shown have been slightly modernized to account for the fact that the original set of symbols did not allow for some of the dependence of the aerodynamic forces on yaw angle. The same logic as that used by the aeronautical community was applied to affix the subscripts *0*, α, α^2 and α^3 to the original symbols.

NOTE: Equations (92) and (94) use the small angle assumption $\cos\alpha = (1 - \sin^2\alpha)^{1/2}$ approximately equal to $1 - \frac{1}{2}\alpha^2$. If instead one assumes $\cos\alpha$ is approximately equal to 1, then (92) and (94) become $C_{D_{\alpha^2}} = C_{x_{\alpha^2}} + C_{z_\alpha}$ and $C_{L_{\alpha^3}} = C_{z_{\alpha^3}}$, respectively. If one uses higher order coefficients, such as $C_{D_{\alpha^4}}$ and $C_{L_{\alpha^5}}$, (92) and (94) may still be used with a negilable effect on precision. The axial drag force and the drag force, $\overrightarrow{DF}$, used in this STANAG are assumed to act in the same direction.

Table 4-1. Aerodynamic Coefficient Symbols

Symbol	***Other Symbols***		***C-to-K Relationship***	***Definition***
	NACA	***Ballistic***		
C_{D_0}	C_{x_0}	K_{D_0}	$K_{D_0} = \frac{\pi}{8} C_{D_0}$	Drag force coefficient
$C_{D_{\alpha^2}}$	$C_{x_{\alpha^2}}$	$K_{D_{\alpha^2}}$	$K_{D_{\alpha^2}} = \frac{\pi}{8} C_{D_{\alpha^2}}$	Quadratic yaw drag force coefficient
$C_{D_{\alpha^4}}$	$C_{x_{\alpha^4}}$	$K_{D_{\alpha^4}}$	$K_{D_{\alpha^4}} = \frac{\pi}{8} C_{D_{\alpha^4}}$	Quartic yaw drag force coefficient
C_{L_α}	$-C_{z_\alpha}$	K_{L_α}	$K_{L_\alpha} = \frac{\pi}{8} C_{L_\alpha}$	Lift force coefficient
$C_{L_{\alpha^3}}$	$C_{z_{\alpha^3}}$	$K_{L_{\alpha^3}}$	$K_{L_{\alpha^3}} = \frac{\pi}{8} C_{L_{\alpha^3}}$	Cubic lift force coefficient
$C_{L_{\alpha^5}}$	$C_{z_{\alpha^5}}$	$K_{L_{\alpha^5}}$	$K_{L_{\alpha^5}} = \frac{\pi}{8} C_{L_{\alpha^5}}$	Quintic lift force coefficient
C_{M_α}	C_{M_α}	K_{M_α}	$K_{M_\alpha} = \frac{\pi}{8} C_{M_\alpha}$	Overturning moment coefficient
$C_{M_\alpha{}^3}$	$C_{M_\alpha{}^3}$	$K_{M_\alpha{}^3}$	$K_{M_\alpha{}^3} = \frac{\pi}{8} C_{M_{\alpha^3}}$	Cubic overturning moment coefficient
C_{mag-f}	$C_{y_{p\alpha}}$	K_F	$K_F = -\frac{\pi}{8} C_{mag-f}$	Magnus force coefficient
C_{mag-m}	$C_{n_{p\alpha}}$	K_T	$K_T = -\frac{\pi}{8} C_{mag-m}$	Magnus moment coefficient
$(C_{N_q} + C_{N_{\dot\alpha}})$	$(C_{Z_q} + C_{Z_{\dot\alpha}})$	K_S	$K_S = -\frac{\pi}{8} (C_{N_q} + C_{N_{\dot\alpha}})$	Damping force coefficient
$(C_{M_q} + C_{M_{\dot\alpha}})$	$(C_{m_q} + C_{m_{\dot\alpha}})$	K_H	$K_H = -\frac{\pi}{8} (C_{M_q} + C_{M_{\dot\alpha}})$	Damping moment coefficient
C_{spin}	C_{l_p}	K_A	$K_A = -\frac{\pi}{8} C_{spin}$	Spin damping moment coefficient
C_{l_δ}	*none*	K_E	$K_E = \frac{\pi}{8} C_{l_\delta}$	Fin cant coefficient

NOTE: Special symbols $C_{mag\text{-}f}$ and C_{spin} are defined in place of $C_{Np\alpha}$ and C_{lp} to avoid possible confusion where these symbols have been used differently in published data (notably in the UK and US), where:

$C_{mag\text{-}f} = C_{N_{p\alpha}}$ for data nondimensionalized using *pd/v* (95a)

$= (1/2)\ C_{y_{p\alpha}}$ for data nondimensionalized using *pd/2v* (95b)

$C_{mag-m} = C_{M_{p\alpha}}$ for data nondimensionalized using *pd*/*v* (96a)

$= (1/2)\, C_{n_{p\alpha}}$ for data nondimensionalized using *pd*/2*v* (96b)

$C_{spin} = C_{l_p}$ for data nondimensionalized using *pd/v* (97a)

$= (1/2)\ C_{l_p}$ for data nondimensionalized using *pd/2v* (97b)

4.5 LIST OF DATA REQUIREMENTS

Physical Data Requirements	***Fin-Stabilized***	***Spin-Stabilized***
Initial speed of projectile with-respect-to ground (muzzle velocity)	u_0	u_0
Twist of rifling at muzzle		t_c
Initial mass of fuzed projectile	m_0	m_0
Reference mass of fuzed projectile	m_r	m_r
Reference diameter	d	d
Initial axial moment of inertia	I_{x_0}	I_{x_0}
Axial spin rate of rocket at (t_L)	$p_{(t_L)}$	
Axial moment of inertia at (t_L)	$I_{X_{(t_L)}}$	
Initial transverse moment of inertia	I_{Y_0}	
Transverse moment of inertia at (t_L)	$I_{Y_{(t_L)}}$	
Specific impulse of rocket fuel	I_{SP}	
Mass flow rate of the motor fuel	$\dot{m}_f$	
Coefficient of friction	μ_f	
Fin cant angle	ε	
Distance from body center of mass to motor nozzle exit	r_e	
Radius of motors mass flow exit	r_{ne}	
Distance from body center of mass to motor nozzle throat	r_t	

Aerodynamic Data Requirements	***Fin-Stabilized***	***Spin-Stabilized***
Zero yaw drag force coefficient	C_{D_0}	C_{D_0}
Quadratic yaw drag force coefficient	$C_{D_{\alpha^2}}$	$C_{D_{\alpha^2}}$
Quartic yaw drag force coefficient		$C_{D_{\alpha^4}}$
Total drag force coefficient	C_D	
Lift force coefficient	C_{L_α}	C_{L_α}
Cubic lift force coefficient	$C_{L_{\alpha^3}}$	$C_{L_{\alpha^3}}$
Quintic lift force coefficient		$C_{L_{\alpha^5}}$
Magnus force coefficient	$C_{mag\text{-}f}$	$C_{mag\text{-}f}$
Overturning moment coefficient	C_{M_α}	C_{M_α}
Cubic overturning moment coefficient	$C_{M_{\alpha^3}}$	$C_{M_{\alpha^3}}$
Spin damping moment coefficient	C_{spin}	C_{spin}
Magnus moment coefficient	C_{mag-m}	
Pitch damping moment coefficient	$C_{M_q} + C_{M_{\dot{\alpha}}}$	
Pitch damping force coefficient	$C_{N_q} + C_{N_{\dot{\alpha}}}$	
Fin cant moment coefficient	C_{l_δ}	

NOTE: Aerodynamic coefficients for fin-stabilized rockets are required for both the fin closed and fin open configurations.

Fitting Factor Data Requirement	***Fin-Stabilized***	***Spin-Stabilized***
Quadrant Elevation Fitting		
Form Factor	i	i
Ballistic Coefficient		C
Mach Number Fitting		
Thrust Factor	f_T	
Drag Factor		f_D
Quadrant Elevation and Mach Number Fitting		
Adjustment to azimuth – difference between actual and computed deflection – for fin-stabilized rockets	$\Delta(\Delta AZ)$	
Lift Factor	f_L	f_L
Yaw Drag Factor		Q_D
Magnus Factor		Q_M
Exit area of motor jet	A_e	
Transverse vertical angular velocity of the body at (t_L)	$\omega_{y_{(t_L)}}$	
Transverse horizontal angular velocity of the body at (t_L)	$\omega_{z_{(t_L)}}$	
Adjustment to time-of-flight – difference between actual and computed time-of-flight	ΔToF	ΔToF

CHAPTER 5 IMPLEMENTATION OF THE AGREEMENT

This STANAG is implemented when a nation has issued instructions to the agencies concerned to use the Lieske Modified Point Mass Trajectory Model for spin-stabilized projectiles and a Five Degrees of Freedom Model for exterior ballistic trajectory simulation of fin-stabilized rockets as detailed in this agreement.

ANNEX A FORMS OF FIRE CONTROL INPUT DATA

1. Aerodynamic coefficients

Aerodynamic coefficients are given as a function of Mach number. These functions are in the form of polynomials of fourth degree or less. They are defined over regions of Mach number, from $M_{MAX_{i-1}}$ up to and including M_{MAX_i}.

Each aerodynamic coefficient is described by a series of polynomials of the form:

$$C_i = a_0 + a_1 M + a_2 M^2 + a_3 M^3 + a_4 M^4 \qquad \text{(A.1)}$$

C_i is a particular aerodynamic coefficient
M is Mach number

2. Fitting Factor:
   a. Functions of Quadrant Elevation

Form factor (i) or ballistic coefficient (C) and lift factor (f_L) are given for each charge as follows:

$$f = a_0 + a_1(QE) + a_2(QE)^2 + a_3(QE)^3 \qquad \text{(A.2)}$$

where $f = i$, C, or f_L

Yaw drag factor (Q_D) and Magnus force factor (Q_M) have been chosen as constants. (See Table A-1)

   b. Functions of Mach Number:

Drag factor (f_D) and lift factor (f_L) are quartic polynomials of Mach number. Yaw drag factor (Q_D) and Magnus force factor (Q_M) have been chosen as constants. (See Table A-1)

   c. Function of Computed Time

The modeling of time used in this document may require a correction to the computed time of flight for each charge as follows:

$$T = t + a_0 + a_1 t + a_2 t^2 + a_3 t^3 \qquad \text{(A.3)}$$

T is time of flight
t is computed time of flight

FACTORS IN EQUATIONS FOR MATCHING OBSERVED RANGE FIRING DATA

Two fitting systems are used, quadrant elevation or Mach number as shown below:

Table A-1. Basic Fitting Data

Fitting to	***Fitting Data as a Function of***	
	Quadrant Elevation [One function for each charge]	***Mach Number [Same function for all charges]***
First order range, all elevations	*Form factor: i (Drag factor: $f_D = 1$)	Drag factor: f_D (Form factor: $i = 1$)
Drift	Lift factor: f_L	Lift factor: f_L
Second order range, high angle	Yaw drag factor: Q_D	Yaw drag factor: Q_D
Vertex height and time of flight	Magnus force factor: Q_M	Magnus force factor: Q_M

*In many countries a ballistic coefficient, $C = m_r / i\, d^2$, is in use as a fitting factor instead of the non-dimensional form factor *i*.

To compensate for the approximations in the equations of motion, aerodynamic coefficients, rocket, projectile, rocket-assisted motor, and base burn motor performance, the factors contained in Table A-2 are applied in order to create correspondence between the computed and the observed range testing results.

Table A-2. Fitting factors for matching observed range firing data

Range Firing Data	***Fitting Factors***			
	5 DoF	***Modified Point Mass***		
	Fin-Stabilized Rockets	***Projectiles***	***Rocket-Assisted Projectiles***	***Base-Burn Projectiles***
Motor Burn Time	$f_{BT_p} \equiv 0$ $f_{BT_P} \equiv 0$	$f_{BT_p} \equiv 0$ $f_{BT_P} \equiv 0$	$f_{BT_p}{}^{*}$ $f_{BT_P} \equiv 0$	f_{BT_p} f_{BT_P}
Velocity After Rocket Burning Change in Radial Velocity During Rocket Burning	f_T A_e	$f_T \equiv 0$ $A_e \equiv 0$	f_T A_e	$f_T \equiv 0$ $A_e \equiv 0$
Velocity Vertical and Horizontal Angle after Rocket Burning	$\omega_{y(t_L)}$ $\omega_{z(t_L)}$			
Range	i $f(i_{BB,MT}) \equiv 0$	i $f(i_{BB,MT}) \equiv 0$	i $f(i_{BB,MT}) \equiv 0$	i $f(i_{BB,MT})$
Deflection	$\Delta(\Delta AZ)$ $f_L \equiv 1$	$\Delta(\Delta AZ) \equiv 0$ f_L	$\Delta(\Delta AZ) \equiv 0$ f_L	$\Delta(\Delta AZ) \equiv 0$ f_L
Time-of-Flight	ΔToF	ΔToF	ΔToF	ΔToF

*Optional

NOTE: See Annex C or D for further fitting factors for base-burn and rocket-assisted projectiles

3. Fuze Setting

Fuze setting is given as a function of time of flight and initial spin as follows:

$$FS = a_0 + a_1 T + a_2 p_0 + a_3 T p_0 + a_4 T {p_0}^2 + a_5 {p_0}^2 \quad \text{(A.4)}$$

or,

$$FS = \frac{T + a_0 + a_2 p_0}{b_0 + b_1 p_0} \quad \text{(A.5)}$$

FS is fuze setting
T is time of flight
p_0 is initial axial spin of projectile

4. Muzzle Velocity Corrections

a. Muzzle Velocity Correction for Propellant Temperature

Muzzle velocity correction for propellant temperature is given for each charge as follows:

$$\Delta U_{pt} = a_0 + a_1(PT - 21) + a_2(PT - 21)^2 + a_3(PT - 21)^3 \quad \text{(A.6)}$$

ΔU_{pt} is incremental change in muzzle velocity
PT is propellant temperature

b. Muzzle Velocity Correction for Cannon (Tube) Wear

The muzzle velocity correction for cannon (tube) wear for a specific charge/projectile/cannon combination is given by

$$\Delta U_w = \frac{\Delta U_r (a_0 + a_1(EFC) + a_2(EFC)^2)}{a_{0,i} + a_{1,i}(EFC) + a_{2,i}(EFC)^2 + a_{3,i}(EFC)^3} \quad \text{(A.7)}$$

ΔU_w is incremental change in muzzle velocity

$\Delta U_r(EFC)$ is incremental change in muzzle velocity for the reference charge, i.e., the maximum charge compatible with the projectile/cannon combination evaluated at the current EFC count.

EFC is the current number of Equivalent Full Charge firings from the cannon.

$a_{0,i}$, $a_{1,i}$, $a_{2,i}$ are the coefficients required to calculate the ratio of the incremental change in muzzle velocity for the reference change (ΔU_r) to the corresponding incremental change in muzzle velocity for the i^{th} charge at the specified EFC. This ratio is derived from the interior ballistics models or actual firing trials.

c. Muzzle Velocity Correction for Projectile Mass

Muzzle velocity correction for projectile mass is given for each charge as follows:

$$\Delta U_m = n_i U_i (m - m_r)/m_r \quad \text{(A.8)}$$

ΔU_m is incremental change in muzzle velocity

n_i is a constant factor derived from interior ballistic models or projectile mass firings

U_i is firing table muzzle velocity for the i^{th} charge corrected for calibration, propellant temperature and cannon wear

m is fuzed projectile mass

m_r is reference mass of fuzed projectile

5. List of Additional Symbols for Forms of Fire Control Data

Symbol	Definition	Units
a_i	Constant coefficient	*none*
b_i	Constant coefficient	*none*
FS	Fuze setting	*none*
n	Constant coefficient	*none*
PT	Propellant temperature	^oC

T	Time of flight	*s*
U	Firing table muzzle velocity	*m/s*
ΔU_m	Change in muzzle velocity due to nonstandard Projectile mass	*m/s*
ΔU_{pt}	Change in muzzle velocity due to nonstandard Propellant temperature	*m/s*
ΔU_w	Change in muzzle velocity due to cannon (tube) wear	*m/s*
$\Delta(\Delta AZ)$	Adjustment to azimuth – difference between actual and computed deflection – for fin-stabilized rockets	*mil*

ANNEX B ADDITIONAL TERMS FOR PROJECTILES WITH BOURRELET NUBS

The presence of nubs introduces terms in the expressions for certain of the aerodynamic forces and moments, which are proportional to the nub setting angle and independent of the spin rate.

1. Equations of Motion

Define $C_{mag\text{-}f}$ and C_{spin} as follows:

$$C_{mag-f} = C_{N_{p\alpha}} + C_{N_{\delta_n}}\ \delta_n /(pd/v) \quad \text{for data nondimensionalized using } pd/v \quad \text{(B.1)}$$

$$= [C_{y_{p\alpha}} + C_{y_{\delta_n}}\ \delta_n /(pd/2v)]/2 \quad \text{for data nondimensionalized using } pd/2v \quad \text{(B.2)}$$

$$C_{spin} = C_{l_p} + C_{l_{\delta_n}}\ \delta_n /(pd/v) \quad \text{for data nondimensionalized using } pd/v \quad \text{(B.3)}$$

$$= [C_{l_p} + C_{l_{\delta_n}}\ \delta_n /(pd/2v)]/2 \quad \text{for data nondimensionalized using } pd/2v \quad \text{(B.4)}$$

2. List of Additional Symbols

Symbol	Definition	Units
$C_{l_{\delta_n}}$	Spin moment coefficient, due to canted bourrelet nubs, at zero spin	*1/rad*
$C_{N_{\delta_n}}$ or $C_{y_{\delta_n}}$	Side force coefficient, due to canted bourrelet nubs, at zero spin	*1/rad*
δ_n	Orientation of nub principal axis with-respect-to a plane containing the projectile axis and the nub geometrical center. Positive δn produces a positive rolling moment.	*rad*

3. Additional Data Requirements

Physical Data	***Symbol***
Nub orientation	δ_n

Aerodynamic Data	***Symbol***
Spin moment coefficient at zero spin	$C_{l_{\delta_n}}$
Side force coefficient at zero spin	$C_{N_{\delta_n}}$ or $C_{y_{\delta_n}}$

ANNEX C ADDITIONAL TERMS FOR SPIN-STABILIZED ROCKET-ASSISTED PROJECTILES, SPIN-STABILIZED BASE-BURN PROJECTILES, AND FIN-STABILIZED ROCKETS – METHOD 1

1. Introduction

This annex provides the equations required to simulate the flight of rocket-assisted projectiles and the specific equations required to simulate the flight of base-burn projectiles and fin-stabilized rockets.

2. Additional Terms for Spin-Stabilized Rocket-Assisted Projectiles

a. Add the following thrust term to the equation of motion of the center of mass of the projectile shown at Eq. (1):

$$\frac{\overrightarrow{TF}}{m} = \frac{T^*}{m}\left(\frac{\vec{v}\cos\alpha_e}{v} + \vec{\alpha}_e\right) \tag{C.1}$$

b. Zero yaw drag coefficient during the burning phase ($t_{DI} \le t \le t_B$) is $C_{D_{0_T}}$.

c. Thrust during the burning phase ($t_{DI} \le t \le t_B$) is as follows:

$$T^* = f_T T_R + (P_r - P)A_e, \tag{C.2}$$

where:

$$T_R = T_{ST}\left(t_{DI_{ST}} - t_{B_{ST}}\right)/(t_{DI} - t_B), \tag{C.3}$$

and

$$t^* = (t - t_{DI})\left[\left(t_{DI_{ST}} - t_{B_{ST}}\right)/(t_{DI} - t_B)\right] + t_{DI_{ST}} \tag{C.4}$$

d. Mass of the projectile is given by:

mass at $t = 0$ is $m = m_0$ (C.5)

for $t < t_{DI}$

$$\dot{m} = -m_{DI} / t_{DI} \quad \text{(C.6)}$$

mass at $t = t_{DI}$ is $m = m_0 - m_{DI} - m_{DOB}$ (C.7)

for $t_{DI} \leq t < t_B$

$$\dot{m} = -T_R / I_{SP} \quad \text{(C.8)}$$

for $t \geq t_B$

$$\dot{m} = 0 \quad \text{(C.9)}$$

$$m = m_B \quad \text{(C.10)}$$

where:

$$m_B = m_0 - m_{DI} - m_{DOB} - m_f \quad \text{(C.11)}$$

3. Additional Terms for Spin-Stabilized Base-Burn Projectiles

a. The change in acceleration due to the base drag reduction of a base-burn motor, $\overrightarrow{BB}$, during burning ($t_{DI} \leq t$ and $m \geq m_B$) is added to the equation of motion of the center of mass of the projectile which follows from Equation (1) of the main body of this STANAG:

$$\overrightarrow{BB} = -\left[\frac{\left(\frac{\pi}{8}\right)\rho\, d^2\, v^2\, C_{x_{BB}}\, f(I)\, f(i_{BB}, MT)}{m}\right]\left(\frac{\vec{v}\cos\alpha_e}{v} + \vec{\alpha}_e\right) \quad \text{(C.12)}$$

b. The coefficient $C_{x_{BB}}$ is the drag reduction coefficient during the burning phase. As with other aerodynamic coefficients, values of this coefficient are given by polynomial functions of Mach number of fourth degree or less.

c. The characteristic flow rate function of the base-burn motor is given as follows:

$f(I) = I/I_0$ If $I \leq I_0$ (C.13)

$f(I) = 1$ If $I \geq I_0$ (C.14)

where: I is the base-burn motor fuel injection parameter;

$$I = \frac{4\,\dot{m}_f}{\pi\, d_b{}^2\, \rho\, v}, \quad \text{(C.15)}$$

and I_0 is the injection parameter permitting optimum efficiency of the base-burn motor. It is given as a function of Mach number. These functions are in the form of polynomials of one degree or less. They are defined over regions of Mach number, from $M_{MAX_{i-1}}$ up to and including M_{MAX_i}.

NOTE: The function $f(I) = I/I_0$ is principally used for emptying phase and eventually at the start of the burning phase.

d. The coefficient i_{BB} is a fitting factor which can be used, if necessary, to adjust the drag reduction. i_{BB} is expressed as a polynomial function of the quadrant elevation, QE, of third degree or less. It is included for matching observed firing data during the base-burn phase.

e. Mass of the projectile is given by:

for $0 \leq t < t_{DI}$

$m = m_0 - m_{CB_0}$ (C.16)

for $t_{DI} \leq t$ and $m \geq m_B$

$$\dot{m} = \dot{m}_f \tag{C.17}$$

$$\dot{m}_f = -V_C \ \rho_p \ S_C \left(m_{CB}\right) \tag{C.18}$$

where:

$$m_B = m_0 - m_f \tag{C.19}$$

$$m_{CB} = m_0 - m \tag{C.20}$$

m_{CB_0} is the mass of fuel burnt in the barrel;

V_C is the combustion rate;

ρ_p is the density of fuel;

$S_C\ (m_{CB})$ is the area of combustion at time t and will be expressed in the form of a function of the mass of fuel burnt:

$$S_C = a_i + b_i\, m_{CB}; \tag{C.21}$$

for $m_{CB_i} < m_{CB} \leq m_{CB_{i+1}}$

a_i and b_i are defined over regions of m_{CB}, from $m_{CB_{i\,=\,0}}$ up to and including $m_{CB_{i\,=\,n}}$.

The combustion rate is given by:

$$V_C = V_{C_0}\, f(MT)\, g(P)\, K(p) \tag{C.22}$$

where:

V_{C_0} is the combustion rate obtained on the strand burner at standard pressure and temperature

MT is the motor fuel temperature

$$f(MT) = e^{\beta(MT-21)} \tag{C.23}$$

P is the local atmospheric air pressure

$$g(P) = k\ P^n \tag{C.24}$$

p is the axial spin of the projectile

K(p) is determined from experiments to take into account the influence of axial spin on the combustion rate, *K(p)* is a linear function of spin for each charge.

The time of motor burnout, t_B, is the time for which $m = m_B$ and it is a program output.

4. Fitting Factors

To compensate for the approximations in this annex, certain fitting factors are applied in order to create correspondence between the computed and the observed range testing results.

Table C-1. Fitting Factors for Rocket-Assisted and Base Burn Projectiles

Fitting	***Fitting Function***	
	Rocket-assisted Projectiles	***Base-burn Projectiles***
Change in Radial Velocity During Motor Burning	f_T	
Base-burn, Motor-burn Time	t_{DI} $t_B - t_{DI}$	t_{DI} $K(p)$
Range	i	i $f(i_{BB,\ MT})$

5. The location of the center of mass for base burn and rocket-assisted projectiles is given by:

$$X_{CG} = X_{CG_0} + \left[\frac{\left(X_{CG_0} - X_{CG_B}\right)\left(m - m_0\right)}{m_0 - m_B} \right] \qquad \text{(C.25)}$$

6. Common Equations for base burn and rocket-assisted, spin-stabilized projectiles, and fin-stabilized rockets.

a. The overturning moment coefficient of the munition is given by:

$$C_{M_\alpha} = C^*_{M_\alpha} + \left[\frac{\left(X_{CG} - X_{CG_0}\right)\left(C_{D_0} + C_{L_\alpha}\right)}{d}\right] \qquad \text{(C.26)}$$

where: $C^*_{M_\alpha}$ is determined for the initial munition configuration and, when $t_{DI} \le t < t_B$, then C_{D_0} equals $C_{D_{0_T}}$ for rocket-assisted projectiles and fin-stabilized rockets.

b. The cubic overturning moment coefficient of the munition is given by:

$$C_{M_{\alpha^3}} = C^*_{M_{\alpha^3}} + \left[\frac{\left(X_{CG} - X_{CG_0}\right)\left(C_{L_{\alpha^3}} + C_{D_{\alpha^2}} - 1/2\, C_{L_\alpha}\right)}{d}\right] \qquad \text{(C.27)}$$

where: $C^*_{M_{\alpha^3}}$ is determined for the initial munition configuration.

c. The axial moment of inertia of the munition is given by:

$$I_x = I_{x_0} + \left[\frac{\left(I_{x_0} - I_{x_B}\right)\left(m - m_0\right)}{m_0 - m_B}\right] \qquad \text{(C.28)}$$

7. The location of the center of mass, motor nozzle exit, motor nozzle throat, and transverse moment of inertia for fin-stabilized rockets.

a. The location of the center of mass is given by:

$$X_{CG} = X_{CG_B} + \left[\frac{\left(X_{CG_{f_0}} - X_{CG_B}\right)\left(m - m_B\right)}{m}\right] \qquad \text{(C.29)}$$

where:

$$X_{CG_{f0}} = X_{CG_B} + \frac{(X_{CG_0} - X_{CG_B})m_0}{(m_0 - m_B)}$$

b. The location of the motor nozzle exit from the center of the mass is given by:

$$r_e = \ell - X_{CG} \qquad \text{(C.30)}$$

c. The location of the motor nozzle throat from the center of mass is given by:

$$r_t = r_e - r_{t-t} \qquad \text{(C.31)}$$

d. The transverse moment of inertia of a fin-stabilized rocket is given by:

$$I_Y = I_{Y_0} - (m_0 - m)\, r_f^2 + m_0 \left(X_{CG_{f_0}} - X_{CG_0}\right)^2 - m \left(X_{CG_f} - X_{CG}\right)^2 \qquad \text{(C.32)}$$

where: r_f is the radius of gyration of the fuel mass.

Figure C-1 illustrates the distances used for the determination of the transverse moment of inertia of the rocket or projectile during motor burning.

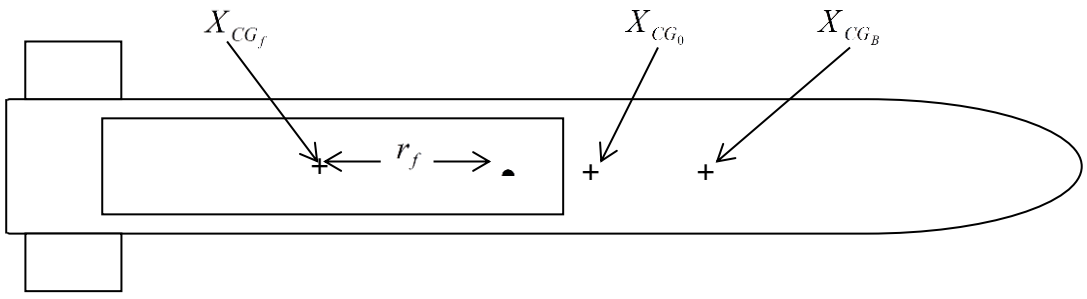

Figure C-1. Distances Used for the Determination of the Transverse Moment of Inertia

8. List of Additional Symbols for Rocket-Assisted and Base-Burn Projectiles

Symbol	Definition	Units
A_e	Exit area of jet	m^2
a_i	Coefficient (constant)	*none*
b_i	Coefficient (constant)	*none*
$\overrightarrow{BB}$	Acceleration due to drag reduction of base-burn motor	m/s^2
$C_{D_{0_T}}$	Zero yaw drag coefficient (thrust on)	*none*
$C^*_{M_\alpha}$	Overturning moment coefficient for initial projectile configuration	*none*
$C_{x_{bb}}$	Drag reduction coefficient during base-burn motor burning	*none*
d	Reference diameter of projectile	m
d_b	Diameter of projectile base	m
e	Base of natural logarithms	*none*
$f(i_{BB,\,MT})$	Base-burn factor	*none*
$f(I)$	Function I	*none*
$f(MT)$	Combustion rate as a function of motor fuel temperature	*none*
f_T	Thrust Factor	*none*
$g(P)$	Combustion rate as a function of atmospheric air pressure	*none*
i_{BB}	Fitting factor to adjust the drag reduction as a function of quadrant elevation	*none*
I	Base-burn motor fuel injection parameter	*none*
I_0	Base-burn motor fuel injection parameter for optimum efficiency	*none*
I_{SP}	Specific impulse	Ns/kg

I_x	Axial moment of inertia of the projectile	$kg\ m^2$
I_{x_0}	Initial axial moment of inertia	$kg\ m^2$
I_{x_B}	Axial moment of inertia at burnout	$kg\ m^2$
I_y	Transverse moment of inertia	$kg\ m^2$
I_{y_0}	Initial transverse moment of inertia	$kg\ m^2$
k	Constant in burning rate versus pressure formula	*none*
$K(p)$	Axial spin burning rate factor	*none*
ℓ	Distance of the motor nozzle exit from nose	m
m_0	Initial fuzed projectile mass	kg
m_B	Fuzed projectile mass at burnout	kg
m_{CB}	Mass of motor fuel burnt	kg
m_{CB_0}	Mass of motor fuel burnt in the barrel	kg
m_{DI}	Ignition delay element mass	kg
m_{DOB}	Delay obturator mass	kg
m_f	Projectile fuel mass	kg
$\dot{m}_f$	Mass flow rate of the motor fuel	kg/s
MT	Temperature of motor fuel	$°C$
n	Exponent in burning rate versus pressure formula	*none*
P	Air pressure	Pa
P_r	Reference air pressure for standard thrust	Pa
r_e	Distance from the body center-of-mass to the motor nozzle exit	m

r_f	Radius of gyration of the motor fuel mass	m
r_t	Distance from the body center-of-mass to the motor nozzle throat	m
$r_{t\text{-}t}$	Distance of the motor nozzle exit from the motor nozzle throat	m
S_C	Area of combustion at time t	m^2
t	Computed time of flight	s
t^*	Pseudo-computed time for mapping of thrust at nonstandard conditions	s
t_B	Time of rocket motor burnout	s
$t_{B_{ST}}$	Standard time of rocket motor burnout	s
t_{DI}	Time of rocket motor ignition delay	s
$t_{DI_{ST}}$	Standard time of rocket motor ignition delay	s
T_R	Thrust produced by rocket motor at time t	N
T_{ST}	Standard thrust as function of burning time	N
T^*	Effective thrust	N
V_C	Combustion rate of base-burn fuel	m/s
V_{C_0}	Combustion rate of base-burn fuel on strand burner	m/s
X_{CG}	Distance of center of mass from nose at time t	m
X_{CG_0}	Initial distance of center of mass from nose	m
X_{CG_B}	Distance of center of mass from nose at burnout	m
$X_{CG_{f_0}}$	Distance of center-of-mass of the rocket motor fuel from nose, initially	m
β	Base-burn motor temperature fuel burning coefficient	$none$
ρ_p	Density of base-burn motor fuel	kg/m^3

9. Additional Data Requirements for Rocket-Assisted and Base-Burn Projectiles

(1) Physical Data	***Symbol***
Exit area of jet	A_e
Reference diameter of projectile	d
Axial moment of inertia of the projectile	I_x
Initial axial moment of inertia of the projectile	I_{x_0}
Axial moment of inertia of the projectile at motor burnout	I_{x_B}
Transverse moment of inertia of the rocket, initially	I_{Y_0}
Distance of the motor nozzle exit from nose	ℓ
Fuzed projectile mass at burnout	m_B
Initial mass of fuzed projectile	m_0
Radius of gyration of motor fuel mass	r_f
Distance of the motor nozzle exit from the motor nozzle throat	$r_{t\text{-}t}$
Initial distance of center of mass from nose	X_{CG_0}
Distance of center of mass from nose at burnout	X_{CG_B}

(2) Aerodynamic Data	***Symbol***
Zero Yaw drag coefficient (thrust on)	$C_{D_{0_T}}$
Overturning moment coefficient for initial fuzed projectile	$C^*_{M_\alpha}$
Drag reduction coefficient during base-burn motor burning	$C_{x_{BB}}$

(3) Motor Data – Rocket-Assisted	*Symbol*
Specific impulse	I_{SP}
Ignition delay element mass	m_{DI}
Delay obturator mass	m_{dob}
Mass of rocket motor fuel	m_f
Reference air pressure for standard thrust	P_r
Time of rocket motor burnout	t_B
Standard time of motor burnout	$t_{B_{ST}}$
Time of rocket motor ignition delay	t_{DI}
Standard time of rocket motor ignition delay	$t_{DI_{ST}}$
Standard thrust as function of pseudo-time	T_{ST}

(4) Motor Data – Base-Burn	*Symbol*
Base-burn motor fuel injection parameter for optimum efficiency	I_0
Mass of fuel burnt in the barrel	m_{CB_0}
Mass of motor fuel	m_f
Area of combustion expression in the form of a function of the mass of fuel burnt $S_C = a_i + b_i\, m_{CB}$; for $m_{CB_i} < m_{CB} \leq m_{CB_{i+1}}$ a_i and b_i are defined over regions of m_{CB}, from $m_{CB_{i=0}}$ up to and including $m_{CB_{i=n}}$	S_C
Combustion rate of base-burn fuel on strand burner	V_{C_0}
Base-burn motor temperature fuel burning coefficient	β
Exponent in burning rate versus pressure formula	n
Density of base-burn motor fuel	ρ_p
Constant in burning rate versus pressure formula	k

10. Fire Control Data for Rocket-Assisted and Base-Burn Motors

a. Rocket-Assisted Motor

Time of rocket ignition delay (t_{DI}), time of rocket motor burn ($t_B - t_{DI}$) and thrust factor (f_T) are given as a function of rocket motor temperature for each charge as follows:

$$f = a_0 + a_1(MT - 21) + a_2(MT - 21)^2 + a_3(MT - 21)^3 \quad \text{(C.33)}$$

where:

$$f = t_{DI},\ t_B - t_{DI},\ \text{or}\ f_T \quad \text{(C.34)}$$

MT is rocket motor temperature

Standard Thrust is given as a function of pseudo-computed time (t^*) as follows:

$$T_{ST} = a_0 + a_1 t^* + a_2 t^{*2} + a_3 t^{*3} \quad \text{(C.35)}$$

b. Base-Burn Motor

The axial spin influence on burning rate factor $K(p)$, is given as a linear function of spin for each charge.

I_0 is a linear function of Mach number.

The factor, $f(i_{BB,MT})$, for a base-burn projectile is given as a function of quadrant elevation, *QE*, and motor temperature, *MT*, for each charge as follows:

$$i_{BB_{(MT=21)}} = a_0 + a_1 QE + a_2 QE^2 + a_3 QE^3 \quad \text{(C.36)}$$

and

$$f(i_{BB,MT}) = i_{BB_{(MT=21)}} + b_1(MT - 21) + b_2(MT - 21)^2 + b_3(MT - 21)^3 + b_4(MT - 21)^4 \quad \text{(C.37)}$$

Time of base-burn ignition delay (t_{DI}) is given as a function of motor temperature for each charge.

$$t_{DI} = a_0 + a_1(MT - 21) + a_2(MT - 21)^2 + a_3(MT - 21)^3 \qquad \text{(C.38)}$$

MT is rocket motor temperature.

ANNEX D ADDITIONAL TERMS FOR SPIN-STABILIZED ROCKET-ASSISTED PROJECTILES, SPIN-STABILIZED BASE-BURN PROJECTILES, AND FIN-STABILIZED ROCKETS – METHOD 2

1. Introduction

This annex provides the equations required to simulate the flight of spin-stabilized rocket-assisted projectiles, spin-stabilized base-burn projectiles, and fin-stabilized rockets

2. Equations for spin-stabilized rocket-assisted projectiles, spin-stabilized base-burn projectiles, and fin-stabilized rockets

a. For rocket-assisted projectiles:

The acceleration due to thrust force of the rocket motor, $\frac{\overrightarrow{TF}}{m}$, during burning ($t_{DI} \le t \le t_B$) is added to the equation of motion of the center of mass of the unassisted projectile:

$$\frac{\overrightarrow{TF}}{m} = \left[\frac{f_T \dot{m}_f I_{SP} + (P_r - P)A_e}{m}\right]\left(\frac{\vec{v}\ \cos\alpha_e}{v} + \vec{\alpha}_e\right) \qquad \text{(D.1)}$$

During rocket motor burning the aerodynamic zero-yaw coefficient is C_{Do_T} and if $\dot{m}_f \le \dot{m}_p$ then $(P_r - P)\, A_e = 0$.

b. For base-burn projectiles:

The base drag reduction due to a base-burn motor during burning ($t_{DI} \le t \le t_B$) is added to the drag term $\left(\frac{\overrightarrow{DF}}{m}\right)$ of the projectile.

$$\frac{\overrightarrow{DF}}{m} = -\frac{\pi \rho d^2 i}{8m}\left\{C_{Do} - f\left(i_{BB,MT}\right)\left[\frac{I\left(\frac{\delta\ BP}{\delta\ I}\right)}{\left(\frac{\gamma}{2}\right)M^2\left(\frac{d}{d_b}\right)^2}\right] + C_{D_{\alpha^2}}(Q_D\alpha_e)^2 + C_{D_{\alpha^4}}(Q_D\alpha_e)^4\right\} v\vec{v} \qquad \text{(D.2)}$$

where:

$$I = \frac{4\dot{m}_f}{\pi \rho v d_b^{\ 2}} \qquad \text{(D.3)}$$

$$f\left(i_{BB,MT}\right)\left[\frac{\left(\frac{\dot{m}_f}{\rho v A_b}\right)\left(\frac{\delta BP}{\delta I}\right)}{\left(\frac{\gamma}{2}\right)M^2\left(\frac{d}{d_b}\right)^2}\right]$$

is used to represent the drag reduction due to the mass flow ($\dot{m}_f$) of the base-burn motor. The factor $f(i_{BB,MT})$ is included for matching observed range firing data.

c. For fin-stabilized rockets:
See Eq. (16) and (25) in main document.

3. Common Equations for base-burn and rocket-assisted, spin-stabilized projectiles, and fin-stabilized rockets.

a. The mass flow for spin-stabilized projectiles and fin-stabilized rockets is given by:

at $t = 0$

$$m = m_0 \tag{D.4}$$

$$\dot{m} = 0 \tag{D.5}$$

for $0 < t < t_{DI}$

$$\dot{m} = -\frac{m_{DI}}{t_{DI}} \tag{D.6}$$

$$m = -\int_0^{t_{DI}}\left(\frac{m_{DI}}{t_{DI}}\right)dt + m_0 \tag{D.7}$$

for $t_{DI} \le t < t_B$

$$\dot{m} = -\dot{m}_f \tag{D.8}$$

$$m = -\int_{t_{DI}}^{t_B}\dot{m}_f\ dt - \int_0^{t_{DI}}\left(\frac{m_{DI}}{t_{DI}}\right)dt + m_0 \tag{D.9}$$

$$\dot{m}_f = \left(\frac{t_B^* - t_{(t)}^*}{t_{B_{(t)}} - t} \right) \dot{m}_f^* \tag{D.10}$$

$$\dot{t}_{(t)}^* = \frac{t_B^* - t_{(t)}^*}{t_{B_{(t)}} - t} \tag{D.11}$$

$$\dot{t}_{B_{(t)}} = \left(t_{B_{(t)}} - t \right) \left[f_{BT_p} \left(\frac{\dot{p}}{p} \right) + f_{BT_P} \left(\frac{\dot{P}}{P} \right) \right] \tag{D.12}$$

where:

$$\dot{P} = \frac{\Delta P}{\Delta t} = \frac{\Delta P}{\Delta E_2} u_2 \tag{D.13}$$

and at t_{DI}

$$t_{(t_{DI})}^* = t_{DI}^* \tag{D.14}$$

$$t_{B_{(t_{DI})}} = t_{DI} + \left[\left(t_B - t_{DI} \right) \left(\frac{p_{(t_{DI})}}{p_r} \right)^{f_{BT_p}} \left(\frac{P_{(t_{DI})}}{P_r} \right)^{f_{BT_P}} \right] \tag{D.15}$$

(Time-of-motor burnout as a function of t_{DI})

p_r	=	Reference axial spin rate for motor mass flow
$p_{(t_{DI})}$	=	Actual spin rate for motor mass flow at t_{DI}
P_r	=	Standard atmospheric air pressure
$P_{(t_{DI})}$	=	Actual atmospheric air pressure at t_{DI}

for $t \geq t_B$

$$m_B = m_0 - m_{DI} - m_f \tag{D.16}$$

$$\dot{m} = 0 \tag{D.17}$$

b. The location of the center of mass of the munition is given by:

$$X_{CG} = X_{CG_B} + \left[\frac{\left(X_{CG_{f0}} - X_{CG_B} \right)\left(m - m_B \right)}{m} \right] \quad \text{(D.18)}$$

where:

$$X_{CG_{f0}} = X_{CG_B} + \frac{(X_{CG_0} - X_{CG_B})m_0}{(m_0 - m_B)} \quad \text{(D.19)}$$

c. The location of the motor nozzle exit from the center of the mass is given by:

$$r_e = \ell - X_{CG} \quad \text{(D.20)}$$

d. The location of the motor nozzle throat from the center of mass is given by:

$$r_t = r_e - r_{t-t} \quad \text{(D.21)}$$

e. The overturning moment coefficient of the munition is given by:

$$C_{M_\alpha} = C^*_{M_\alpha} + \left[\frac{\left(X_{CG} - X_{CG_0} \right)\left(C_{D_0} + C_{L_\alpha} \right)}{d} \right] \quad \text{(D.22)}$$

where: $C^*_{M_\alpha}$ is determined for the initial munition configuration and, when $t_{DI} \leq t < t_B$, then C_{D_0} equals $C_{D_{0_T}}$ for rocket-assisted projectiles and fin-stabilized rockets. The aerodynamic coefficients are considered to be dimensionless, with unit = 1, in this formulation.

f. The cubic overturning moment coefficient of the munition is given by:

$$C_{M_{\alpha^3}} = C^*_{M_{\alpha^3}} + \left[\frac{\left(X_{CG} - X_{CG_0} \right)\left(C_{L_{\alpha^3}} + C_{D_{\alpha^2}} - 1/2\, C_{L_\alpha} \right)}{d} \right] \quad \text{(D.23)}$$

where: $C^*_{M_{\alpha^3}}$ is determined for the initial munition configuration. The aerodynamic coefficients are considered to be dimensionless, with unit =1, in this formulation.

g. The axial moment of inertia of the munition is given by:

$$I_x = I_{x_0} + \left[\frac{\left(I_{x_0} - I_{x_B}\right)\left(m - m_0\right)}{m_0 - m_B} \right] \qquad \text{(D.24)}$$

4. The transverse moment of inertia of a fin-stabilized rocket is given by:

$$I_Y = I_{Y_0} - \left(m_0 - m\right) r_f^2 + m_0 \left(X_{CG_{f_0}} - X_{CG_0}\right)^2 - m \left(X_{CG_f} - X_{CG}\right)^2 \qquad \text{(D.25)}$$

Figure D-1 illustrates the distances used for the determination of the transverse moment of inertia of the rocket during motor burning.

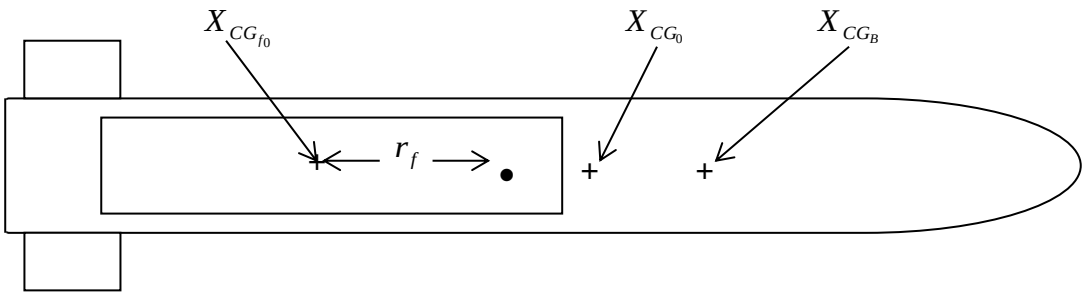

Figure D-1. Distances Used for the Determination of the Transverse Moment of Inertia

5. List of Additional Symbols

Symbol	Definition	Units
A_b	Area of projectile base	m^2
A_e	Exit area of the motor jet	m^2
C_{D_0}	Zero yaw drag coefficient	*none*
$C_{D_{0_T}}$	Zero yaw drag coefficient during rocket motor burning	*none*
$C^*_{M_\alpha}$	Overturning moment coefficient for initial fuzed munition	*none*
$C^*_{M_\alpha{}^3}$	Cubic overturning moment coefficient for initial fuzed munition	$1/rad^2$
d_b	Diameter of projectile base	*m*
f_T	Thrust factor	*none*
$f(i_{BB,\,MT})$	Base-burn factor	*none*
f_{BT_p}	Base-burn motor spin rate burning-time factor	*none*
f_{BT_P}	Base-burn motor atmospheric air pressure burning-time factor	*none*
I	Base-burn motor fuel injection parameter	*none*
i_{BB}	Fitting factor to adjust the drag reduction as a function of quadrant elevation	*none*
I_x	Axial moment of inertia of the munition at time t	$kg\ m^2$
I_{x_0}	Axial moment of inertia of the munition, initially	$kg\ m^2$
I_{x_B}	Axial moment of inertia of the munition at motor burnout	$kg\ m^2$
I_Y	Transverse moment of inertia of the rocket at time t	$kg\ m^2$
I_{Y_0}	Transverse moment of inertia of the rocket, initially	$kg\ m^2$
ℓ	Distance of the motor nozzle exit from nose	*m*

m_0	Fuzed munition mass, initially	kg
m_B	Fuzed munition mass at burnout	kg
m_{DI}	Mass of ignition delay element	kg
m_f	Mass of motor fuel	kg
$\dot{m}_f^*$	Reference mass flow rate of the motor fuel as a function of t* pseudo-time-of-motor burning	kg/s
$\dot{m}_P$	Minimum mass flow rate of the motor fuel for air pressure term	kg/s
MT	Temperature of motor fuel	$°C$
p	Axial spin rate of projectile	rad/s
p_r	Reference axial spin rate for motor mass flow	rad/s
r_e	Distance from the body center-of-mass to the motor nozzle exit	m
r_f	Radius of gyration of the motor fuel mass	m
r_t	Distance from the body center-of-mass to the motor nozzle throat	m
$r_{t\text{-}t}$	Distance of the motor nozzle exit from the motor nozzle throat	m
t^*	Pseudo-time-of-motor burning	s
t_B	Time-of-motor burnout	s
t_B^*	Reference time-of-motor burnout	s
t_{DI}	Time-of-motor ignition delay	s
t_{DI}^*	Reference time-of-motor ignition delay	s
X_{CG}	Distance of center of mass of the munition from nose at time t	m

X_{CG_0}	Distance of center of mass of the munition from nose at time t0	m
X_{CG_B}	Distance of center of mass of the munition from nose at time tB	m
$X_{CG_{f_0}}$	Distance of center-of-mass of the rocket motor fuel from nose at time t0	m
$\frac{\delta BP}{\delta I}$	Change in non-dimensional base pressure for a change in the base-burn motor injection parameter	*none*
$\frac{\Delta P}{\Delta t}$	Rate of change of atmospheric air pressure as seen by the munition	*Pa/s*

6. Additional Data Requirements

Physical data	***Symbol***
Area of projectile base	A_b
Exit area of motor jet	A_e
Diameter of projectile base	d_b
Axial moment of inertia of the munition, initially	I_{x_0}
Axial moment of inertia of the munition at motor burnout	I_{x_B}
Transverse moment of inertia of the rocket, initially	I_{Y_0}
Distance of the motor nozzle exit from nose	ℓ
Fuzed munition mass, initially	m_0
Fuzed munition mass at burnout	m_B
Mass of ignition delay element	m_{DI}
Mass of motor fuel	m_f
Minimum mass flow rate of the fuel for air pressure term	$\dot{m}_p$
Radius of gyration of motor fuel mass	r_f
Distance of the motor nozzle exit from the motor nozzle throat	$r_{t\text{-}t}$
Distance of center of mass of the munition from nose, initially	X_{CG_0}
Distance of center of mass of the munition from nose at motor burnout	X_{CG_B}

Aerodynamic data	***Symbol***
Zero yaw drag coefficient during rocket motor burning	$C_{D_{0_T}}$
Overturning moment coefficient for initial fuzed munition	$C^*_{M_\alpha}$
Nonlinear overturning moment coefficient for initial fuzed munition	$C^*_{M_{\alpha^3}}$

Motor data	***Symbol***
Reference mass flow rate of the motor fuel as a function of pseudo-time-of motor burning, t^* $\dot{m}^*_f = a_0 + a_1 t^* + a_2 t^{*2}$; for $t^*_i < t^* \le t^*_{i+1}$ a_0 and a_1 are defined over regions of t^*, from $t^*_{i=0}$ up to and including $t^*_{i=n}$	$\dot{m}^*_f$
Reference axial spin rate for motor mass flow	p_r
Standard atmospheric air pressure at sea level	P_r
Time-of-motor burnout	t_B
Reference time-of-motor burnout	t^*_B
Time-of-motor ignition delay	t_{DI}
Reference time-of-motor ignition delay	t^*_{DI}
Specific impulse of motor fuel	I_{SP}
Change in non-dimensional base pressure for a change in the base-burn motor injection parameter as a function of Mach number and injection parameter	$\frac{\delta BP}{\delta I}$

$\frac{\delta BP}{\delta I}$ is given, for up to five values of I, as a function of Mach number in the form of polynomials of fourth degree or less. They are defined over regions of Mach number, from MMAXi = 1 up to and including MMAX.

$$\left(\frac{\delta BP}{\delta I}\right)_I = a_0 + a_1 M + a_2 M^2 + a_3 M^3 + a_4 M^4 \qquad \text{(D.26)}$$

7. Fire Control Data for Projectile Motor
(for a complete fitting factor table, see Annex A)

a. The time-of-motor ignition delay, t_{DI}, and time-of-motor burn, (t_B - t_{DI}), for rocket-assisted and base-burn projectiles are given as a function of motor temperature, *MT*, for each charge as follows:

$$t_{DI} = a_0 + a_1(MT-21) + a_2(MT-21)^2 + a_3(MT-21)^3 \quad \text{(D.27)}$$

$$(t_B - t_{DI}) = a_0 + a_1(MT-21) + a_2(MT-21)^2 + a_3(MT-21)^3 \quad \text{(D.28)}$$

b. The thrust factor, f_T, for a rocket-assisted projectile is given as a function of motor temperature, *MT*, for each charge as follows:

$$f_T = a_0 + a_1(MT-21) + a_2(MT-21)^2 + a_3(MT-21)^3 \quad \text{(D.29)}$$

c. The spin rate burning-time factor, f_{BT_p}, for a base-burn projectile is given as a constant for each charge.

d. The atmospheric air pressure burning-time factor, f_{BT_P}, for a base-burn projectile is given as a constant for each charge.

e. The factor, $f(i_{BB,MT})$, for a base-burn projectile is given as a function of quadrant elevation, *QE*, and motor temperature, *MT*, for each charge as follows:

$$i_{BB_{(MT=21)}} = a_0 + a_1 QE + a_2 QE^2 + a_3 QE^3 \quad \text{(D.30)}$$

and

$$f(i_{BB,MT}) = i_{BB_{(MT=21)}} + b_1(MT-21) + b_2(MT-21)^2 + b_3(MT-21)^3 + b_4(MT-21)^4 \quad \text{(D.31)}$$

8. Fire Control Data for Fin Stabilized Rockets
(for a complete fitting factor table, see Annex A)

a. The mass of ignition delay element, m_{DI}, time of motor ignition delay, t_{DI}, spin rate burning-time factor, f_{BT_p}, and the atmospheric air pressure burning-time factor, f_{BT_P}, are zero.

b. The time of first motion, t_{FM}, time of launch, t_L, time of rocket fin opening, t_{FO}, time of motor burn, (t_B - t_{DI}), is given by, t_B, time of end of five degrees of freedom, $t_{E5D,}$ and thrust factor, f_T, are given as a function of motor temperature, *MT*, as follows:

$$t_{FM} = a_0 + a_1(MT-21) + a_2(MT-21)^2 + a_3(MT-21)^3 \quad \text{(D.32)}$$

$$t_L = a_0 + a_1(MT-21) + a_2(MT-21)^2 + a_3(MT-21)^3 \quad \text{(D.33)}$$

$$t_{FO} = a_0 + a_1(MT-21) + a_2(MT-21)^2 + a_3(MT-21)^3 \quad \text{(D.34)}$$

$$t_B = a_0 + a_1(MT-21) + a_2(MT-21)^2 + a_3(MT-21)^3 \quad \text{(D.35)}$$

$$t_{E5D} = a_0 + a_1 (MT - 21) + a_2 (MT - 21)^2 + a_3 (MT - 21)^3$$

(D.36)

$$f_T = a_0 + a_1(MT-21) + a_2(MT-21)^2 + a_3(MT-21)^3 \quad \text{(D.37)}$$

c. At time, t_L, the initial angular velocity (spin) of the fin stabilized rocket is, $p_{(t_L)}$, a constant and the initial transverse angular velocities of the fin stabilized rocket, $\omega_{y_{(t_L)}}$ and $\omega_{z_{(t_L)}}$, are given as a function of quadrant elevation, *QE*, as follows:

$$p_{(t_L)} = a_0 \quad \text{(D.38)}$$

$$\omega_{y_{(t_L(MT=21))}} = a_0 + a_1 QE + a_2 QE^2 + a_3 QE^3 \quad \text{(D.39)}$$

and $\omega_{y_{(t_L)}} = \omega_{y_{(t_L(MT=21))}} + b_1(MT-21) + b_2(MT-21)^2 + b_3(MT-21)^3$

$$\omega_{z_{(t_L(MT=21))}} = a_0 + a_1 QE + a_2 QE^2 + a_3 QE^3 \quad \text{(D.40)}$$

and $\omega_{z_{(t_L)}} = \omega_{z_{(t_L(MT=21))}} + b_1(MT-21) + b_2(MT-21)^2 + b_3(MT-21)^3$

d. The form factor, i, and adjustment to azimuth, $\Delta(\Delta AZ)$, are given as a function of quadrant elevation, *QE*, as follows:

$$i = a_0 + a_1 QE + a_2 QE^2 + a_3 QE^3 \quad \text{(D.41)}$$

$$\Delta(\Delta AZ) = a_0 + a_1 QE + a_2 QE^2 + a_3 QE^3 \quad \text{(D.42)}$$

e. The modeling of time used for fin stabilized rockets may require a correction to time of flight as follows:

$$T = t + \Delta ToF \quad \text{(D.43)}$$

$$\Delta ToF = a_0 + a_1 t + a_2 t^2 + a_3 t^3 \quad \text{(D.44)}$$

ANNEX E CALCULATION OF SUBMUNITION TRAJECTORIES

1. Introduction

This annex provides the methods for calculating submunition trajectories. Submunition trajectories are the trajectories for submunitions ejected from the carrier shell in flight.

a. Submunition trajectories may represent trajectories for:

(1) Cargo bomblets
(2) Mines
(3) Smoke canisters
(4) Illuminating canisters
(5) Canister for sensor-fuzed submunition

b. This Annex describes methods for the calculation of:

(1) the base separation point
(2) the submunition trajectories with a point mass trajectory model
(3) simple trajectory calculation using a closed form solution
(4) submunition dispersion
(5) empty carrier trajectory

Figure E-1 defines the nomenclature for the different phases. A collective name for the different phases is *submunition trajectory*. Note that *terminal phase* should always be used for the phase in which the submunition hits the ground or functions.

2. Rules for the Calculation of the Base Separation Point

The base separation point is the point where the fuze of the carrier shell activates the first phase of the submunition trajectories. Calculation of the position of the base separation point can be done using either of the following rules:

a. a predefined *height of burst* (*HOB*) above the target, or by
b. requiring a certain *time of fall* (T_{fs}) for the center submunition.

Both can be given either as a constant or as a polynomial function of the superelevation. Thus for rule (a.) and rule (b.) we respectively get

$$\begin{aligned} HOB = a_0 + a_1(QE - A_S) + a_2(QE - A_S)^2 + a_3(QE - A_S)^3 + \\ \left(a_4 + a_5(QE - A_S) + a_6(QE - A_S)^2 + a_7(QE - A_S)^3\right) Alt_w \end{aligned} \quad \text{(E.1)}$$

and

$$T_{fs} = b_0 + b_1(QE - A_S) + b_2(QE - A_S)^2 + b_3(QE - A_S)^3 \qquad \text{(E.2)}$$

Rule (a.) is designed to ensure that a specified fraction of all base separation points occur at a certain height. Rule (b.) is designed to ensure that a specified fraction of submunitions hits the ground before the self-destruct time.

The starting velocity of any phase, which includes point-mass and closed-form-biases:

$$\vec{u}_{s1} = \vec{u}_{carrier} + \Delta u_{s1}\vec{c} \qquad \text{(E.3)}$$

where: $\vec{c} = \frac{\vec{v}}{v}\cos\alpha_e + \vec{\alpha}_e$ is the axis of the carrier shell at the end of the previous phase, and the vector $\vec{\alpha}_e$ is the yaw of repose.

$\Delta u_{sn} = a_{0,n} + a_{1,n}\, p_{n-1}$ is the ejection speed of the submunition,

and p_{n-1} is the magnitude of the spin at the end of the previous phase

For a more detailed description of ejection velocity from a spin-stabilized projectile used to estimate the maximum dimension of submunition pattern on the ground, see equation E.34.

NOTE: See Figure E-2 for explanation of additional terms

3. Calculation of Submunition Trajectories with a Point Mass Model

NOTE: See Annex F for Point Mass Model implementation.

The acceleration due to aerodynamic drag, $\vec{D}$, is computed as

$$\vec{D}_{sn} = -i_{sn} C_{D_{sn}} \frac{\rho S_{sn}}{2 m_{sn}} v_{sn}\, \vec{v}_{sn} \qquad \text{(E.4)}$$

where: the subscripts *s* and *n* represent submunition and the phase number respectively. S_{sn} is the effective presented cross sectional area of the submunition unit and m_{sn} is its mass. They can both be given as linear functions of time.

The wind velocity, $\vec{w}$, is accounted for through

$$\vec{v}_{sn} = \vec{u}_{sn} - \vec{w} \qquad \text{(E.5)}$$

If necessary the spin damping can be calculated according to the expression

$$\dot{p}_{sn} = \frac{2\rho}{\pi I_{x_{sn}}} S_{sn}^2 \, p_{sn} \, C_{spin_{sn}} \, v_{sn} \qquad \text{(E.6)}$$

Drag coefficient can be formatted in two ways, one of which is dependent on Mach number only and one of which is dependent on Mach number, velocity, and spin.

Drag coefficient is given as a function of the Mach number (M_{sn}) of the submunition. The function is in the form of a linear function. It is defined over regions of Mach number similar to that of Annex A, paragraph 1. Thus in each interval

$$C_{D_{sn}} = a_{0,n} + a_{1,n} \, M_{sn} \qquad \text{(E.7)}$$

$C_{D_{sn}}$ value depends on the Mach number and the quotient of velocity and spin as follows.

$$C_{D_{sn}} = \frac{1.0}{i_{sn}} + \left[a_{0,n} + a_{1,n} \, M_{sn}\right]\left(\frac{S_{ball\_sn} - S_{sn}}{S_{sn}}\right) \qquad \text{(E.8)}$$

where:
$$S_{ball\_sn} = \frac{\pi}{4} d_{sn}^2 \qquad \text{(E.9)}$$

and
$$d_{sn} = a_{0,sn} + \frac{a_{1,sn}}{1 + a_{2,sn}\left(\frac{|p_{sn}|}{u_{sn}}\right)^{a_{3,sn}}} \qquad \text{(E.10)}$$

where: the coefficients $a_{k,sn}$ *(k=0,1,2,3)* are constant fitting factors for the submunition *s* in the phase *n*.

p_{sn} The spin of the submunition *s* in the phase *n* (rad/s)
u_{sn} The velocity of the submunition *s* in the phase *n* (m/s)

The form factor, i_{sn}, is given as a polynomial function of HOB

$$i_{sn} = b_0 + b_1\left(HOB_{sn}\right) + b_2\left(HOB_{sn}\right)^2 + b_3\left(HOB_{sn}\right)^3 \qquad \text{(E.11)}$$

Mass of submunition unit, m_{sn}, is given as a quadratic polynomial of *t*

$$m_{sn} = a_0 + a_1 t + a_2 t^2 \qquad \text{(E.12)}$$

Reference cross sectional area, S_n, is given as a quadratic polynomial function of t

$$S_n = a_0 + a_1 t + a_2 t^2 \tag{E.13}$$

and the corrected time is given by

$$T_{sn} = t_{sn} + a\, t_{sn} \tag{E.14}$$

for each phase.

The end of the phase is determined either by height above the ground and/or the duration of the phase and is calculated by one of the following equations:

$$H_{phase} = a \tag{E.15}$$

or

$$T_{f,sn} = a_0 + a_1(QE - A_S) + a_2(QE - A_S)^2 + a_3(QE - A_S)^3 + \frac{b_1}{u_{sn}} \tag{E.16}$$

u_{sn} is the velocity of the submunition at the beginning of the phase.

4. Calculation Using Simplified Formulas

The ballistic trajectory of a phase can be calculated in closed form either by

a. Closed Form A
assuming a drag proportional to a velocity reference and constant meteorological parameters throughout the phase using the vector equation

$$\vec{x}_{n+1} = \vec{x}_n + \left(\frac{\vec{v}_{sn}}{k_s} - \frac{\vec{g}}{k_s^2}\right)\left[1 - \exp(-T_{sn} k_s)\right] + T_{sn}\left(\vec{w} + \frac{\vec{g}}{k_s}\right) \tag{E.17}$$

where:

$$k_s = C_{D_{sn}}\, \rho \frac{S_{sn}}{2m_{sn}} v_{sn} \tag{E.18}$$

$$\vec{g} = \begin{bmatrix} 0 \\ -g_0 \\ 0 \end{bmatrix} \tag{E.19}$$

and

$$\vec{w} = \begin{bmatrix} w_1 \\ w_2 \\ w_3 \end{bmatrix} \quad \text{(E.20)}$$

or

b. Closed Form B

assuming a constant velocity of fall and constant wind throughout the phase where the heights of burst and time of fall are related by

$$T_{f_{sn}} = \frac{HOB_n - HOB_{n+1}}{\left| v_{sn,2} \right|} \quad \text{(E.21)}$$

where $v_{sn,2}$ is the vertical component of $\vec{v}_{sn}$. HOB_n is the height of burst at the start of phase *n*. If *n* is the last phase then $HOB_{n+1} = 0$ meaning that the submunition terminates at ground level.

The displacement due to wind is $T_{f_{sn}} \vec{w}_h$ where $\vec{w}_h$ is the horizontal wind vector.

If HOB_n and HOB_{n+1} are in different met zones, a fall time is calculated for each zone

$$T_{f_{sn}}(Z) = \frac{HOB_n - H_{Z-1}}{\left| v_{sn,2} \right|} \quad \text{(E.22)}$$

$$T_{f_{sn}}(z) = \frac{H_z - H_{z-1}}{\left| v_{sn,2} \right|} \quad \text{(E.23)}$$

$$T_{f_{sn}}(Z_0) = \frac{H_{Z_0} - HOB_{n+1}}{\left| v_{sn,2} \right|} \quad \text{(E.24)}$$

where Z is the met zone of HOB_n, Z_0 is the met zone of HOB_{n+1} and *z* is any met zone $Z < z < Z_0$. H_z is the upper height of met zone *z*. When *n* is the last submunition phase, equation (E.21) becomes zero.
The displacement due to horizontal wind is the sum of contributions from applicable met zones.

$$\vec{d} = \sum_{s=Z_0}^{Z} T_{f_{sn}}(z)\vec{w}_h(z) \quad \text{(E.25)}$$

where $\vec{d}$ is the displacement vector and $\vec{w}_h(z)$ the horizontal wind vector of met zone z (assumed constant throughout the zone).

The displacement due to wind may for certain types of submunition, e.g. illumination canisters, be used to make an offset to the aim point. The offset is

$$\vec{o} = -\vec{d}\min\left(a, \frac{o_{\max}}{|\vec{d}|}\right) \quad \text{(E.26)}$$

where: $\vec{o}$ is the offset vector, $a \leq 0.5$ is a factor indicating the relation between the displacement and the offset. The offset should not exceed a certain horizontal distance o_{max}. The minus sign indicates that the offset vector is in the opposite direction as the horizontal wind vector.

For illumination canisters the maximum offset is

$$o_{max} = \sqrt{R_{ill}{}^2 - HOB^2} \quad \text{(E.27)}$$

where: R_{ill} is the illumination radius (maximum absolute distance between illumination canister and target). HOB is the height at which the illumination canister ignites.

or

c. Displacement

by fitting observed data (for phase 1) to the form

$$\Delta X_{1,1} = \left(\frac{v_{carrier,1}}{\sqrt{v_{carrier,1}{}^2 + v_{carrier,3}{}^2}}\right)\left(a_0 + a_1 \sqrt{v_{carrier,1}{}^2 + v_{carrier,3}{}^2}\right) \quad \text{(E.28)}$$

$$\Delta X_{1,2} = b_0 + b_1 \; v_{carrier,2} \quad \text{(E.29)}$$

$$\Delta X_{1,3} = \left(\frac{v_{carrier,3}}{\sqrt{v_{carrier,1}{}^2 + v_{carrier,3}{}^2}}\right)\left(a_0 + a_1 \sqrt{v_{carrier,1}{}^2 + v_{carrier,3}{}^2}\right) \quad \text{(E.30)}$$

$$\Delta t = c_0 = \text{time displacement} \quad \text{(E.31)}$$

or

d. Closed Form Biases

The offset is calculated using closed form rule for certain types of sensor-fuzed munitions.
This describes the change of the submunition data from the ejection of the carrier shell to the time where a deceleration device is fully deployed.
The change of the flight conditions from the base separation point after ejection to the point where the deceleration devices (eg. ballutes, parachutes) are fully deployed, are calculated by polynomial functions.

The separation phase is described by the following equations, where the index *s* represents the submunition.

For a detailed description of the coefficients used, see chapter List of Symbols.

The change in position $\Delta\vec{X}_s$ is given as

$$\Delta\vec{X}_s = a_{0s}\begin{bmatrix}\cos\Gamma_0\cos\psi_0\\ \sin\Gamma_0\\ \cos\Gamma_0\sin\psi_0\end{bmatrix} \quad \text{(E.32)}$$

where Γ_0 is the vertical angle of fall and ψ_0 is the horizontal angle of fall at the start of the phase.
The change in velocity is given as

$$\Delta u_s = a_0 + a_1\,u_0 + a_2\,\Gamma_0 + a_3\,u_0\,\Gamma_0 \quad \text{(E.33)}$$

where u_0 is the velocity and Γ_0 is the vertical angle of fall at the start of the phase.

The change in the vertical angle of fall is given as

$$\Delta\Gamma_s = a_0 + a_1\,u_0 + a_2\,u_0^2 + \left(b_0 + b_1\,u_0 + b_2\,u_0^2\right)\Gamma_0 + \left(c_0 + c_1\,u_0 + c_2\,u_0^2\right)\Gamma_0^2 \quad \text{(E.34)}$$

where u_0 is the velocity and Γ_0 is the vertical angle of fall at the start of the phase.

The change in spin is given by

$$\Delta p_s = a_0 + a_1\,p_0 + a_2\,u_0 + a_3\,p_0\,u_0 \quad \text{(E.35)}$$

where p_0 is the spin and u_0 is the velocity at the start of the phase.

The duration of the phase is given by

$$\Delta t_s = a_0 + a_1\,u_0 + a_2\,u_0^2 \quad \text{(E.36)}$$

where u_0 is the velocity at the start of the phase.

5. Calculation of Submunition Dispersion

a. Concentric submunitions
The axis of the shell will not in general be parallel to the shell velocity vector due to a non-zero yaw of repose. This effect may be accounted for as shown in the following dispersion calculation.

The axis of the carrier shell is the vector $\vec{c}$ and the yaw of repose is defined by the vector $\vec{\alpha}_e$. Thus we have

$$\vec{c} = \frac{\vec{v}}{v}\cos\alpha_e + \vec{\alpha}_e \tag{E.37}$$

The ejection velocity of any central bomblet (a bomblet lying concentric with the axis of the shell), we get

$$\vec{u}_{s1} = \vec{u}_{carrier} + \Delta u_{s1}\vec{c} \tag{E.38}$$

where: $$\Delta u_{s1} = a_0 + a_1 p \tag{E.39}$$

is the ejection speed of the submunition, and p is the magnitude of projectile's spin at time of fuze function.

b. Eccentric submunitions

For a cross-sectional layer of submunitions, the ejection velocity of eccentric submunitions in the plane normal to the shell axis may be calculated by

$$\vec{u}_{s,\,normal} = i_D\left(\vec{p}\times\vec{r}_s\right) \tag{E.40}$$

where: $\vec{p}$ is the spin vector at base separation and $\vec{r}_s$ is the vector from the axis of the carrier shell to the center of gravity of the individual submunition. i_D is a fitting factor. The configuration is shown in Figure E-2.

In order to find the ejection velocity we first have to find the horizontal vector $\vec{e}$ that is normal to $\vec{c}$ and the vector $\vec{d} = \vec{e} \times \vec{c}$. These are also shown in Figure E-2. The vector $\vec{e}$ can be written as

$$\vec{e} = \frac{\vec{c} \times \vec{y}}{\left| \vec{c} \times \vec{y} \right|} \tag{E.41}$$

where $\vec{y}$ is defined as a unit vector in the positive 2-direction.

If we now define ϕ as the angle between the vector $\vec{d}$ and the position of the submunition as shown in Figure E-2, the position vector of the submunition from the axis is

$$\vec{r}_s = r_s \left(\vec{e} \sin\phi + \vec{d} \cos\phi \right) \tag{E.42}$$

In the modified point mass model, we always have $\vec{p} = p\vec{c}$ and when inserted into (E.40)

$$\vec{u}_{s,normal} = i_D \left(p\vec{c} \times \vec{r}_s \right) \tag{E.43}$$

After combining (E.38-39) and adding the velocity for the central bomblets we get

$$\vec{u}_{s1} = \vec{u}_{carrier} + \Delta u_{s1}\vec{c} + i_D p r_s \left(-\vec{d} \sin\phi + \vec{e} \cos\phi \right) \tag{E.44}$$

where: $$\Delta u_{s1} = a_0 + a_1 p \tag{E.45}$$

is the ejection speed of the submunition, and *p* is the magnitude of the projectile's spin at the time of fuze function.

In the case when $|\vec{c} \times \vec{y}|$ = 0, both $\vec{d}$ and $\vec{e}$ are in the horizontal plane.

In this case, choose $\vec{d}$ to be the unit vector in the direction of the projection of the initial projectile velocity onto the horizontal plane.

c. Submunition trajectories

The ballistic trajectory of the submunitions can be determined by the same methods as described in sections 3 and 4.

This pattern is defined by the impact point of four virtual submunitions defined relative to the vertical plane of the trajectory of the carrier:

(1) the submunition ejected in the vertical plane above the shell trajectory,
(2) the submunition ejected in the vertical plane below the shell trajectory,
(3) the submunition whose tangential ejection velocity component is normal to the vertical plane in the negative 3-direction,
(4) the submunition whose tangential ejection velocity component is normal to the vertical plane in the positive 3-direction.

The initial velocities for these submunitions at the base separation point are respectively

$$\vec{u}_{lower} = \vec{u}_{carrier} + \Delta u_{s1}\vec{c} - i_D pr_s \vec{e} \qquad (\phi = 180^o) \qquad (E.46)$$

$$\vec{u}_{upper} = \vec{u}_{carrier} + \Delta u_{s1}\vec{c} + i_D pr_s \vec{e} \qquad (\phi = 0^o) \qquad (E.47)$$

$$\vec{u}_{right} = \vec{u}_{carrier} + \Delta u_{s1}\vec{c} - i_D pr_s \vec{d} \qquad (\phi = 90^o) \qquad (E.48)$$

$$\vec{u}_{left} = \vec{u}_{carrier} + \Delta u_{s1}\vec{c} + i_D pr_s \vec{d} \qquad (\phi = 270^o) \qquad (E.49)$$

In cases (3) and (4) it is anticipated that the ejection takes place at such a height that the descent is close to vertical at the end of the terminal phase.

6. Empty Carrier Trajectory

The trajectory of the empty carrier left after the base separation point can be calculated assuming that the carrier has the same aerodynamic properties as the original shell. The empty carrier will at base separation get a velocity, a mass and a moment of inertia, which are different to the original shell. The calculation of the trajectory could be done according to the Modified Point Mass Model in the main text or the Point Mass Model in Annex F.

The velocity of the empty carrier is found by

$$\vec{u}_{ec} = \vec{u}_{carrier} + \Delta u_{ec}\vec{c} \qquad \text{(E.50)}$$

The sign of Δu_{ec} is opposite to Δu_{s1}. The mass of the empty carrier m_{ec}, its moment of inertia $I_{x_{ec}}$, and Δu_{ec} must be entered separately.

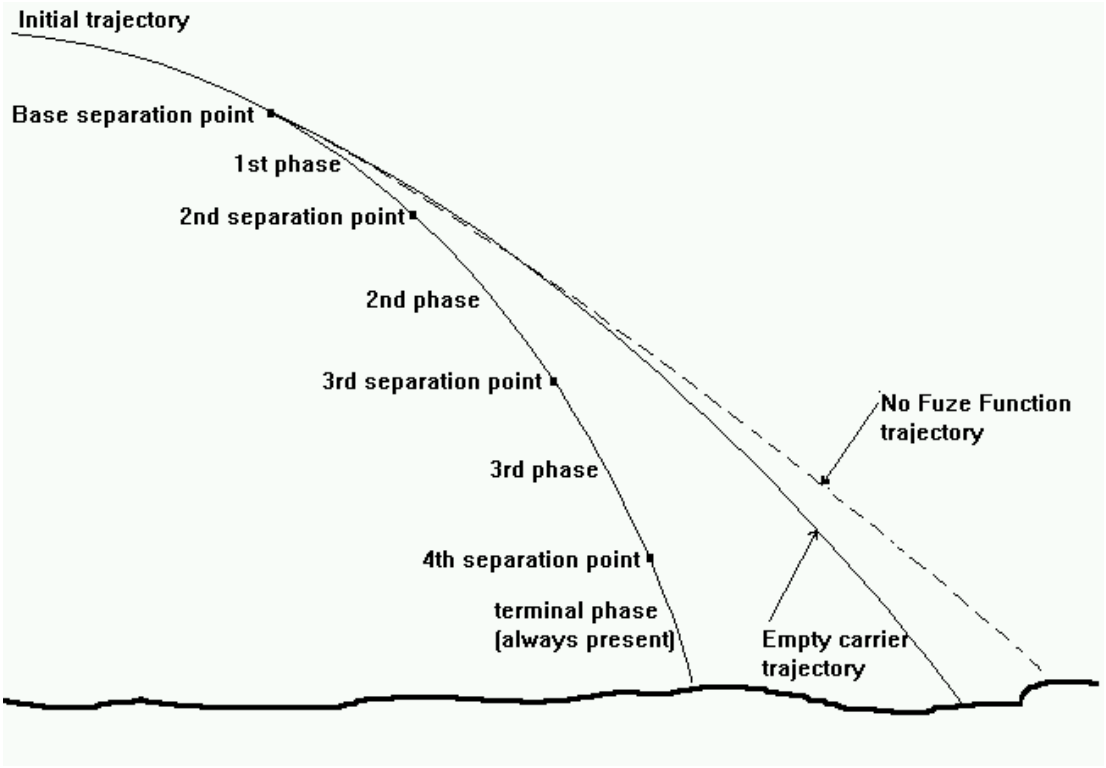

Figure E-1. Definition of concepts for submunition trajectories

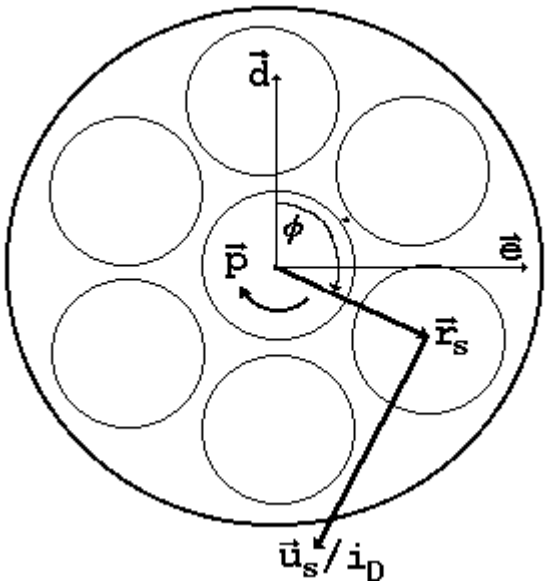

Figure E-2. Geometry of tangential ejection velocity

7. List of Additional Symbols

Symbol	Definition	Units
Alt_w	Altitude of weapon above sea level	m
A_s	Angle of site	mil
$a_0, a_1 \ldots b_0, b_1 \ldots$	Auxiliary coefficients	$none$
$\vec{c}$	Axis of carrier shell	$none$
C_D	Drag coefficient	$none$
C_{spin}	Spin damping coefficient	$none$
$\vec{d}$	Displacement vector due to wind	m
HOB	Height of burst	m
H_z	Upper height of met zone z	m
i_D	Fitting factor for dispersion of submunition	$none$
m_s	Mass of submunition unit	kg
$\vec{o}$	Offset vector	m
QE	Quadrant elevation	mil
r_s	Distance from carrier axis to center of gravity of submunition	m
S	Reference cross sectional area	m^2
t	Simulation time since start of phase	s
T_f	Fall time of submunition (duration of phase)	s
T_s	Time since start of phase	s
$\vec{w}_h$	Horizontal wind velocity	m/s
$\vec{x}_n$	Position at nth separation point	m

z	Met zone index	*none*
Δu	Axial ejection velocity of submunition or velocity change of empty carrier due to ejection	*m/s*
Γ_0	Vertical angle of fall at the start of the phase	*rad*
ϕ	Positional angle of submunition at ejection (clockwise from positive vertical, see Figure E-2)	*rad*
ψ_0	Horizontal angle of fall at the start of the phase	*rad*
ρ	Density of air	kg/m^3

Subscripts	(multiple subscripts occur)
carrier	property of carrier shell at base separation
ec	property of empty carrier shell
n (or a *digit*)	property in terminal phase *n* (or phase number as given by *digit*)
s	property of submunition
1, 2, 3	(when following a comma) component in the 1-2-3 system

Symbols without vector indicator symbolize the scalar value of the vector

ANNEX F POINT MASS TRAJECTORY MODEL

1. The following equations constitute a mathematical model representing the flight of a projectile. The modeling is accomplished by simplifying the modified point mass equations given in Chapter 4 of this document to those representing a point having mass and spin only.

2. Newton's law of motion for a point mass is:

$$\vec{F} = m\dot{\vec{u}} = \overrightarrow{DF} + m\vec{g} + m\vec{\Lambda} \tag{F.1}$$

where:

acceleration due to drag force is:

when *i* is used as a fitting factor,

$$\frac{\overrightarrow{DF}}{m} = -\left(\frac{\pi \rho\, i d^2}{8\, m}\right) C_D\, v\vec{v} \tag{F.2}$$

or when *C* is used as a fitting factor,

$$\frac{\overrightarrow{DF}}{m} = -\left(\frac{\pi \rho m_r}{8\, C m}\right) C_D\, v\vec{v} \tag{F.3}$$

or when f_D is used as a fitting factor,

$$\frac{\overrightarrow{DF}}{m} = -\left(\frac{\pi \rho d^2}{8m}\right)\left(f_D\, C_D\right) v\vec{v} \tag{F.4}$$

acceleration due to gravity is:

$$\vec{g} = -g_0\left(\frac{R^2}{r^3}\right)\vec{r} = -g_0\begin{bmatrix} \frac{X_1}{R} \\ 1-\frac{2X_2}{R} \\ \frac{X_3}{R} \end{bmatrix} \tag{F.5}$$

where: $g_0 = 9.80665\ [\ 1 - .0026 \cos (2\ lat)\ ]$ (F.6)

$$\vec{r} = \vec{X} - \vec{R}, \tag{F.7}$$

$$\vec{R} = \begin{bmatrix} 0 \\ -R \\ 0 \end{bmatrix} \tag{F.8}$$

and $R = 6.356766 \times 10^6$ meters

acceleration due to the effect of the Coriolis force is:

$$\vec{A} = -2(\vec{\omega} \times \vec{u}) \tag{F.9}$$

where:

$$\vec{\omega} = \begin{bmatrix} \Omega \cos(lat) \cos(AZ) \\ \Omega \sin(lat) \\ -\Omega \cos(lat) \sin(AZ) \end{bmatrix} \tag{F.10}$$

and $\Omega = 7.292115 \times 10^{-5}$ *rad/s*

NOTE: For southern hemisphere, *lat* is negative.

3. The magnitude of spin acceleration is given by:

$$\dot{p} = \frac{\pi \rho\ d^4\ p v\ C_{spin}}{8\ I_x} \tag{F.11}$$

where:

$$p = p_0 + \int_0^t \dot{p}\ dt \tag{F.12}$$

is the magnitude of spin at time = t and

$$p_0 = \frac{2\pi\, u_0}{t_c\, d} \tag{F.13}$$

is the magnitude of the initial spin of the projectile at the muzzle.

4. The velocity of the projectile with-respect-to the ground fixed axes at time = t is:

$$\vec{u} = \vec{u}_0 + \int_0^t \dot{\vec{u}}\; dt \tag{F.14}$$

where:
$$\vec{u}_0 = \begin{bmatrix} u_0\ \cos(QE)\cos(\Delta AZ) \\ u_0\ \sin(QE) \\ u_0\ \cos(QE)\sin(\Delta AZ) \end{bmatrix} \tag{F.15}$$

5. The velocity of the projectile with-respect-to the air is given by:

$$\vec{v} = \vec{u} - \vec{w} \tag{F.16}$$

and Mach number by:

$$M = v\ /\ a \tag{F.17}$$

where a is the speed of sound as defined at paragraph 21 on Page 14.

6. The position of the projectile with-respect-to the ground axes is given by:

$$\vec{X} = \vec{X}_0 + \int_0^t \vec{u}\; dt \tag{F.18}$$

where:

$$\vec{X}_0 = \begin{bmatrix} l_W\ \cos(QE)\ \cos(\Delta AZ) \\ X_{2_W} + l_W\ \sin(QE) \\ l_W\ \cos(QE)\ \sin(\Delta AZ) \end{bmatrix} \tag{F.19}$$

is the location of the muzzle, i.e., initial position of the center of mass of the projectile.

7. The position of the projectile with-respect-to the spherical earth's surface is given by the approximation:

$$\vec{E} = \begin{bmatrix} X_1 \\ X_2 + \dfrac{\left(X_1{}^2 + X_3{}^2\right)}{2R} \\ X_3 \end{bmatrix} \qquad \text{(F.20)}$$

8. For some applications, especially where the flight path of the projectile is short, the model described above may be simplified further:

   the effects of height above the earth's surface on gravity may be ignored, in which case

$$\vec{g} = -g_0 \begin{bmatrix} 0 \\ 1 \\ 0 \end{bmatrix} \qquad \text{(F.21)}$$

   the effects of spin of the earth may be ignored, in which case

$$\Omega \equiv 0 \qquad \text{(F.22)}$$

   the effects of projectile spin may be ignored, in which case

$$p_0 = \dot{p} \equiv 0 \qquad \text{(F.23)}$$

   the earth's surface may be considered a flat plane, in which case

$$\vec{E} = \begin{bmatrix} X_1 \\ X_2 \\ X_3 \end{bmatrix} \qquad \text{(F.24)}$$

9. The List of Symbols found at Sections 4.3 and 4.4 of the main document contain all the symbols required for this annex with one exception, namely, C_D is defined as the total drag force coefficient (dimensionless).

10. The List of Data Requirements related to this annex are as follows:

Physical Data	***Symbol***
Initial speed of projectile with-respect-to ground (muzzle velocity)	u_0
Rifling twist at muzzle	t_c
Mass of fuzed projectile	m
Mass of fuzed reference projectile	m_r
Reference diameter	d
Initial axial moment of inertia (optional)	I_{x_0}

Aerodynamic Data	***Symbol***
Total drag force coefficient	C_D
Spin damping moment coefficient (optional)	C_{spin}

a. Fitting Factors for Range Estimation

Since the point mass equations do not explicitly model the effects of yaw of repose, the fitting factors for the range estimation must be used to account for this fact. As a result, the forms will vary from those forms used with the MPM equations. Following are some typical forms used in fire control systems.

Quadrant Elevation Fitting

Ballistic coefficient (C):

$$C = a_0 + a_1(QE) + a_2(QE)^2 + a_3(QE)^3 \qquad \text{(F.25)}$$

Form factor (i):

$$i = b_0 + b_1(QE) + b_2(QE)^2 + b_3(QE)^3 \quad \text{(F.26a)}$$

or

$$i = b_0 + b_1(QE - A_s) + b_2(QE - A_s)^2 + b_3(QE - A_s)^3 \quad \text{(F.26b)}$$

The equations are applicable over the QE intervals bounded by QE_{j-1} to and including QE_j. The functions must be continuous and smooth at each breakpoint. The minimum and maximum values of QE are determined by the weapon and ammunition characteristics but, typically, range from zero mils to the maximum trail angle. The degree of the polynomial is dependent upon the desired quality of the range estimation.

Mach Number Fitting

Drag factor (f_D) can be fitted as a function of Mach number.

b. Drift Correction

Since the point mass equations do not include the drift effects associated with spinning projectiles, the drift (which is perpendicular to the vertical plane containing the line of fire) is generally represented by a function based on the observed fall of shot results. The following are typical expressions for drift expressed in mil:

$$Drift = tan\,(QE)\, f\,(QE) \quad \text{(F.27)}$$

where:

$$f\,(QE) = a_0 + a_1\,(QE) + a_2\,(QE)^2 + a_3\,(QE)^3 \quad \text{(F.28)}$$

or

$$Drift = b_0\, tan\,(QE) + b_1\, tan^2\,(QE) \quad \text{(F.29)}$$

or

$$Drift = c_0\, QE \,/\, (QE + c_1) \qquad \text{(F.30)}$$

or

$$Drift = \arctan\left((d_0 + d_1 T + d_2 T^2 + d_3 T^3)/x_1\right) \qquad \text{(F.31)}$$

where: x_1 is the range (m) to impact along the $\vec{1}$ axis.

or

$$Drift = d_0 + d_1 (SE) + d_2 (SE)^2 + d_3 (SE)^3 \qquad \text{(F.32)}$$

where: the superelevation (mils), SE = QE – Angle of Site.

c. Time of Flight Correction

In order to account for the difference between the actual time of flight (T) and the time of flight predicted by the point mass model the following forms can be used:

$$T = a_0 + a_1 t + a_2 t^2 + a_3 t^3 \qquad \text{(F.33)}$$

Or, if approximating Δt as a function of t,

$$T = t + \Delta t \qquad \text{(F.34)}$$

and $$\Delta t = b_0 + b_1 t + b_2 t^2 + b_3 t^3 \qquad \text{(F.35)}$$

Where the equation is applicable over the time (t) intervals bounded by t_{j-1} to and including t_j. The functions must be continuous and smooth at each breakpoint. The minimum and maximum values of T are determined by the weapon and ammunition characteristics but, typically, range from zero seconds to the maximum time of flight. The degree of the polynomial is dependent upon the desired quality of the time estimation.

ANNEX G COORDINATE CONVERSION REQUIRED BY COURSE CORRECTING FUZES

1. Introduction

This section describes the equations for the coordinate conversions required by course correcting fuzes. There are two coordinate conversions that are required to support course correcting fuzes: gun frame to North, East, Down (NED) and Lat/Long to Earth-Center, Earth-Fixed (ECEF).

The gun frame to NED conversion starts with vectors oriented in a coordinate frame with an origin at mean sea level directly below the trunnion the weapon being fired, where the x_1 axis is tangent to the earth's surface at the origin and points along the gun-target line, the x_2 axis is in the vertical plane perpendicular to the surface of the earth (or ellipsoidal representation of the surface), and the x_3 axis is perpendicular to the plane formed by the other two axes so as to define a right hand Cartesian coordinate system. The x_1 axis is positive in the direction of target, the x_2 axis is positive above the surface of the earth, and the x_3 axis is positive to the right of the gun location when facing the target. The gun-target azimuth is the clockwise angular measure between true north and the gun-target line taken at the gun. The transformation converts to a reference frame where the vectors are represented with the origin of the coordinate frame located at the target, and the axes of the system pointing northward, eastward, and downward. The North-East plane is tangent to the WGS84 ellipsoid at the target. Thus the downward axis is perpendicular to the WGS84 ellipsoid at the target. The North axis is positive north of the target, the East axis is positive east of the target, and the Down axis is positive for points below the target.

The Lat/Long to ECEF conversion, used in the gun frame to NED transformation, converts coordinates given in terms of latitude, longitude, and altitude with respect to the WGS84 ellipsoid to a coordinate system where the origin is the mass center of the earth and the axes are: out through the intersection of the equator and the prime meridian, the rotational axis of the earth, and the final axis is perpendicular to the plane formed by the other two axes so as to satisfy the right-hand rule. The earth is modeled as an ellipsoid as described in the earth model WGS84.

2. Gun Frame to NED Conversion

a. Inputs

The following data are required as input:

1) Gun-target azimuth, Az_{gt} (radians) clockwise with respect to true north
2) Projectile position with respect to gun frame (wrt/ MSL), $\bar{x}$ (m)
3) Projectile velocity components with respect to gun frame, $\bar{u}$ (m/s)
4) Latitude of target, ϕ_{target} (radians)
5) Latitude of gun, ϕ_{gun} (radians)
6) Longitude of target, λ_{target} (radians)
7) Longitude of gun, λ_{gun} (radians)
8) Height of target above WGS84 ellipsoid, h_{target} (m)
9) Height of gun above WGS84 ellipsoid, h_{gun} (m)
10) Height of gun above mean sea level, alt_{gun} (m)

b. Known Values

From the WGS84 model:

$$R_{equator} = 6{,}378{,}137 \text{ meters}$$

$$f = \frac{1}{298.257223563}$$

$$e^2 = 1-(1-f)^2 \cong 0.006694379990141$$

c. Determine ECEF Coordinates

Compute the ECEF coordinates such that the z-axis points northward along the Earth's rotation axis, the x-axis points outward along the intersection of the Earth's equatorial plane and prime meridian, and the y-axis points into the eastward quadrant, perpendicular to the x-z plane so as to satisfy the right-hand rule.

$$N_L = \frac{R_{equator}}{\sqrt{1-e^2\sin^2(\phi_L)}} \tag{G.1}$$

$$\bar{r}_L = \begin{bmatrix} X \\ Y \\ Z \end{bmatrix}_L = \begin{bmatrix} (N_L + h_L)\cos(\phi_L)\cos(\lambda_L) \\ (N_L + h_L)\cos(\phi_L)\sin(\lambda_L) \\ (N_L(1-e^2) + h_L)\sin(\phi_L) \end{bmatrix} \tag{G.2}$$

Where the subscript L can be either the gun or target location.

d. Computation of Direction Cosine Matrix

The direction cosine matrix (DCM) used to transform ECEF coordinates to the NED frame is:

$$\left[\mathrm{DCM}_{\mathrm{L}}\right] = \begin{bmatrix} -\sin(\phi_{\mathrm{L}})\cos(\lambda_{\mathrm{L}}) & -\sin(\phi_{\mathrm{L}})\sin(\lambda_{\mathrm{L}}) & \cos(\phi_{\mathrm{L}}) \\ -\sin(\lambda_{\mathrm{L}}) & \cos(\lambda_{\mathrm{L}}) & 0 \\ -\cos(\phi_{\mathrm{L}})\cos(\lambda_{\mathrm{L}}) & -\cos(\phi_{\mathrm{L}})\sin(\lambda_{\mathrm{L}}) & -\sin(\phi_{\mathrm{L}}) \end{bmatrix} \quad \text{(G.3)}$$

Again the subscript L is either the gun or target location.

e. Determine the Projectile Location in a Gun-Centered NED Frame

This is accomplished by rotating about the opposite of the gun-target azimuth about the x_2/Down axis.

$$\overline{\mathrm{x}}_{\mathrm{NED}_{\mathrm{gun}}} = \begin{bmatrix} \mathrm{North}_{\mathrm{gun}} \\ \mathrm{East}_{\mathrm{gun}} \\ \mathrm{Down}_{\mathrm{gun}} \end{bmatrix} = \begin{bmatrix} \cos(Az_{\mathrm{gt}}) & 0 & -\sin(Az_{\mathrm{gt}}) \\ \sin(Az_{\mathrm{gt}}) & 0 & \cos(Az_{\mathrm{gt}}) \\ 0 & -1 & 0 \end{bmatrix} \begin{bmatrix} x_1 \\ x_2 - alt_{\mathrm{gun}} \\ x_3 \end{bmatrix} \quad \text{(G.4)}$$

f. Determine the ECEF Vector Components from Gun-to-Projectile

Transform the projectile NED vector into a vector oriented in the ECEF frame using the gun's DCM.

$$\left[\mathrm{DCM}_{\mathrm{gun}}\right]\overline{\mathrm{X}}_{\mathrm{gun}} = \overline{\mathrm{x}}_{\mathrm{NED}_{\mathrm{gun}}} \quad \text{(G.5)}$$

Note: Solve for $\overline{\mathrm{X}}_{\mathrm{gun}}$

g. Calculate the ECEF Vector Components from Target-to-Projectile

This is done by, first, finding the vector from the center of the ellipsoid to the projectile. This vector is simply the sum of the gun ECEF vector and the gun-to-projectile ECEF vector. Then by subtracting from this center-of-ellipsoid-to-projectile vector the target ECEF vector.

$$\overline{X}_{target} = \bar{r}_{gun} + \overline{X}_{gun} - \bar{r}_{target} \quad \text{(G.6)}$$

h. Obtain the Position of the Projectile in the NED Target-Centered Frame

Transform the target-to-projectile ECEF vector into a vector oriented in the target's NED frame using the target's DCM.

$$\bar{x}_{NED} = \left[DCM_{target}\right]\overline{X}_{target} \quad \text{(G.7)}$$

i. Obtain the Velocity of the Projectile in the NED Target-Centered Frame

This transformation is similar to the steps above.

1) Determine the Projectile Velocity in a Gun-Centered NED Frame

This is accomplished by rotating about the opposite of the azimuth to target about the x_2/Down axis.

$$\bar{u}_{NED_{gun}} = \begin{bmatrix} \dot{North}_{gun} \\ \dot{East}_{gun} \\ \dot{Down}_{gun} \end{bmatrix} = \begin{bmatrix} \cos(Az_{gt}) & 0 & -\sin(Az_{gt}) \\ \sin(Az_{gt}) & 0 & \cos(Az_{gt}) \\ 0 & -1 & 0 \end{bmatrix} \begin{bmatrix} u_1 \\ u_2 \\ u_3 \end{bmatrix} \quad \text{(G.8)}$$

2) Determine the ECEF Vector Components of the Projectile Velocity

Transform the projectile NED vector into a vector oriented in the ECEF frame using the gun's DCM.

$$\left[DCM_{gun}\right]\overline{U} = \bar{u}_{NED_{gun}} \quad \text{(G.9)}$$

Note: Solve for $\overline{U}$

3) Obtain the Velocity of the Projectile in the NED Target-Centered Frame

Transform the projectile ECEF vector into a vector oriented in the target's NED frame using the target's DCM.

$$\bar{u}_{NED} = \left[DCM_{target}\right]\bar{U} \qquad \text{(G.10)}$$

3. Computation of Euler Angles in the NED Frame

The Euler angles (ψ, θ) of the projectile velocity in the NED frame are:

$$\psi = \tan^{-1}\frac{u_E}{u_N} \qquad -\pi \le \psi \le \pi \qquad \text{(G.11)}$$

$$\theta = \tan^{-1}\frac{-u_D}{\sqrt{u_E^2 + u_N^2}} \qquad -\frac{\pi}{2} \le \theta \le \frac{\pi}{2} \qquad \text{(G.12)}$$

Where u_E, u_N and u_D are, respectively, the eastward, northward and downward components of projectile velocity in the target-centered NED frame.

4. List of Symbols

Symbol	Definition	Units
alt_{gun}	Altitude of the gun wrt/ mean sea level	m
Az_{gt}	Gun-target azimuth	rad
DCM	Direction cosine matrix	-
DCM_{gun}	Direction cosine matrix to convert ECEF to NED for the gun	-
DCM_{target}	Direction cosine matrix to convert ECEF to NED for the target	-
e	Eccentricity	-
ECEF	Earth-centered, earth-fixed coordinate system	-
f	Flattening of the earth	-

h	Height above WGS84 ellipsoid	*m*
h_{gun}	Height of gun above WGS84 ellipsoid	*m*
h_{target}	Height of target above WGS84 ellipsoid	*m*
MSL	Mean sea level	-
N	Distance from surface of ellipsoid to polar axis along line normal to the ellipsoid surface	*m*
R_{equator}	Equatorial radius of the earth	*m*
$\bar{\text{r}}_{\text{gun}}$	ECEF position vector of gun	*m*
$\bar{\text{r}}_{\text{target}}$	ECEF position vector of target	*m*
$\bar{\text{u}}$	Projectile velocity vector in the gun frame	*m/s*
u_1, u_2, u_3	Components of projectile velocity in the gun frame	*m/s*
$\bar{\text{u}}_{\text{NED}}$	Projectile velocity vector in target-centered NED frame	*m/s*
$u_{\text{N}}, u_{\text{E}}, u_{\text{D}}$	Northward, eastward and downward components of projectile velocity in target-centered NED frame	*m/s*
$\bar{\text{u}}_{\text{NED}_{\text{gun}}}$	Projectile velocity vector in gun-centered NED frame	*m/s*
$\bar{\text{U}}$	Projectile velocity vector in earth-centered, earth-fixed coordinate system	*m/s*
x_1 axis	Axis which runs from the gun to the target	-
x_2 axis	Axis oriented perpendicular to the WGS84 model's surface of the earth	-
x_3 axis	Axis oriented perpendicular to the x1-x2 plane so as to satisfy the right-hand rule	-
$\bar{\text{x}}$	Projectile position vector in the gun frame	*m*

x_1, x_2, x_3	Components of projectile position in the gun frame (x2 component given wrt/ mean sea level)	m
$\overline{\mathrm{x}}_{\mathrm{NED}}$	Projectile position vector in target-centered NED frame	m
$\overline{\mathrm{x}}_{\mathrm{NED_{gun}}}$	Projectile position vector in gun-centered NED frame	m
$\overline{\mathrm{X}}_{\mathrm{gun}}$	Gun-to-projectile vector in earth-centered, earth-fixed coordinate system	m
$\overline{\mathrm{X}}_{\mathrm{target}}$	Target-to-projectile vector in earth-centered, earth-fixed coordinate system	m
$\overline{\mathrm{X}}_{\mathrm{NED_{target}}}$	Projectile position vector in target-centered NED frame	m
λ	Longitude	rad
λ_{gun}	Longitude of gun	rad
$\lambda_{\mathrm{target}}$	Longitude of target	rad
ϕ	Geodetic latitude	rad
ϕ_{gun}	Geodetic latitude of gun	rad
ϕ_{target}	Geodetic latitude of target	Rad

ANNEX H ADDITIONAL TERMS FOR GUIDED MUNITIONS

1. Introduction

This annex presents two methods for extending the use of a modified point mass trajectory for guided munitions. The first method concerns guided munitions using Global Positioning System (GPS) and Inertial Navigation System (INS) incorporating estimates for the vertical and horizontal angles of yaw to simulate the flight of the guided munition. The second method of guidance concerns maintained munition pointing, or attitude hold gliding, for laser guided munitions. The equations in this annex are to be used during the guided and terminal phases of the trajectory, where the munition departs from a ballistic trajectory $\left(t \geq t_g\right)$.

2. Modified Point Mass for GPS Guided Munitions

The figure below shows the phases of a trajectory for GPS guided munitions. The trajectory follows three phases: ballistic, proportional navigation, and terminal. The first phase is an unguided ballistic phase occurring from muzzle exit until the projectile reaches the time to initiate guidance, t_g. Once $t > t_g$, the trajectory is modeled with proportional navigation until the trajectory reaches terminal conditions. Once in the terminal phase, the trajectory is modeled as a beam rider to the target impact point.

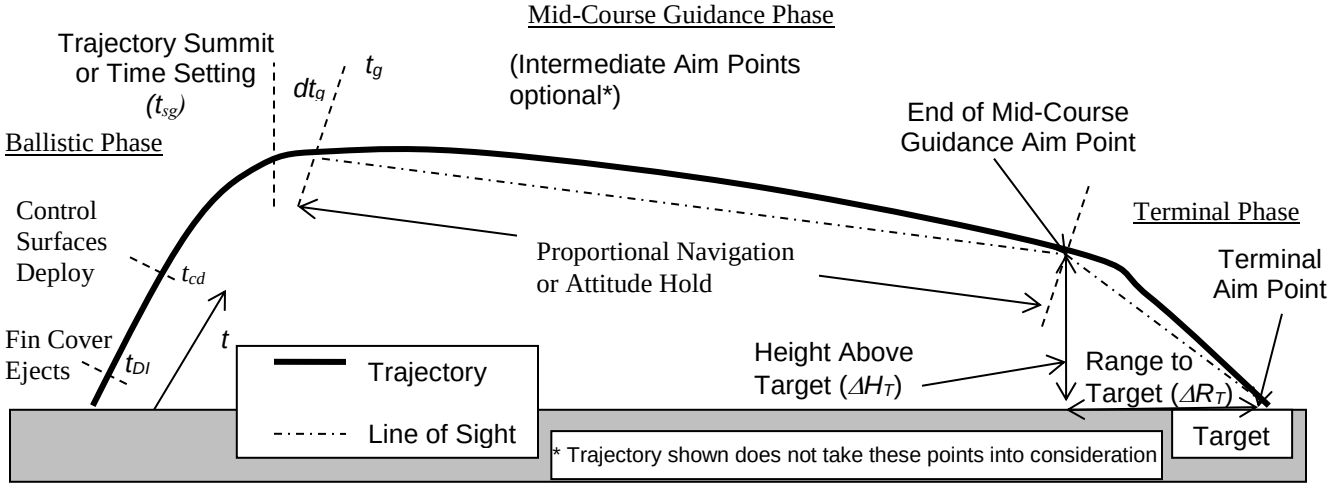

Figure H-1. Phases of GPS Guided Munition Trajectory

If the control surfaces are deployed at time t_{cd} during the ballistic phase, the form factor and zero-yaw drag force coefficient are $i_{b_{cd}}$ and $C_{D_{0g}}$ respectively.

3. Pointing of Munition

The pointing of the munition is assumed to be the same as the pointing of the velocity vector. The projection of the velocity vector on the vertical (γ_v) and horizontal (γ_h) planes is given by:

$$\gamma_v = \arcsin\left(\frac{v_2}{v}\right) \tag{H.1}$$

$$\gamma_h = \arctan\left(\frac{v_3}{v_1}\right) \tag{H.2}$$

Then define a unit vector along the longitudinal axis of the munition including an estimate of the angles of yaw to simulate the guidance technologies during the guidance phase.

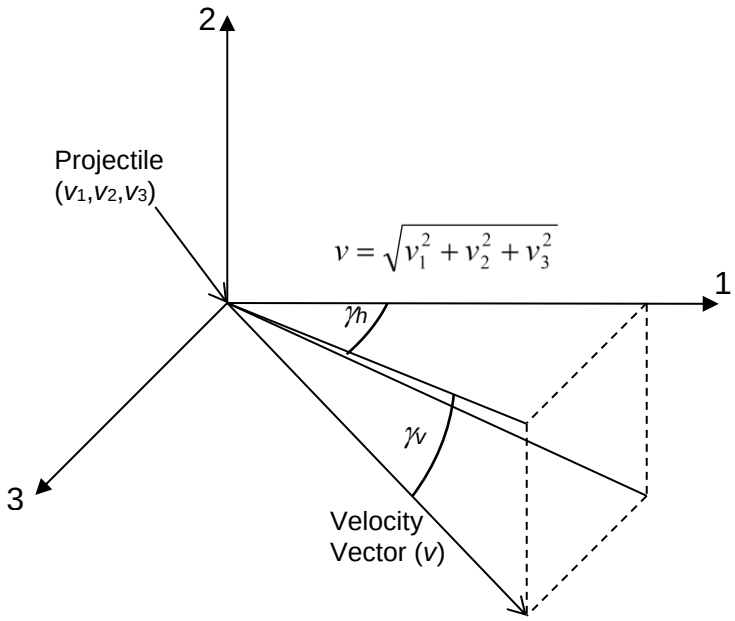

Figure H-2. Angles for Pointing of Munition

4. Proportional Navigation Guidance to an Aim Point

The unit vector along the longitudinal axis of the munition to proportionally navigate to an aim point beginning at the initiation of guidance (t_g) is given by:

$$\vec{x} = \begin{Bmatrix} \cos(\gamma_v + f_{\alpha_v}\alpha_{v_{pn}} + f_{gb}\alpha_{v_{gb}} + f_{rb_v}\alpha_{v_{rb}})\cos\left[\gamma_h + \left(\frac{f_{\alpha_h}\alpha_{h_{pn}}}{\cos\gamma_v}\right)\right] \\ \sin(\gamma_v + f_{\alpha_v}\alpha_{v_{pn}} + f_{gb}\alpha_{v_{gb}} + f_{rb_v}\alpha_{v_{rb}}) \\ \cos(\gamma_v + f_{\alpha_v}\alpha_{v_{pn}} + f_{gb}\alpha_{v_{gb}} + f_{rb_v}\alpha_{v_{rb}})\sin\left[\gamma_h + \left(\frac{f_{\alpha_h}\alpha_{h_{pn}}}{\cos\gamma_v}\right)\right] \end{Bmatrix} \quad \text{(H.3)}$$

where:

$$\alpha_{v_{pn}} = -\frac{8\,m\,N_v\dot{\lambda}_v}{\pi\,\rho\,d^2\left(C_{L_{\alpha_g}} + C_{L_{\alpha_g{}^3}}\alpha_g{}^2\right)v} \quad \text{(H.4)}$$

$$\alpha_{h_{pn}} = -\frac{8\,m\,N_h\dot{\lambda}_h}{\pi\,\rho\,d^2\left(C_{L_{\alpha_g}} + C_{L_{\alpha_g{}^3}}\alpha_g{}^2\right)v} \quad \text{(H.5)}$$

N_v and N_h are the vertical and horizontal plane navigation ratios, respectively. They are treated as functions of time from time-of-guidance ($t - t_g$).

The pointing angle or angles of line-of-sight vector (from munition to aim point) in inertial space are obtained from the known aim point position and the munition position (for all aim points in the guidance phase) from GPS by:

$$\lambda_v = \arctan\left(\frac{X_{2_{ap}} - X_2}{\sqrt{\left(X_{1_{ap}} - X_1\right)^2 + \left(X_{3_{ap}} - X_3\right)^2}}\right) \quad \text{(H.6)}$$

$$\lambda_h = \arctan\left(\frac{X_{3_{ap}} - X_3}{X_{1_{ap}} - X_1}\right) \quad \text{(H.7)}$$

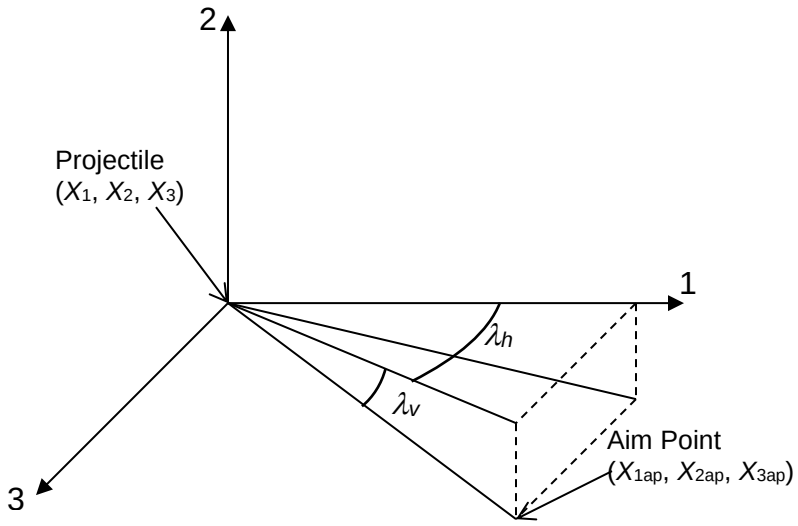

Figure H-3. Pointing Angles (Line of Sight Vector)

Then the rate of change of the pointing angles to the aim point are given by:

$$\dot{\lambda}_v = \frac{\left[\left(X_{1_{ap}} - X_1\right)^2 + \left(X_{3_{ap}} - X_3\right)^2\right]\dot{X}_2 - \left(X_{2_{ap}} - X_2\right)\left[\left(X_{1_{ap}} - X_1\right)\dot{X}_1 + \left(X_{3_{ap}} - X_3\right)\dot{X}_3\right]}{\left[\left(X_{1_{ap}} - X_1\right)^2 + \left(X_{2_{ap}} - X_2\right)^2 + \left(X_{3_{ap}} - X_3\right)^2\right]\sqrt{\left(X_{1_{ap}} - X_1\right)^2 + \left(X_{3_{ap}} - X_3\right)^2}} \quad \text{(H.8)}$$

$$\dot{\lambda}_h = \frac{\left(X_{1_{ap}} - X_1\right)\dot{X}_3 - \left(X_{3_{ap}} - X_3\right)\dot{X}_1}{\left(X_{1_{ap}} - X_1\right)^2 + \left(X_{3_{ap}} - X_3\right)^2} \quad \text{(H.9)}$$

gravity bias ($\alpha_{v_{gb}}$), which is determined as a function of time, is given by:

$$\alpha_{v_{gb}} = -\frac{8 g_2 m \cos\gamma_v}{\pi\, \rho\, d^2 \left(C_{L_{\alpha_g}} + C_{L_{\alpha_g{}^3}}\, \alpha^2{}_g\right) v^2} \quad \text{(H.10)}$$

NOTE: g_2 represents the vertical component of the gravity vector.

and rate bias ($\alpha_{v_{rb}}$), which is determined as a function of ground distance to aim point and provides the trajectory shaping, is given by:

$$\alpha_{v_{rb}} = -\frac{8m\left(\gamma_{v_{AP}} - \gamma_v\right)RB_v}{\pi\,\rho\,d^2\left(C_{L_{\alpha_g}} + C_{L_{\alpha_g{}^3}}\,\alpha^2{}_g\right)v^2} \qquad \text{(H.11)}$$

Where RB_v is the value of the rate bias term for the ground distance to aim point at time *t*.

To compensate for the approximations in the equations of motion, the fitting factors f_{α_v}, f_{α_h}, f_{gb}, and f_{rb_v} are applied in order to match the computed and observed results. The factor on gravity bias (f_{gb}) is reduced linearly starting at a distance from the aim point to 0 at a closer distance to the aim point. Fitting factors are defined in Table H-1.

The total angle of yaw during the guidance phase, $\vec{\alpha}_g$, is given by:

$$\vec{\alpha}_g = \vec{x} - \left(\vec{x}\cdot\vec{v}\right)\left(\frac{\vec{v}}{v^2}\right) \qquad \text{(H.12)}$$

5. Maximum Angles of Yaw

The total angle of yaw combining the horizontal and vertical directions will not be allowed to exceed certain constraints. A vertical upward angle of attack $\left(f_{\alpha_v}\alpha_{v_{pn}} + f_{gb}\alpha_{v_{gb}} + f_{rbv}\alpha_{rbv}\right)$ will increase the range by increasing lift and reduce the range by increasing the drag. These opposing effects are balanced to avoid a decrease in maximum range by defining a vertical upward angle of attack limit $\alpha_{vu_{\max}}$ that yields the maximum lift-to-drag ratio; and $\left(f_{\alpha_h}\alpha_{h_{pn}}\right)$ must vanish as $\left(f_{\alpha_v}\alpha_{v_{pn}} + f_{gb}\alpha_{v_{gb}} + f_{rbv}\alpha_{rbv}\right)$ approaches $\alpha_{vu_{\max}}$ or the total drag will be increased beyond the maximum lift-to-drag ratio.

Therefore, for $\left(f_{\alpha_v}\alpha_{v_{pn}} + f_{gb}\alpha_{v_{gb}} + f_{rbv}\alpha_{rbv}\right) > 0$: the limitation on the vertical upward angle of yaw $\left(f_{\alpha_v}\alpha_{v_{pn}} + f_{gb}\alpha_{v_{gb}} + f_{rbv}\alpha_{rbv}\right)$ is $\alpha_{vu_{\max}}$. The limitation on $\left(f_{\alpha_h}\alpha_{h_{pn}}\right)$ will be dependent on the magnitude of $\left(f_{\alpha_v}\alpha_{v_{pn}} + f_{gb}\alpha_{v_{gb}} + f_{rbv}\alpha_{rbv}\right)$. If $\alpha_{vu_{\max}}$ is the limit on $\left(f_{\alpha_h}\alpha_{h_{pn}}\right)$ when $\left(f_{\alpha_v}\alpha_{v_{pn}} + f_{gb}\alpha_{v_{gb}} + f_{rbv}\alpha_{rbv}\right) = 0$, then when $\left(f_{\alpha_v}\alpha_{v_{pn}} + f_{gb}\alpha_{v_{gb}} + f_{rbv}\alpha_{rbv}\right) > 0$, $\alpha_{vu_{\max}}$ must be

reduced to prevent $\left(f_{\alpha_h}\alpha_{h_{pn}}\right)$ from adding drag that would compromise the maximum lift-to-drag criteria.

The horizontal angle of attack is limited as follows:

$$\left|\left(f_{h_v}\ \alpha_{h_{pn}}\right)_{\max}\right| = \alpha_{h_{\max}}\sqrt{1-\frac{\left(f_{\alpha_v}\ \alpha_{v_{pn}} + f_{gb}\ \alpha_{v_{gb}} + f_{rbv}\alpha_{rbv}\right)^2}{\alpha_{vu_{\max}}{}^2}} + \alpha_{hg} \qquad \text{(H.13)}$$

For $\left(f_{\alpha_v}\alpha_{v_{pn}} + f_{gb}\alpha_{v_{gb}} + f_{rbv}\alpha_{rbv}\right) \le 0$: the maximum lift-to-drag ratio no longer applies, since the downward lift and drag no longer oppose one another, so the primary limiter can be $\left(f_{\alpha_h}\alpha_{h_{pn}}\right)$.

Therefore, for $\left(f_{\alpha_v}\alpha_{v_{pn}} + f_{gb}\alpha_{v_{gb}} + f_{rbv}\alpha_{rbv}\right) \le 0$: the limitation on $\left|\left(f_{\alpha_h}\alpha_{h_{pn}}\right)\right|$ will be $\alpha_{h_{\max}}$ and the limitation on $\left(f_{\alpha_v}\alpha_{v_{pn}} + f_{gb}\alpha_{v_{gb}} + f_{rbv}\alpha_{rbv}\right)$ will be dependent on the magnitude of $\left(f_{\alpha_h}\alpha_{h_{pn}}\right)$ and the maximum vertical downward angle of attack $\alpha_{vd_{\max}}$.

The vertical downward angle of attack is limited as follows:

$$\left(f_{\alpha_v}\ \alpha_{v_{pn}} + f_{gb}\ \alpha_{v_{gb}} + f_{rbv}\alpha_{rbv}\right)_{\max} = -\alpha_{vd_{\max}}\sqrt{1-\frac{\left(f_{\alpha_h}\ \alpha_{h_{pn}}\right)^2}{\alpha_{h_{\max}}{}^2}} \qquad \text{(H.14)}$$

The maximum vertical upward ($\alpha_{vu_{\max}}$), vertical downward ($\alpha_{vd_{\max}}$), and horizontal ($\alpha_{h_{\max}}$) angles of attack are functions of Mach number.

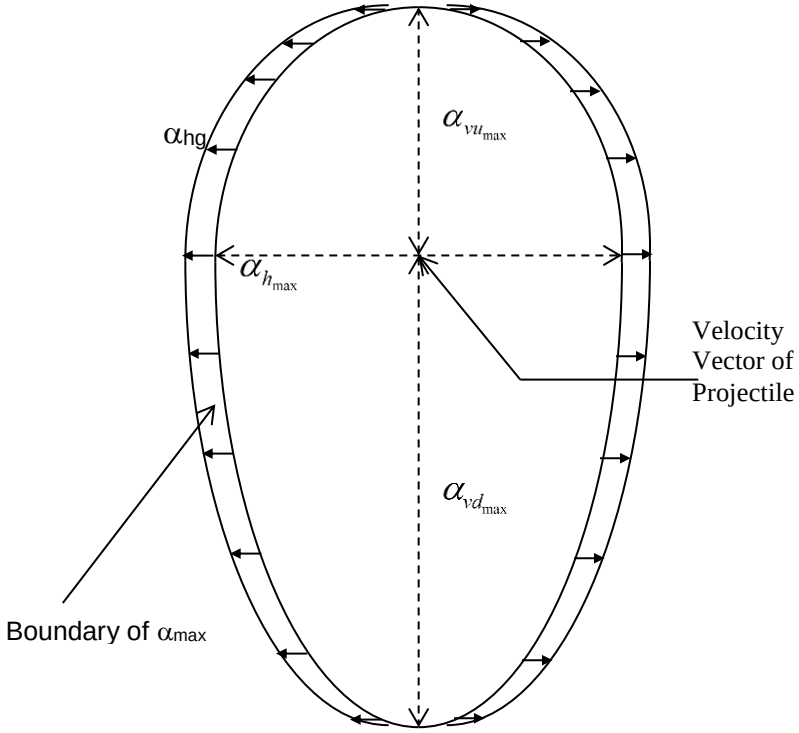

Figure H-4. Maximum Angles of Yaw

α_{hg} is the additional guided horizontal angle of yaw constant applied to the horizontal guided yaw in order to provide horizontal maneuverability when the projectile was at the alpha vertical max/min.

6. Terminal Phase (Beam Rider):

The following equations compute the vector of the velocity of the projectile in relation to the line-of-sight to the target angle and the angle of fall. The terminal phase is initiated when both of the following conditions occur after t_g:

$$\lambda_v \leq \lambda_{v\max} \quad \textbf{\textit{and}} \quad \gamma_v \leq \gamma_{v\max} \tag{H.15}$$

Proportional navigation yields unpredictable behavior as γ_v approaches a vertical dive angle. If the above conditions are met, equation H.12 must be modified as follows in

order to compensate for this limitation in proportional navigation for the remainder of the trajectory:

$$\vec{\alpha}_g = \frac{v^2\left(\Delta\vec{E}\right) - \left(\vec{v}\cdot\Delta\vec{E}\right)\vec{v}}{v^2\left(\left|\Delta\vec{E}\right|\right)} \tag{H.16}$$

where:

$$\Delta\vec{E} = \begin{bmatrix} E_{1_{ap}} - E_1 \\ E_{2_{ap}} - E_2 \\ E_{3_{ap}} - E_3 \end{bmatrix} \tag{H.17}$$

To give the projectile a realistic flight path and to avoid an immediate turn of the projectile to the line-of-sight vector, equation H.17 is limited with a predefined maximum angle of attack α_{gmax}, in radians, such that once α_g exceeds this angle the yaw vector becomes the following:

$$\vec{\alpha}_g = \alpha_{g\max}\left(\frac{\vec{\alpha}_g}{\alpha_g}\right) \tag{H.18}$$

The lift factor f_L is also modified by the terminal lift factor term $f_{Lt,}$ such that the lift factor becomes the following:

$$f_L = f_{Lt}\left(f_L\right) \tag{H.19}$$

7. Fitting Factor

Table H-1. Fitting Factors

Fitting Factor Data Requirement	***Symbol***	***Function***
Vertical angle of yaw*	f_{α_v}	$f_{\alpha_v} = a_0 + a_1(\lambda_v) + a_2(\lambda_v)^2$
Gravity Bias angle of yaw*	f_{gb}	$f_{gb} = a_0 + a_1(\lambda_v) + a_2(\lambda_v)^2$
Horizontal angle of yaw*	f_{α_h}	$f_{\alpha_h} = a_0 + a_1(\lambda_h) + a_2(\lambda_h)^2$
Rate Bias*	f_{rb_v}	$f_{rb_v} = a_0 + a_1(\lambda_v) + a_2(\lambda_v)^2$
Lift During Terminal Phase	f_{L_t}	$f_{L_t} = a_0$

*Note: λ_h and λ_v are evaluated at t_g

8. Maintain Munition Pointing (Attitude Hold) for Laser Guided Munition

Mid-Course Guidance Phase

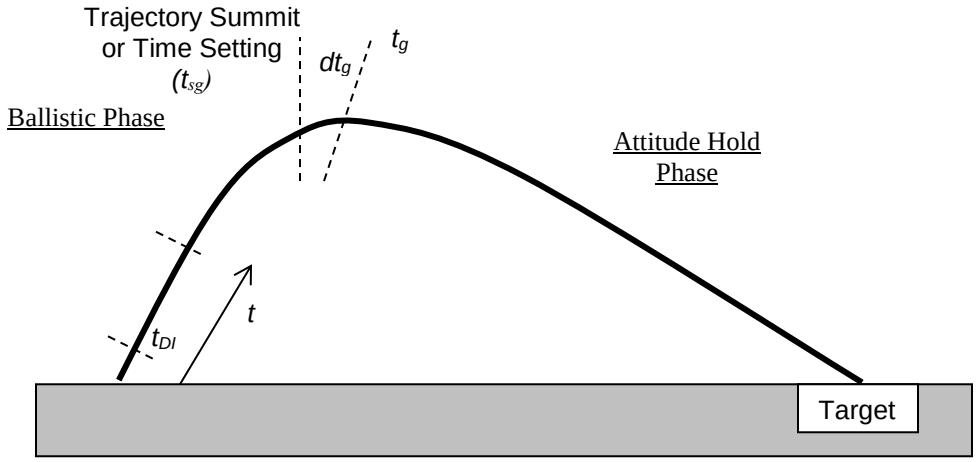

Figure H-5. Phases of Laser Guide Munition Trajectory

Laser guided munitions follow a ballistic trajectory until time *t* is greater than the sum of the time setting t_{sg} and delay time d_{tg}. At the time of glide initiation t_g, munition pointing of the projectile is maintained. This is represented by the following equation:

$$\vec{x} = \begin{Bmatrix} \cos\gamma_{v_{t_g}} & \cos\gamma_{h_{t_g}} \\ \sin\gamma_{v_{t_g}} & \\ \cos\gamma_{v_{t_g}} & \sin\gamma_{h_{t_g}} \end{Bmatrix} \qquad \text{(H.20)}$$

The unit vector remains fixed as above as long as α_g, the total angle of yaw during the guidance phase, is $\leq \alpha_{vu_{\max}}$. When $\alpha_g > \alpha_{vu_{\max}}$ due to the path of the trajectory falling away from the pointing vector of the munition, the attitude must be allowed to drift downward to prevent α_g from becoming too large and causing the munition to stall.

During guidance, when $\alpha_g > \alpha_{vu_{\max}}$ the unit vector is:

$$\vec{x} = \begin{Bmatrix} \cos\left(\gamma_{v_{t_g}} + \alpha_{vu_{\max}}\right)\cos\gamma_{h_{t_g}} \\ \sin\left(\gamma_{v_{t_g}} + \alpha_{vu_{\max}}\right) \\ \cos\left(\gamma_{v_{t_g}} + \alpha_{vu_{\max}}\right)\sin\gamma_{h_{t_g}} \end{Bmatrix} \qquad \text{(H.21)}$$

9. List of Additional Symbols

Symbol	Definition	Units
$C_{D_{0_g}}$	Zero yaw drag force coefficient with control surfaces deployed	*none*
$C_{L_{\alpha_g}}$	Lift force coefficient during guidance phase	*1/rad*
$C_{L_{\alpha^3{}_g}}$	Cubic lift force coefficient during guidance phase	$1/rad^3$
dt_g	Time between the end of ballistic phase and start of guidance (t_g)	*s*
f_{α_v}	Fitting factor on vertical angle of yaw	*none*
f_{α_h}	Fitting factor on horizontal angle of yaw	*none*
f_{gb}	Fitting factor on gravity bias	*none*
f_{gb}	Fitting factor on vertical rate bias	*none*
f_{Lt}	Fitting factor on terminal lift factor	*none*
$i_{b_{cd}}$	Form factor during ballistic phase with control surfaces deployed	*none*
N_v	Vertical plane navigation ratio	*none*
N_h	Horizontal plane navigation ratio	*none*
RB_v	Vertical Rate Bias	*none*
t_{cd}	Time-of-control surfaces deployment	*s*
t_g	Time-of-guidance or glide	*s*

t_{sg}	Time-setting for-guidance or glide	s
v_1	Velocity along 1-axis	m/s
v_2	Velocity along 2-axis	m/s
v_3	Velocity along 3-axis	m/s
X_1	Position of projectile along 1-axis	m
X_2	Position of projectile along 2-axis	m
X_3	Position of projectile along 3-axis	m
$X_{1_{ap}}$	Position of aim point in the ground-fixed coordinate system along 1-axis	m
$X_{2_{ap}}$	Position of aim point in the ground-fixed coordinate system along 2-axis	m
$X_{3_{ap}}$	Position of aim point in the ground-fixed coordinate system along 3-axis	m
α_g	Angle of yaw during guidance	rad
$\vec{\alpha}_g$	Total angle of yaw during guidance phase	rad
α_{h_g}	Guided horizontal angle of yaw constant	rad
$\alpha_{h_{\max}}$	Maximum horizontal angle of attack	rad
$\alpha_{h_{pn}}$	Proportional navigation horizontal angle of yaw	rad
$\alpha_{\max}$	Maximum angle of attack	rad

$\alpha_{vd_{\max}}$	Maximum vertical downward angle of attack	rad
$\alpha_{v_{gb}}$	Gravity bias vertical angle of yaw	rad
$\alpha_{v_{pn}}$	Proportional navigation vertical angle of yaw	rad
α_{rbv}	Vertical Rate Bias vertical angle of yaw	rad
$\alpha_{vu_{\max}}$	Maximum vertical upward angle of attack	rad
ΔH_T	Difference in height between the End of Mid-Course Guidance Aim Point and the target	m
ΔR_T	Difference in range between the End of Mid-Course Guidance Aim Point and the target	m
γ_h	Angle of projection on the horizontal plane	rad
γ_v	Angle of projection on the vertical plane	rad
λ_h	Horizontal inertial line-of-sight angle	rad
λ_v	Vertical inertial line-of-sight angle	rad

ANNEX I GLOSSARY OF TERMS

1. Reference Frame and Axes

All vectors have as a frame of reference a right-handed, orthonormal, ground-fixed, Cartesian coordinate system (and) where:

a. the origin is the point where the local vertical line, perpendicular to the surface of the geoid, through the weapon trunnion, intersects the geoid.

b. the axis is the intersection of the vertical plane of fire and the horizontal plane and pointing along the gun to target line.

c. the axis is parallel to the gravity vector, , and opposite in direction.

d. the axis completes the right-handed coordinate system.

The geoid is the surface within or around the earth that is everywhere normal to the direction of gravity and coincides with mean sea level.

2. Geophysical Approximations

The following geophysical approximations are used in this document.

a. The geoid is locally approximated by a sphere with a radius (R) of 6,356,766 metres.

b. The gravitational acceleration, , has the scalar magnitude

$$g_0 = 9.80665\ [1 - .0026 \cos (2\ lat)]$$

at the surface of the above-mentioned sphere and is inversely proportional to the square of the distance from the center of the sphere. The term *"lat"* is the latitude of the origin of the coordinate system.

3. Coriolis

The origin of the coordinate system is fixed to the rotating earth, therefore, a Coriolis acceleration term, , is included.

4. Yaw of Repose

The Yaw of Repose is defined by an approximation to the particular solution of the classical linearized equations of yawing motion for a dynamically stable projectile possessing at least trigonal symmetry.

NOTE: Based on comparisons of test firings and modified point mass simulations, it has been determined that quadrant elevations corresponding to a yaw of repose of 0.6 radians provide a good approximation of a weapon system's practical maximum quadrant elevation. Quadrant elevations exceeding this limit can lead to erratic flight behavior reflected by increased dispersion in the deflection plane. Details can be found in the reference, Collings, W.Z. and Lieske, R.F., "A study of Artillery Shell Drift at High Angle of Fire Using Solar Aspect Sensors," BRL-MR-2244, U.S. Army Ballistic Research Laboratory, Aberdeen Proving Ground, Maryland, November 1972.

5. Windage Jump

Windage Jump corrects for the effect of a transient yaw caused by a wind shear. This gives the "Modified Point Mass Model" the ability to perform the correct second order response to wind, range effect due to a cross wind, and the deflection effect due to a range wind.

6. Fitting

To compensate for the approximations in the "Lieske Modified Point Mass Model" and the aerodynamic data, certain fitting factors are applied in order to create correspondence between the computed and the observed values of range, deflection and the time of flight.

Two fitting systems are used, quadrant elevation or Mach number as shown in Table I-1 below:

Table I-1. Fitting Data

Fitting to	***Fitting Data as a Function of***	
	Quadrant Elevation ***[One function for each charge]***	***Mach Number*** ***[Same function for all charges]***
First Order Range, all elevations	*Form factor: i (Drag factor: $f_D = 1$)	Drag factor: f_D (Form factor: $i = 1$)
Drift	Lift factor: f_L	Lift factor: f_L
Second Order Range, high angle	Yaw drag factor: Q_D	Yaw drag factor: Q_D
Vertex height and time of flight	Magnus force factor: Q_M	Magnus force factor: Q_M

*In many countries a ballistic coefficient, $C = m_r / i\, d^2$, is in use as a fitting factor instead of the non-dimensional form factor i.

ANNEX J SELECTED BIBLIOGRAPHY

Title	Topic
Textbook of Ballistics and gunnery. Volumes I and II, Her Majesty's Stationary Office, London, 1987	Complete general background to trajectory modeling P(I) (External Ballistics) and use of MPM P(III) (Fire Control Data).
Equations of Motion for a Modified Point Mass Trajectory. R. Lieske & M. Reiter, Feb 1966, LCB 199	Definition and derivation of original model
The Modified Point Mass Trajectory Model, NATO D/161 (UK Source)	Specifications of Model for current use by NATO countries
Introduction to Equation of Motion in Ballistics (and Related Topics), W.G. Dotson, Jr., BRL 1964	Mathematical description of point mass trajectories in ballistics
Äussere Ballistick, H. Molitz, R. Strobel, Springer Verlag, 1963	General textbook on ballistics. Chapter: Lineares Widerstandsgesetz (linear drag law)
American Standard Letter Symbols for Aeronautical Sciences, ASA Y 10.7-1954	NACA Aerodynamic Symbols
The Calibration of a Modified Point Mass Model by Mach Number Fitting SCICON Jan 1982	Reports use of linearized MPM to aid trials design and automated analysis techniques.
Procedures to Determine the Fire Control Inputs for Use in Fire Control Systems. NATO STANAG 4144	Specified measurements to be taken during R&A trials and gives some indication of numbers of rounds that might be fired.
A note on recent progress in the design and analysis of Ballistic Trials of Artillery Shells. P. Fitch, RARDE Branch memo 31/1980	Short resume of first generation analysis method. Contains references to relevant analysis work on the subject.

Title	Topic
A Study of Design and Analysis Methods For Range and Accuracy Trials. SCICON - Jun 1978	Review of work leading to current UK techniques for R&A analysis. Contains references to relevant SCICON work in the area.
Adoption of a Standard Canon Artillery Firing Table Format. NATO STANAG 4119	Contains description of Firing Table content indicating which parametric variations are of interest.
Use of Programmable Hand-Held Calculators for Artillery Fire Control. Col Roberts RARDE Branch Memo 58/1981.	Describes method of programming back-up fire control from Firing Table output.
Base Burn Projectile French Trajectory Model. D. Chargelegue and M.T. Couloumy, Proc. First International Symposium on Basebleed, Athens, Greece, November 1988.	Background information and development of the French trajectory model for base-burn projectiles.
Base Burn Trajectory Model. D. Chargelegue and M.T. Couloumy, Proc. 11th International Symposium on Ballistics, Volume 1, FOLO, Pages 725-733, Brussels Belgium, May 1989	Background information and development of the French trajectory model for base-burn projectiles
Analysis of the Flight Performance of the 155mm M864 Base Burn Projectile. J.E. Danberg, BRL Report No. 3083, U.S. Army Ballistic Research Laboratory, Aberdeen Proving ground, MD, April 1990 (AD A222624)	Comparison of base-burn motor performance modeling and flight test results using M864 projectile.

Title	Topic
Base-Bleed Systems for Gun Projectiles, Nils-Erik Gunners, K. Andersson and R. Hellgren, National Defense Research Institute (FOA) Tumba, Sweden, Chapter 16, Volume 109, 1988, Progress in Astronautics and Aeronautics, Gun Propulsion Technology, Published by the American Institute of Aeronautics and Astronautics, Inc., 370 L'Efant Promenade S.W., Washington, D.C. 20024	Fundamental principles of base flow techniques and comparisons with Swedish munitions
Modified Point Mass Trajectory Simulation for Base-Burn Projectiles. R.F. Lieske and J.E. Danberg, BRL Report No. 3321, U.S. Army Ballistic Research Laboratory, Aberdeen Proving Ground, MD, March 1992 (AD A248292)	Extension of the trajectory simulation to include base-burn projectiles for use in fire control systems. Comparisons with observed performance are included.
A Physically More Direct and Mathematically More Simple Approach To the MPM Trajectory Model. Prof. In. E. Celens – Head Dept Ballistics and Armament Royal Military Academy - Brussels – 10th International Symposium on Ballistics – San Diego, California, 1987	Trajectory modeling.
Modern Exterior Ballistics, The Launch and Flight Dynamics of Symmetric Projectiles. Robert L. McCoy, Shiffer Publishing Ltd., 1999 ISBN: 0-7643-0720-7	Covers the free flight dynamics of symmetric projectiles. Provides many examples of projectile motion illustrating key flight behaviors.

Title	Topic
International Standard ISO 2533: Standard Atmosphere, First Edition International Organization for Standardization, 1975.	Specifies the characteristics of an ISO Standard Atmosphere and is intended for use in calculations and design of flying vehicles. Also recommended in the processing of data from meteorological observations.

INTENTIONALLY BLANK

AOP-4355(A)(1)